SLAC-WP-097

Science Driven Instrumentation for LCLS-II

A White Paper outlining science and scope of instrumentation

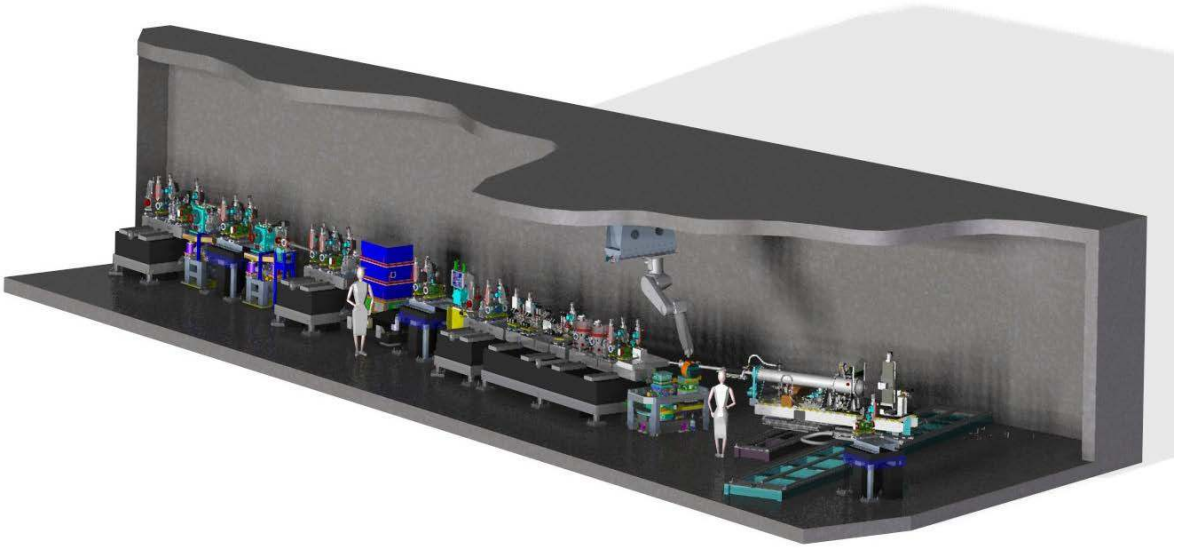

John Arthur, Uwe Bergmann, Axel Brunger, Christoph Bostedt, Sebastien Boutet, John Bozek, Daniele Cocco, Tom Devereaux, Yuantao Ding, Hermann Dürr, David Fritz, Kelly Gaffney, John Galayda, Julia Goldstein, Markus Gühr, Jerome Hastings, Philip Heimann, Keith Hodgson, Zhirong Huang, Nicholas Kelez, Paul Montanez, Aymeric Robert, Michael Rowen, William Schlotter, Marvin Seibert, Joachim Stöhr, Joshua Turner, William White, Juhao Wu, Garth Williams, Vittal Yachandra, Junko Yano

SLAC National Accelerator Laboratory, 2575 Sand Hill Road, Menlo Park, CA 94025

Work supported in part by US Department of Energy under contract DE-AC02-76SF00515.

Table of Contents

I. Executive Summary

The world's first x-ray free electron laser (XFEL), LCLS, has now been operating for more than three years and all six experimental stations are supporting user science and producing high impact scientific results. Other countries are rapidly catching up and a second XFEL, SACLA, is already operating in Japan with others coming on line in Germany, Korea and Switzerland within the next three to five years. In order to increase capability and capacity of LCLS, the Department of Energy has funded LCLS-II.

The LCLS-II baseline project, with delivery of first light in 2018, is a response to overwhelming user demand for more beam time and a key step to remain at the international forefront in capacity and capability. LCLS-II provides a second injector and another 1 km of linac which operate independently from the current LCLS facility, henceforth referred to as LCLS-I. The key expansion steps of LCLS are summarized in Figure I-1.

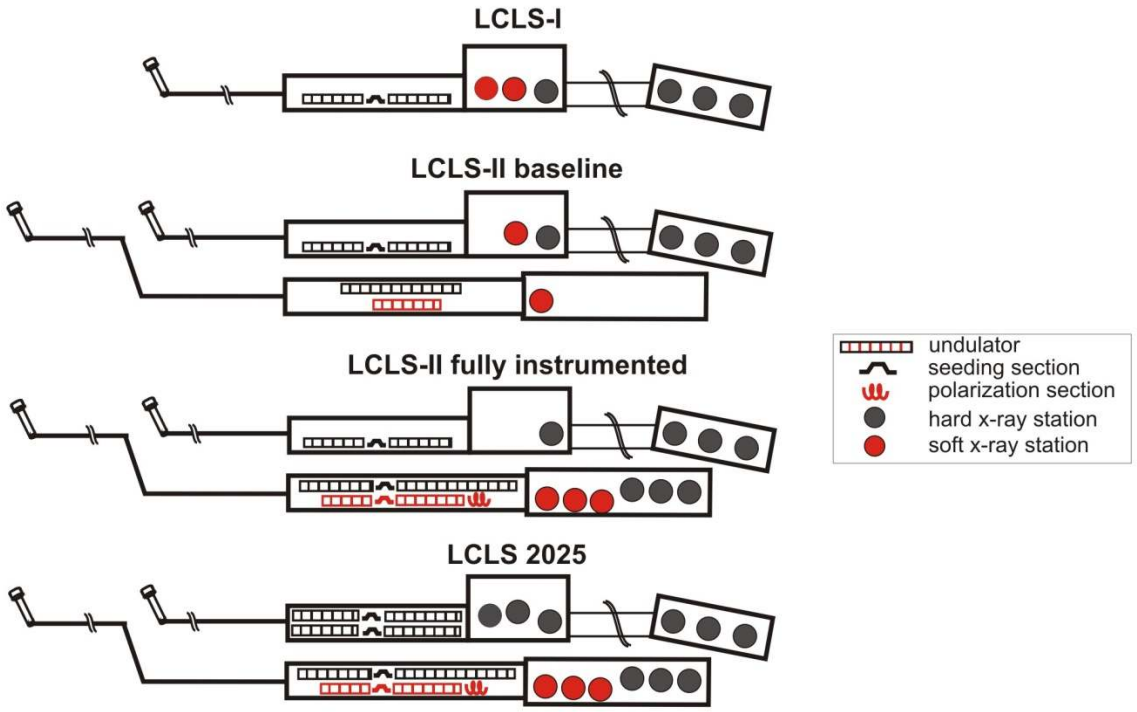

Figure I-1: Key expansion steps of LCLS with soft x-ray undulators and stations shown in red and hard x-ray capabilities in black. Descriptions of the icons are given on the right.

LCLS-II utilizes electron and photon beams that are completely decoupled from LCLS-I, allowing continued operation of LCLS-I during most of LCLS-II construction. The LCLS-II baseline project contains a new injector, an additional 1 km of linac, a new undulator hall with one soft and one hard x-ray SASE undulator and a new experimental hall that is nearly as long as the combined

LCLS-I halls. LCLS-II will be the only facility worldwide to have two independent injectors and linac sections for complete and independent control of electron bunches and x-ray pulses. The baseline project also provides one scientific instrument, which replaces the existing AMO station of LCLS-I.

This white paper outlines the full expansion of LCLS-II as illustrated in Figure I-1, building on the baseline scope of LCLS-II. Besides proposing additional user instruments it also adds capabilities such as seeding and polarization control which had not been demonstrated when the baseline scope of LCLS-II was established. LCLS-II instrumentation consists of additional undulators and seeding sections for pulse control and maximum x-ray power, x-ray optics for manipulation and diagnostics for characterization of the pulses and the addition of five new user instruments in the LCLS-II experimental hall. The key enhancements of a fully instrumented LCLS-II over the current LCLS-I facility are:

- Two independent injectors for flexible x-ray pulses
- Tripling of the number of undulator sources
- Tripling of the simultaneously operating stations
- Decoupling of hard and soft x-ray operation
- Extended photon energy range to lower and higher energies (250eV-18keV)
- Self-seeded, near transform limited soft and hard x-ray pulses
- Pulse enhancements of 1000X in brightness, 10X in power and 100X smaller bandwidth
- Complete soft x-ray polarization control
- X-ray pulse manipulation (split, delay, combine, multi-colors)
- Improved x-ray detectors (single photon sensitivity, dynamic range, number and size of pixels, 120Hz for soft x-rays)
- Pump-probe synchronization to 10 femtoseconds

The build-out of LCLS-II does not complete the full development of LCLS. Because of the rapid development of XFEL science it is prudent to add another facility improvement step later with a horizon around 2025. This envisioned fully built-out LCLS facility, referred to as LCLS 2025 in Figure I-1, will utilize the conventional facilities built for LCLS-I, adding a fourth hard x-ray undulator source in the existing LCLS-I tunnel and two more hard x-ray instruments in the LCLS-I near experimental hall, replacing the AMO and SXR soft x-ray instruments. LCLS 2025 will consist of a total of four seeded undulator sources, each serving three experimental instruments. Three quarters of the instruments will support hard x-ray and one quarter soft x-ray science, complementing the envisioned capability of the Next Generation Light Source.

Figure I-2 illustrates the LCLS capacity growth in terms of the number of undulator sources and experimental stations for the four steps in Figure I-1. LCLS-II will produce first light in 2018.

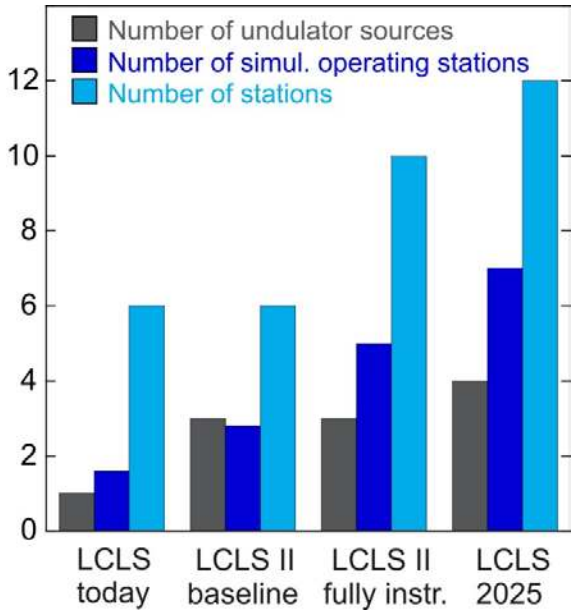

Figure I-2: LCLS growth in number of undulators and stations for the four scenarios shown in Figure I-1.

A fully instrumented LCLS-II by 2018 would keep LCLS at the international forefront as illustrated in Figure I-3. Only Japan's X-FEL facility SACLA will offer the same number of stations as LCLS (four on LCLS-I and six on LCLS-II). Figs. I-2 and I-3 point to the importance of a timely build-out of LCLS-II instrumentation to increase LCLS beamtime for users and keep LCLS internationally competitive.

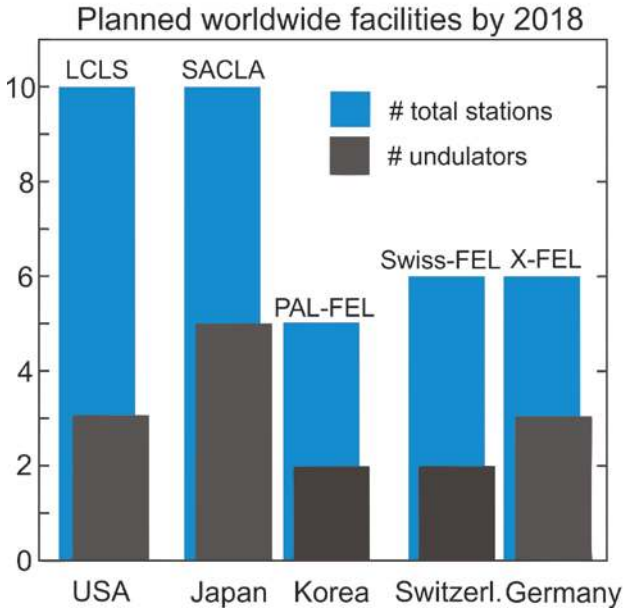

Figure I-3: Snapshot of worldwide X-FEL facilities in 2018, labeled by their names and the host country. For LCLS we have assumed the fully instrumented LCLS-II scenario.

This white paper begins with an introduction to the unique capabilities of x-ray free electron lasers, how they distinguish themselves from conventional lasers and synchrotron radiation sources, and why and how they open the door to revolutionary science.

The second chapter describes scientific challenges in three specific fields. We have deliberately restricted the discussed science to the areas of structural biology, chemical reactivity and novel materials of technological importance. The outlined challenges will greatly benefit from or outright require the use of state-of-the-art XFEL radiation and instrumentation, and if they can be mastered, will directly benefit society by advancing human health, energy production and information technology. Also, the selected science areas address key aspects of the structure and function of the atomic, electronic and spin building blocks of matter. Each scientific section ends with an outline of instrumentation needs whose implementation is the subject of chapter three.

Chapter three gives a science-driven prioritized order of three proposed LCLS-II instrumentation packages. They take advantage of the LCLS-II baseline facilities and are envisioned to lead to the creation of scientific and technological knowledge and breakthroughs. The prioritized beamline packages consist of a step-wise build-out toward the fully instrumented LCLS-II depicted in Figure I-1. Each step increases facility capability/capacity and includes enhancements of the x-ray source (e.g. power, bandwidth, polarization control), improved x-ray transport and diagnostics (e.g. pulse manipulation, characterization and synchronization), and at least one additional user instrument consisting of vacuum tanks, sample introduction and manipulation devices, detectors, and specialized optics.

The coupling of the outlined science case and the three selected prioritized instrumentation packages is illustrated in Figure I-4.

The present white paper outlines envisioned instrumentation. Owing to the fast development of LCLS science the outlined packages will be refined through future user workshops. We also anticipate close collaborations on LCLS-II instrumentation development with other laboratories. The instrumentation packages consist of:

- ***A nanocrystal x-ray diffraction facility*** to create enhanced capabilities and increased capacity for what has been identified as the first “killer application” of LCLS. It supports the structure determination of proteins that cannot be crystallized to sizes required for conventional x-ray diffraction and of samples whose radiation sensitivity currently prevents reliable structure determinations. It also allows studies of proteins in their natural environment at room temperature which is a key requirement for addressing and understanding protein function.

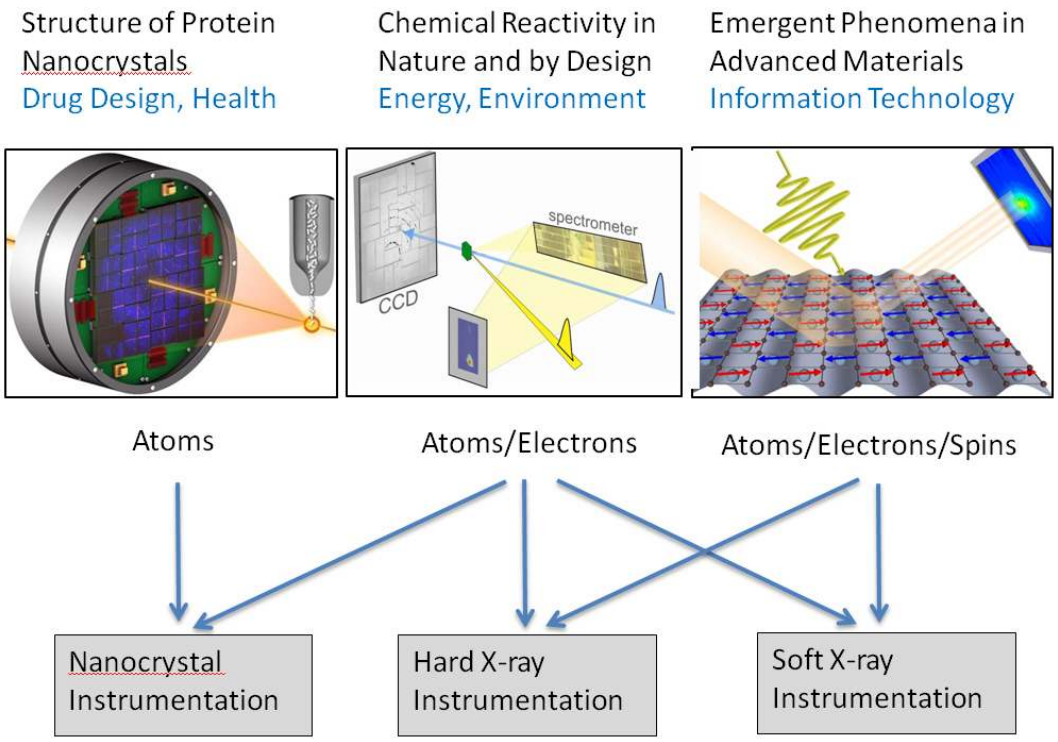

Figure I-4: Schematic of the three discussed science and envisioned impact areas, and their coupling to the three selected instrumentation packages.

- ***A soft x-ray suite*** that covers the spectral range 250 – 2,500 eV with three branch lines for atomic, chemical and materials studies. It adds to the single branch line in the LCLS-II baseline project and offers completely novel capabilities such as an x-ray optical toolbox. It also provides increased soft x-ray capacity over LCLS-I and frees up the existing LCLS-I experimental halls for hard x-rays. This facility enables element specific studies of chemical reactivity and processes involving C, N and O atoms, such as hydrocarbon transformations, nitrogen fixation and the photon induced splitting of water, supporting the dream of man-made production of fuel from sunlight. It also opens the door for understanding and controlling emergent behavior in complex materials, with the goal of controlling fundamentally new materials properties and phenomena for information technologies.
- ***A hard x-ray instrument*** covering the range up to 18 keV, suitable for a wide range of scattering, diffraction and spectroscopy studies. This flexible instrument complements the first two instrumentation packages and supports studies of atomic, electronic and spin based processes in biological and chemical systems and in materials that require unconventional experimental approaches. Examples are in situ studies of systems under operational conditions, such as materials/liquid interfaces in batteries, and

materials in extreme environments produced by pressure, temperature, radiation and field pulses.

An appendix discusses other envisioned instrumentation opportunities toward LCLS 2025. We focus on how to continue complementary use of the experimental stations in LCLS-I and how the stations may be changed to yield new scientific capabilities.

II. Scientific Opportunities with X-Ray Free Electron Lasers

A. The Revolution Enabled by X-Ray Free Electron Lasers

The essence of science is the search for new knowledge that constitutes a major step in our understanding of the structure and the processes in the world around us. Occasionally, steps occur that have such profound impact that we refer to them as paradigm shifts or scientific revolutions, as first popularized by Thomas Kuhn in his 1970 book *The Structure of Scientific Revolutions*.

For many centuries sunlight constituted the primary tool for the investigation of matter. By extending the meaning of "light" to include shorter wavelength x-rays, one may point to five light revolutions as listed in Figure II-1.

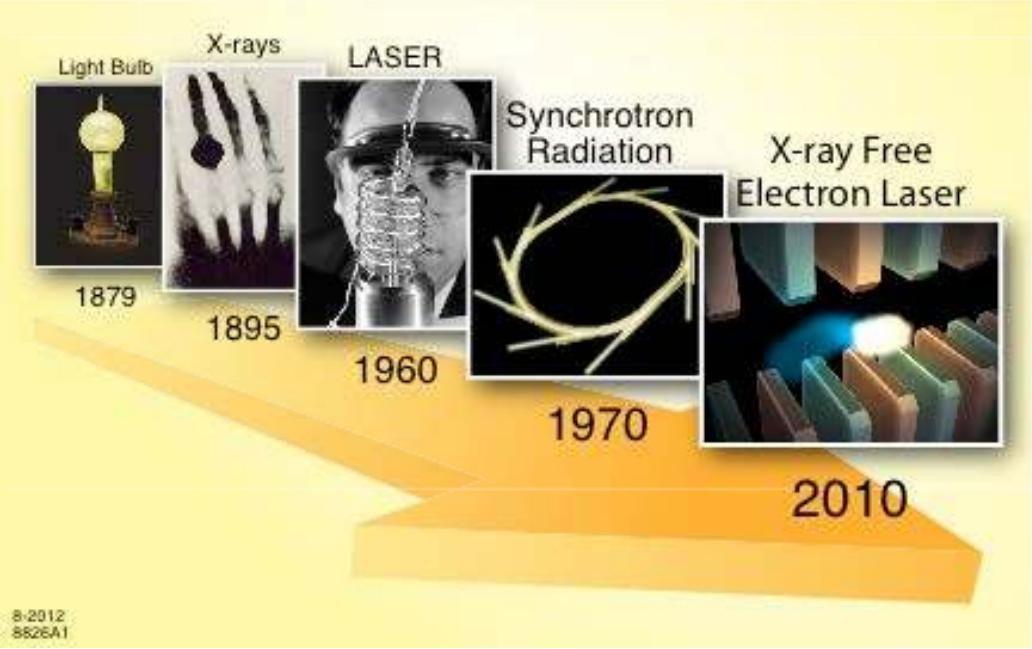

Figure II-1: Revolutions in sources of light

The last two revolutionary developments in Figure II-1 evolved over several years and the listed dates are only approximate milestones. The argument for the scientific impact of synchrotron radiation is now well documented and five Nobel Prizes are based on the use of its revolutionary properties. Free electron lasers (XFELs) at hard x-ray energies became a technological reality around 2010, and we argue that their scientific use will constitute the fifth scientific light revolution. We continue with a brief overview explaining why the availability of XFEL light constitutes the beginning of a new era in science.

Figure II-2 compares the peak brightness of conventional lasers and their extensions into the ultraviolet regime with synchrotron radiation sources and XFELs.

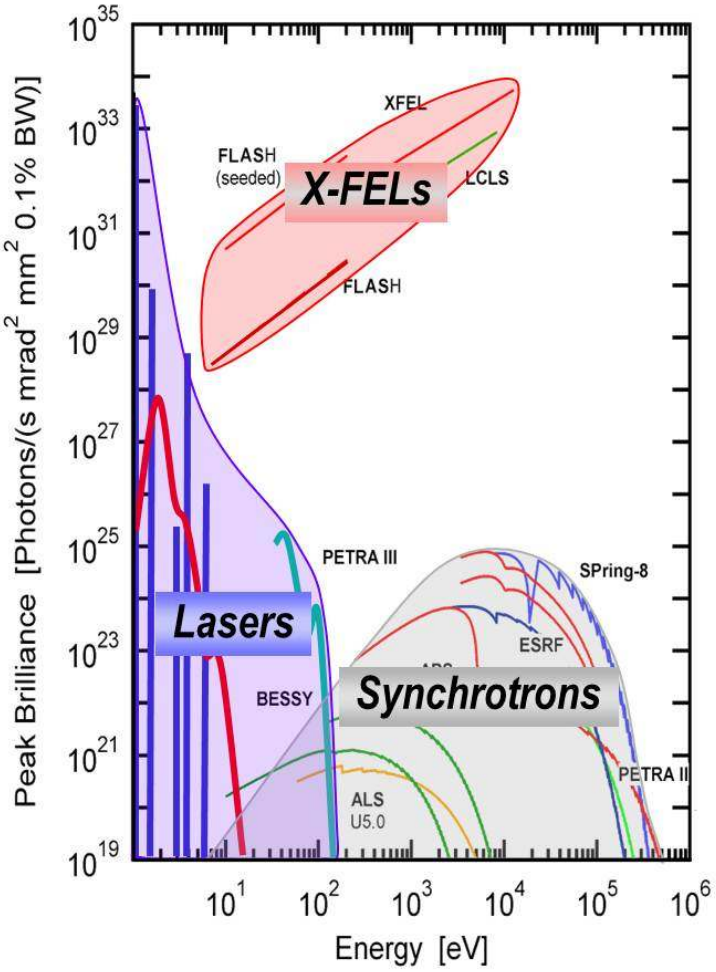

Figure II-2: Peak brilliance or brightness versus photon energy of conventional lasers and higher harmonic generation sources (Lasers, blue envelope) , synchrotron sources (Synchrotrons, gray envelope) and x-ray free electron lasers (X-FELs, red envelope) (from J. Ullrich, A. Rudenko, R. Moshammer, Ann. Rev. Phys. Chem. **63**, 635 (2012)). Note that with LCLS-II the spectral range is greatly increased to 250 eV – 18 keV and the peak brilliance exceeds that of other sources.

XFELs are distinct from conventional lasers and synchrotron radiation sources in the underlying physical principles and the properties of the light.Conventional lasers are based on light-emitting electronic transitions between distinct quantum states in the chosen laser medium. Amplification of the transition intensity is achieved by bringing many electrons into the same excited state (population inversion) and then stimulating many electrons to undergo the same radiative transition. Free electron lasers are based on radiation emitted by relativistic free

electrons travelling along a sinusoidal path. The laws of relativity allow many electrons (~10^{10}) to be bunched into a small volume of micron dimensions. Amplification arises from imposing longitudinal positional order in the electron bunch with a periodicity of the x-ray wavelength so that all electrons wiggle and radiate in complete synchronization. The order may be induced from noise by spontaneous x-ray radiation from the back of the bunch (SASE) or by superimposed monochromatic radiation. Such "seeding" decreases the energy band width of the pulses and increases the longitudinal coherence.

Both optical lasers and XFELs take advantage of the fact that the radiation intensity originating from a system of N electrons is enhanced from N to N^2 assuming that all N particles act in unison rather than individually. XFELs are considerably larger in size than even the most powerful optical lasers but both types of sources deliver similar pulse lengths, coherence and energy per pulse. The most distinguishing property of XFELs is their more than 1000 times shorter wavelength and their continuous wavelength tunability. In comparison to synchrotron radiation, XFEL radiation comes in pulses that are shorter by about a factor of 10^4, contain about 10^6 more photons per bandwidth and comprise photons that are nearly fully coherent laterally and longitudinally. The peak brightness enhancement of XFEL radiation may be as large as 10^{10}.

From a scientific point of view, XFELs open the window to a previously inaccessible region of space-time phase space that links the static and dynamic properties of matter at their fundamental length and time scales. The fundamental length scale of interest here is the size of the atoms and the spatial extent of the electronic charge and spin distributions that bind them together. The fundamental times in this atomic world are set by characteristic times of change in the atomic positions of about 1 picosecond (ps) and in the electronic valence distributions of about 1 femtosecond (fs). These timescales arise from the strength of the electromagnetic force and the inertia associated with the atomic and electronic masses. In practice the characteristic times may be simply estimated from the energy-time correlation $E\,\tau = \hbar = 4$ eV fs, linking characteristic energies E associated either with atomic motion (phonons, meV) or electronic bonds (eV) with the characteristic times of change τ.

Events in the atomic and electronic world may also be viewed from a comparison of fundamental speeds as summarized in Table II-1.

Table II-1: Order of magnitude values for fundamental speeds in our "electromagnetic" world. The listed speed of sound and Fermi velocity are approximate and material dependent. 1 attosecond (as) is 0.001 fs.

Atoms	Speed of sound:	1 nm / 1 ps
Electrons	Fermi velocity:	1 nm / 1 fs
Light	Speed of light:	1 nm / 3 as

The atomic and electronic speeds in Table II-1 are determined by consideration of their characteristic energies and *linear* momenta. Electrons, however, have another fundamental property, the spin. The transport of spins in solids is also determined by the Fermi velocity, but many important phenomena are based on the presence of localized atomic moments which give rise to the macroscopic magnetization of materials. Atomic magnetic moments underlie the practical use of magnetism and of key interest is their direction and the achievable speed of direction reversal. This speed is determined by energy and *angular* momentum. Any rotation in magnetic moments is accompanied by a change in angular momentum that needs to be accounted for. In practice, the angular momentum is transferred to the lattice and since this requires angular atomic motions, the magnetic switching speed is bottlenecked by the speed of sound. Therefore the fundamental speeds listed in Table II-1 also apply to the spin system.

We can obtain information on the fundamental dynamics of atoms, electrons and spins if we employ light because it is intrinsically faster than the speed of atoms or electrons. While the x-ray probing speed is typically dictated by the length of a pulse consisting of many wave cycles, one may nevertheless state:

> *Because of their atomic-size wavelength and their intrinsic speed of light, x-rays uniquely allow the investigation of matter on the fundamental length and time scales of its atomic and valence-electronic building blocks.*

This simple consideration of speeds has important consequences when we combine it with the inherent abilities of x-rays to determine atomic positions and to distinguish different atoms and their chemical state.

We can beat the speed of sound or the motion of atoms with the speed of light of ultrafast x-ray pulses. This allows us to use the principle of “probe before destroy” to capture single shot structural images of fragile protein molecules and chemical reaction centers that in the past were damaged in the process of the measurement itself, yielding inconclusive results. While the employed x-ray pulses are so powerful that they will destroy the sample, the image will already have been recorded by the time destruction occurs.

The shortest femtosecond x-ray pulses today have comparable or faster durations than the fastest electronic processes associated with valence electrons that determine the electronic properties of matter. It is thus possible to study the time evolution of key electronic processes. Because of its importance and ultrafast initiation, the conversion process of sunlight into other forms of energy, such as that stored in chemical bonds, is a prime target of investigation. The element and chemical state specificity of x-rays furthermore provides the unique ability to isolate the signal emanating from the key reaction centers.

While the laws of nature determine the fundamental speed limits in matter, technology today has not reached these limits. The most advanced devices today of ~100 nm size can be switched in about 100 ps, or roughly with the speed of sound. The goal of developing "smaller and faster" electronic devices approaching the 1000-times faster electronic speed limit will therefore remain the key topic of technological developments for years, and most likely decades, to come. X-ray studies of the ultrafast electronic and magnetic nanoworld can pioneer the course of future technologies.

While the first generation of XFEL science has exploited the obvious advantages of XFEL radiation, namely pulse intensity, speed and lateral coherence, we envision more sophisticated uses of X-FELs in the future. One hallmark of lasers is their complete coherence, expressed by a large degeneracy parameter, i.e. the number of photons contained in the volume defined by the product of lateral and longitudinal coherence lengths. Synchrotron radiation sources on average have less than one photon in their coherence volume and therefore all interactions of x-rays with a sample can be described as "one photon at a time". In contrast, XFELs presently have of order 10^9 photons in their coherence volume and this number will increase with seeding.

The large degeneracy parameter of XFELs opens up the entire new field of non-linear x-ray science. Judging from the impact in the visible range we anticipate revolutionary advances at x-ray energies, as well. The Raman process is of particular importance as it provides access to low-lying excited states that cannot be reached by one-photon dipole processes. In the x-ray region, stimulated Raman scattering can be performed resonantly by involving transitions from the ground state through intermediate core hole states that provide atom, chemical and charge/spin specificity. In the soft x-ray region, the resonant Raman cross section is comparable to the non-resonant optical Raman cross section and soft x-ray stimulated Raman scattering appears to be straightforward once suitable instrumentation is available (see Figure II-15). Another advantage of using x-rays is their finite momentum, yielding momentum dependent information of low lying excitations in solids. The beauty of the stimulated Raman technique is that it does not require population inversion in the sample, which, because of the required power, would lead to strong perturbation during the pulse and ensuing damage. The pursuit of non-linear x-ray science, however, requires improvements in pulse control and we propose developing source schemes for producing two colors and construction of a "soft x-ray tool box" that contains pulse splitters and delay lines.

B. Three Scientific Challenges that will Affect the Way we Live

Here we discuss three selected scientific areas where XFEL radiation through its unique properties discussed above is envisioned to lead to significant scientific breakthroughs. The outcomes of research in these areas will influence the way we will live in the future and are envisioned to improve health through drug design, enable environmentally benign energy production and lead to advanced information processing and communication.

The "LCLS-II New Instruments Workshops Report" gives a broader scientific case for XFEL applications and also details specific examples where research can benefit from the enhanced capabilities of LCLS-II (http://slac.stanford.edu/pubs/slacreports/reports19/slac-r-993.pdf). Another source that presents the scientific case for XFELs is the published report "Science and Technology of Future Light Sources" available as ANL-08/39, BNL-81895-2008, LBNL-1090E-2009, SLAC-R-917 or at http://www-ssrl.slac.stanford.edu/aboutssrl/documents/future-x-rays-09.pdf and the Basic Energy Sciences Advisory Committee report "Next-Generation Photon Sources for Grand Challenges in Science and Energy" available at http://science.energy.gov/bes/news-and-resources/reports/basic-research-needs. More generally, XFEL and synchrotron radiation research supports the complete science portfolio of the Basic Energy Sciences Division of DOE outlined in the "Basic research Needs" workshop series at http://science.energy.gov/bes/news-and-resources/reports/basic-research-needs.

We have started to work on the identified scientific challenges with LCLS-I, but the advanced *capabilities* and the enhanced *capacity* delivered by a fully instrumented LCLS-II will ensure that we can successfully meet them. The LCLS-II enhancements were already summarized in the Executive Summary and will be outlined in more detail in the later sections of this white paper.

1. The Biological Cycle of Life: Understanding the Structure and Function of Macromolecular Assemblies

Overview

Structural biologists eagerly anticipated and started the revolution in "x-ray light-driven" science more than a decade before LCLS arrived. A publication entitled "Potential for biomolecular imaging with femtosecond x-ray pulses" (Neutze et al, *Nature,* **406**, 752 (2000)) simulated the interaction between an ultra intense, ultrashort x-ray pulse and two key classes of biological samples: nanocrystals and single molecules. The simulations predicted an astounding effect: increasing the x-ray dose to the level where a single shot destroys the sample completely allows recording structural data to higher resolution than a conventional dose to the same sample that damages it gradually. The diffraction of femtosecond pulses outruns radiation damage processes. This "diffraction-before-destruction" effect has set the stage for a revolution in structural biology because it makes nanocrystals and single particles accessible to structure determination methods for the first time. A recent review has been given by Neutze and Moffat (*Current Opinion in Struct. Biol*. **22**, 651 (2012)).

Although LCLS-I has not quite reached the beam parameters used in these simulations to enable atomic resolution nanocrystallography, diffraction data for known protein structures have already been collected at high resolution with LCLS-I. The peak intensity pulses that will be achievable with LCLS-II can greatly expand the capability for biological experiments with carefully selected new instrumentation.

Introduction

Understanding life and the biochemical processes that sustain it has obvious importance to society at large. It is primarily through structural knowledge, which may be used to deduce function of the proteins, complexes and control pathways involved in disease, that one can begin to devise a cure or treatment. The impacts on human health and quality of life from the explosion of structural biology studies in the coming decades cannot be overstated. In the search for examples of scientific research and discoveries that directly impact society, there can be no better example than the determination of the structure and function of biomolecules and processes involved in a human disease and the use of this information to design new drugs to control or cure the disease. Prominent examples where structures played a key role in drug development include HIV protease, reverse transcriptase, and fusion inhibitors that made HIV a largely manageable disease; the kinase inhibitor Gleevec that is remarkably effective in treating certain types of leukemia; and the recent BRaf kinase inhibitor Zelboraf that is used to treat metastatic melanoma in patients with a certain mutation (about 50% of the patients have this mutation).

X-rays are the primary tool that enables structural studies of large biomolecules such as proteins, enzymes, and complexes, leading to life science breakthroughs that can improve our quality of life, as exemplified by the development of the above mentioned therapeutics. Moreover, as illustrated in Figure II-3, x-ray macromolecular crystallography is today the primary technique used to solve the structure and function of life's machinery on the molecular and atomic levels and it is expected to continue to be equally important in the future.

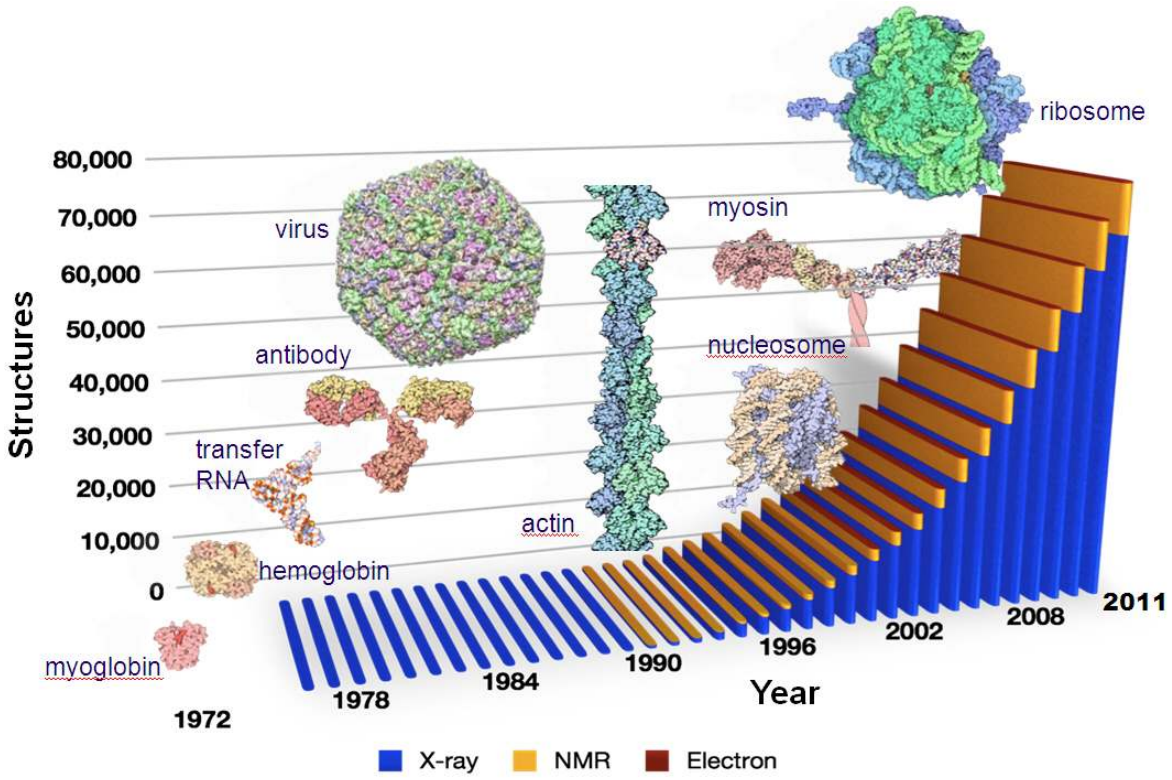

Figure II-3: Cumulative number of structures in the Protein Data Bank and breakdown of structures solved by different techniques. (C. Abad-Zapatero, *Acta Cryst*. **D68** (2012)).

The importance of protein x-ray crystallography is well illustrated by the determination of the structures of two complex molecular machines central to all known life: RNA polymerase (the protein complex which reads DNA and produces messenger RNA) and the structure of the ribosome, which synthesizes proteins based on this RNA message. Nobel prizes were awarded in 2006 and 2009 for this seminal work, demonstrating the role that x-ray crystallography plays at the frontier of life sciences as well as its overall importance.

The technique of macromolecular x-ray crystallography has progressed from studying individual proteins and enzymes in a reductionist approach to biology to providing a system-level view of large protein assemblies, in many cases interacting with DNA and RNA, that carry out many of the key functions in cells. As the macromolecular assemblies being investigated increase in size and complexity, the essential requirement of growing macroscopic diffraction-quality crystals

becomes more and more challenging. Despite more than half a century of intense efforts, determining crystallization conditions for biological macromolecules remains unpredictable and requires exhaustive experimentation. The inability to obtain large enough high-quality, well-diffracting crystals for conventional synchrotron-based studies is a significant limitation to macromolecular crystallography and structure determination of large complexes and of some other classes of proteins. The problem is exacerbated in cases of non-soluble molecules, such as membrane proteins, which are very often more difficult to crystallize than soluble proteins.

This represents a very important challenge in biology because most of the important processes of life occur at the boundary between the cell interior and the outside, *i.e.* at the cell membrane, and many of these processes are today very poorly understood due to the lack of structural information. As of mid 2012, out of more than 82,500 structures deposited in the Protein Data Bank, fewer than 350 represent membrane proteins. Likewise, the number of macromolecular assemblies (complexes) determined is still dwarfed by the number of known individual, uncomplexed structures. Any tool that can be developed to facilitate the structural determination of membrane proteins is of immense value.

In addition to the challenges of crystallization, the problem of x-ray induced radiation damage has hindered progress in structure determination, in particular at high resolution. Nearly all crystals used in synchrotron experiments must be cryogenically cooled to minimize such damage. There are also active centers in some very radiation-sensitive proteins, such as photosystem II, that are rapidly photo-damaged by the synchrotron beam before an intact structure can be determined.

Historically, conventional synchrotron x-ray sources have imposed a lower limit on the size of crystals that can be used for diffraction experiments. Crystals typically need to be at least a few tens of microns in size in order to produce sufficient signal integrated over the measurement period. Simultaneously, there exists an upper limit on the resolution that can be obtained from a crystal of a given size before it is destroyed by radiation damage, due to the relatively lengthy time required to record the diffraction patterns. The very probe used to study the samples deposits energy in the sample through x-ray absorption and causes a degradation of the sample during measurement. The problem can be circumvented by the use of large crystals since the absorbed energy is spread over more copies of the molecule, leading to a smaller dose per molecule while maintaining the signal level. Another approach is to collect data from multiple crystals, scaling the diffraction data to obtain the required 3D data set. If the crystals are too small (smaller than about several cubic microns), these approaches are not feasible even with the best available synchrotron sources.

Serial Femtosecond Crystallography (SFX)

LCLS-I and LCLS-II offer a path to open discovery possibilities for many more difficult-to-crystallize or easily damaged proteins by allowing much smaller crystals to be used successfully when compared to what is possible at conventional synchrotron x-ray sources. The revolutionary ultra-bright and ultra-short x-ray pulses from LCLS-I have removed the link between crystal size and radiation damage. The extremely high peak-power of the pulses permits measurable and interpretable diffraction from crystals that are only a few hundred nanometers in size and in some cases contain fewer than ten repeating unit cells per side. The femtosecond duration of the LCLS pulse lets diffraction outrun radiation damage, leading to a "diffraction-before-destruction" approach that allows x-ray doses far above the conventional damage threshold. By exposing hundreds of thousands of individual crystals to the beam one-by-one, fully hydrated and at room temperature, a complete undamaged diffraction data set can be determined at high resolution, despite the fact that the crystals are destroyed by the beam. Thus, LCLS pulses can be used to achieve higher resolution for crystals that are sensitive to radiation damage, avoiding the loss of resolution caused by even a single exposure at synchrotron sources.

Figure II-4 shows one of millions of diffraction patterns recorded at LCLS-I and the corresponding protein structure. The phases necessary for the computation of the electron density map were obtained based on the previously known crystal structure of lysozyme.

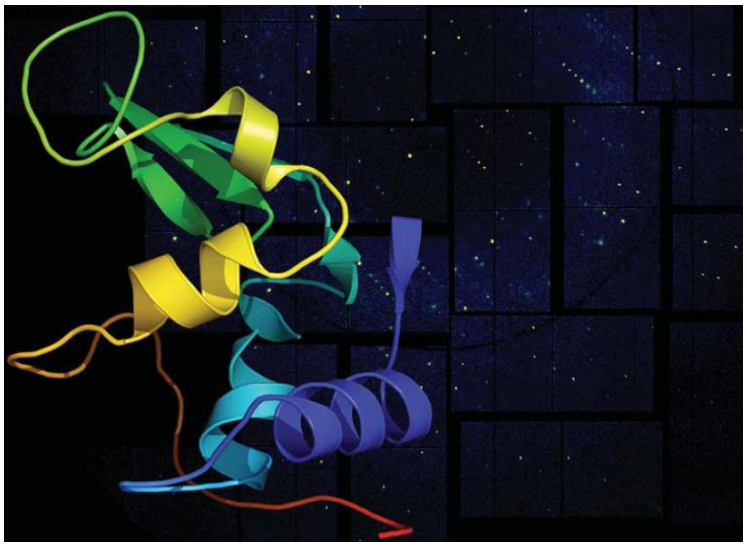

Figure II-4: This rendering shows a lysozyme structural model against its x-ray diffraction pattern recorded a LCLS' CXI instrument. The bright Bragg spots correspond to the spikes in the previous figure. This successful demonstration paves the way for studies of more complex biological structures. *Image courtesy of Anton Barty/DESY* (https://news.slac.stanford.edu/image/lysozyme-analysis)

The experimental setup for this serial femtosecond crystallography technique is illustrated in Figure II-5.

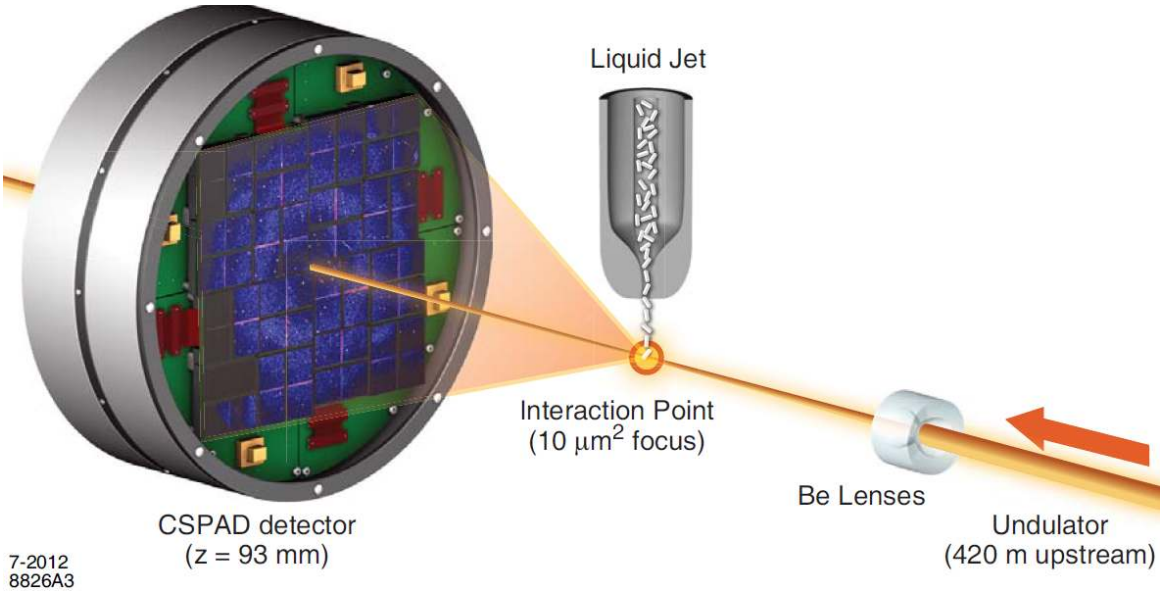

Figure II-5: Serial Femtosecond Crystallography at the Coherent X-ray Imaging (CXI) instrument at LCLS-I (Boutet et al., *Science* **337**, 362 (2012))

The inherently fast measurement of crystal diffraction using the LCLS-II beam lends itself naturally to the study of dynamic processes in biomolecules. The measurement is so fast that it is made before motion of atoms in the sample occurs following the energy deposited by the x-ray pulse. With the introduction of a well-known and well-prepared initial state followed by a stimulus of some kind, the dream of making molecular movies will likely be achievable. Here, the increased capacity provided by the LCLS-II dedicated instrument will be of extreme value by affording sufficient beam time to extremely challenging projects.

The initial success and proof-of-principle studies in crystallography of micro-to-nano-sized crystals at LCLS-I is expected to have wide impact in the field of structural biology and, analogous to the explosion of structural biology at synchrotron sources, a similar increase in the already high demand for LCLS beam time is expected. Although major technological hurdles will have to be overcome to make macromolecular structure determination with LCLS a matter of routine, and to apply it to the most challenging systems, it is likely that the demand for LCLS beam time for biological projects will significantly grow in the next few years. Therefore, the need for increased capacity is expected to justify the development of a dedicated hard x-ray macromolecular crystallography beamline that can fully utilize the beam properties of LCLS-II. Areas of expected growth where LCLS-II can have a unique impact are described below.

Photo-induced dynamics

The example of biological photosynthesis comes immediately to mind as a prototypical case for LCLS-I and LCLS-II. In particular, the detailed understanding of the structural dynamics of water splitting due to the sequential absorption of four photons by photosystem II (PSII) would be a groundbreaking result. Ultrafast x-ray pulses are required for this experiment in order to probe the Kok cycle (see Figure II-6) of this extremely radiation sensitive metal center at room temperature using the probe-before-destroy approach. Note that the evolution times between the indicated "S" states is rather slow as given in the Figure caption but the ultrafast LCLS pulses are needed to avoid radiation damage.

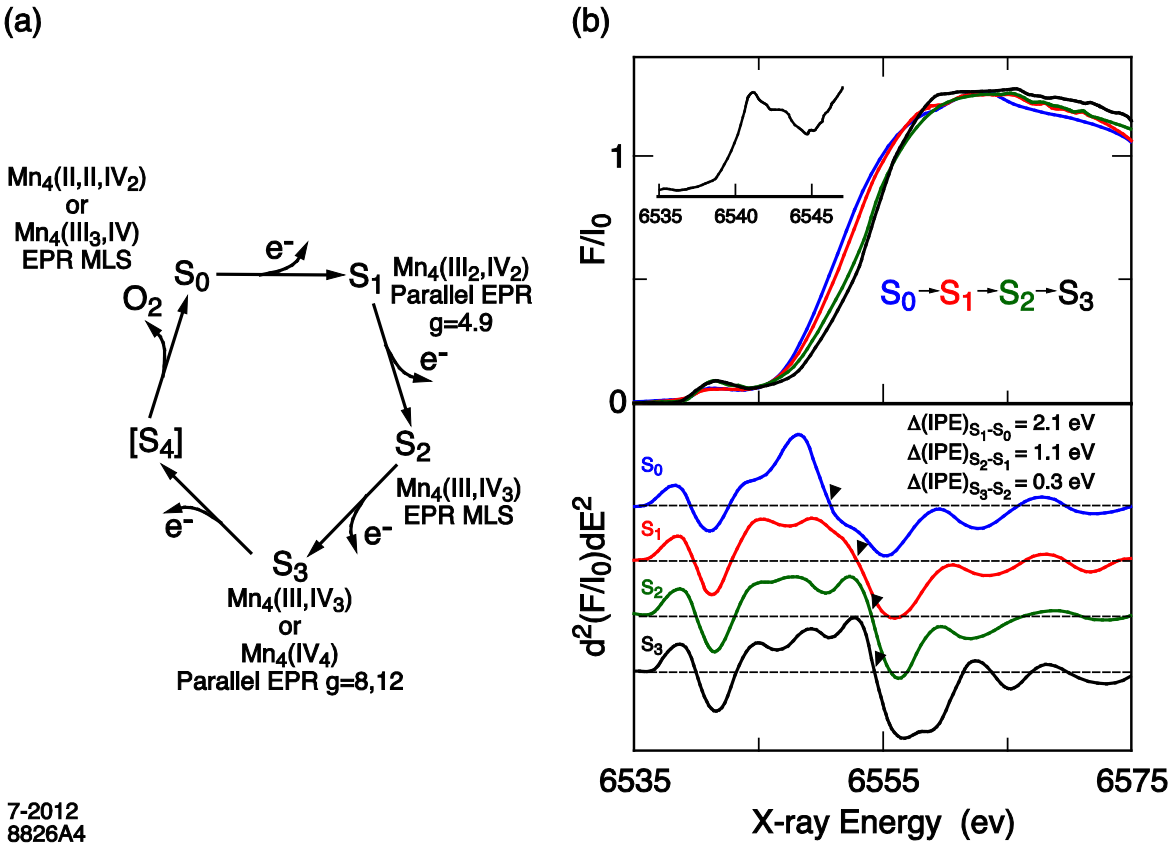

Figure II-6: Kok cycle of water splitting in PSII. The sequential absorption of 4 visible photons produces molecular oxygen from water molecules (from Sauer et al, *Coord Chem Rev* **252**, 318 (2008)). The evolution times are 30μs (S_0-S_1), 70μs (S_1-S_2), 190μs (S_2-S_3), 200μs (S_3-S_4), and 1.1 ms (S_4-S_0).

The key lies in understanding the $S_3 \rightarrow S_4 \rightarrow S_0$ transition, which has never been conclusively observed. It is here where the actual water splitting occurs at room temperature. An understanding of the details of this mechanism could identify a path toward artificial

photosystems capable of rivaling natural systems in efficiency. LCLS-II can integrate instrumentation, such as ultrafast time-resolved X-ray Emission Spectroscopy (XES), to routinely make correlated multi-probe measurements to complement structural data obtained by XRD from the same x-ray pulses. Another key advantage of using intense, ultrafast x-ray pulses for pump-probe studies is the use of small crystals that allow a more uniform illumination of the sample by a pump laser, providing a more uniform population of states throughout the sample and reducing attenuation effects of the laser in the sample.

Chemical reactions with rapid mixing

Another area of potentially high impact is the study of the dynamics of ligand binding to a substrate site. It may be possible, for example, to make a molecular movie at atomic resolution of an enzymatic reaction of substrate binding, chemical reaction and product release. Time-resolved studies could be accomplished by using rapid mixing systems integrated in the liquid jet sample delivery system. Here, the ability of single LCLS-II pulses to provide sufficient signal is key to obtaining a snap-shot structure at a well-defined time. Also, the possibility of again using small crystals provides the enormous advantage of allowing rapid and more uniform diffusion of the reagents into the crystal to produce a uniform concentration throughout the crystal.

Radiation-sensitive systems: metalloproteins

Some macromolecules can produce large crystals, but synchrotron sources tend to cause radiation damage at the active site, so that the structure of metal centers in the molecules can only be determined in a radiation-damaged state. This can often be the case for metallo-proteins, where x-ray absorption in the protein and buffer leads to multiple, very rapid radiation damage events, including photo-reduction of the metal centers. The manganese cluster in PSII is an example where electronic damage to the heavy-atom cluster occurs at a dose that is two orders of magnitude lower than the dose required to obtain the data needed to determine the structure of the entire protein at high resolution. In this case and others, LCLS-I, and the increased capacity and shorter, higher intensity pulses afforded by LCLS-II, represents the only path to a high-resolution structure of the undamaged metal ion active site using the diffraction-before-destruction technique.

Naturally-occurring aggregates

For many important classes of proteins it has thus far been very challenging to obtain crystals large enough to use with synchrotron radiation. Some neurodegenerative diseases, for example Alzheimer's and Parkinson's Diseases, exhibit mis-folded protein segments that form partially ordered fibrils and aggregates. Figure II-7 shows amyloid fibrils that yielded structures with a microfocused synchrotron undulator x-ray beam. LCLS-II will greatly enhance study of naturally

occurring crystalline aggregates due to the ability to use even smaller crystals than ever before in improved sample chambers on a dedicated crystallography end station.

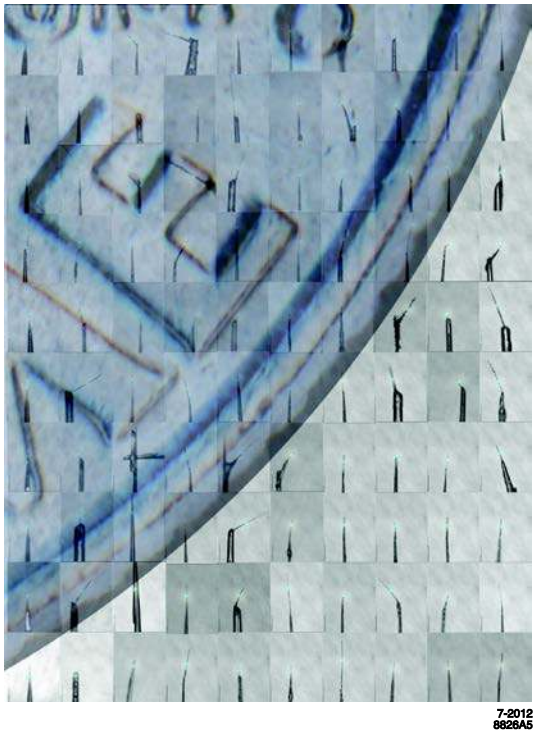

Figure II-7: A montage of 100 micro-crystals used to determine the x-ray structures of amyloid fibril cross-beta spines. Each small circle indicates where the x-ray beam intersects that crystal. To provide scale, the image of a U.S. dime is superimposed. Credit: Michael Sawaya, David Eisenberg/UCLA. Shown by David Eisenberg during the LCLSII New Instruments Workshop. Source: http://www.esrf.eu/news/general-old/general-2007/disease/image/image_view_fullscreen

Crystallography down to the ultimate limit

Whether a systematic quality difference exists between nanoscopic and macroscopic crystals remains an open question. Three competing hypotheses can be formulated:

1. Small crystals are of higher quality, perhaps because the small volume induces less strain, resulting in fewer defects. If the crystal size is smaller than a typical mosaic domain, one could imagine that the crystal quality would be increased.

2. Small crystals are small because they stopped growing due to the early accumulation of defects, leading to a low quality.

3. Size and quality are independent of each other.

The question of how small is the smallest usable crystal for structure determination can be addressed by LCLS-I and LCLS-II. Pushing the crystal size limit downwards requires small focus

capabilities. Such a capability is already provided at the LCLS-I CXI instrument and the increased capacity provided by LCLS-II will allow a broader effort toward imaging smaller crystals and eventually single molecules using the existing CXI instrument with tight focusing.

Crystal screening

An additional question for the crystallography community that arises due to the nanocrystallography capabilities demonstrated at LCLS-I is how readily high-quality nanometer- and micron-sized crystals are obtainable, relative to macroscopic crystals. Showers of tiny crystallites and microcrystals are frequently found during biomacromolecular crystallization trials before conditions for large single crystal growth are established. Serial femtosecond crystallography (SFX) using LCLS-II will be able to generate diffraction patterns from sub-micron crystals. Such materials might conventionally not even be considered for screening with synchrotron light. Nanocrystals useable at LCLS-II could in fact be so small that they might escape the initial crystal detection strategies commonly employed in protein crystallization laboratories, since those frequently use optical light microscopy to identify crystals.

It is therefore plausible that there already exist crystallization protocols in the structural biology community that generate samples suitable for SFX experiments, but not for synchrotron-based crystallography. Moreover, novel crystallization routes employing *in-vivo* crystal growth become feasible when combined with LCLS-I x-ray pulses. Exploiting this opportunity requires far greater capacity for access to beam time for screening and iteratively improving samples than LCLS-I currently offers. A tandem operation of two experiments in series can allow for crystal screening time in a parasitic mode that will not reduce beam time for other efforts. The serial operation of the instrument will effectively create more beam time, for such applications as crystal screening.

Seeded TW pulses

LCLS-II has the potential to generate terawatt (TW) x-ray pulses with very short duration, resulting in maximum signal with minimum damage during exposure, which is ideal for crystallography. The path to TW pulses involves self-seeding, and the use of a seeded beam at LCLS-II will allow a better-defined spectrum of the incident x-ray beam, which could potentially greatly simplify data analysis. One potential concern regarding self-seeding, however, is that it leads to a narrow bandwidth. The effect of such a narrow bandwidth on the ability to analyze the structure of nanocrystals is currently a source of great debate. One possible way of increasing the band width is using much shorter pulses which will allow for fewer partial Bragg peak measurements. On the other hand, the SASE spectrum fluctuates wildly from shot-to-shot and represents a potentially significant source of errors in the Bragg peak integration. Currently, many shots are required to average out all the fluctuations of the LCLS beam for SFX. Reducing these fluctuations could lead to more accurate integration but could also come at the

cost of requiring more crystals. It is currently unknown whether the reduced number of Bragg peaks per shot because of the narrower seeded bandwidth will represent a problem for SFX.

There are other potential advantages of a seeded beam. The ability to provide a beam with a well-defined and controlled energy spectrum could turn out to be critical for future anomalous diffraction measurements near absorption edges (such as Se at 12.6 keV) and provide a critical method for phasing diffraction patterns and solving *de novo* structures.

It is important to note that the much shorter, very intense pulses of the LCLS-II TW seeded beam may overcome damage issues in the smallest and most radiation-sensitive crystals. It is believed that Bragg diffraction in SFX terminates when damage occurs. Shorter pulses lead to more incident photons before the damage occurs and therefore more measurable and interpretable signal from the same sample. This will be a significant advantage for weakly-diffracting and damage-prone samples.

The effects of the limited seeded bandwidth may eventually be overcome and outweighed by the advantages in reduced radiation damage from the short seeded pulses and the better control of the beam properties. We believe there is a need for both wide bandwidth and narrow bandwidth short pulses for nanocrystallography at LCLS-II, which justifies the development of the capability for hard x-ray self-seeding that can lead to TW pulses. It is, however, important that users are able to choose between a seeded or non-seeded beam for their experiments, which is easily accomplished with a self-seeded system by removing the monochromator and bypassing the electron beam chicane.

Opportunities and instrumentation needs

The techniques for structural biology with FELs are rapidly evolving. The strategy for LCLS-II instruments must therefore be tightly integrated with improvements of existing LCLS-I instrumentation and should benefit from their development. Simultaneously, a balance must be struck between increasing capacity and developing new capability. LCLS is facing rapidly growing competition from other FEL facilities pursuing ambitious performance goals. Biology projects have been pursued on four of the six LCLS-I instruments (AMO/CAMP, CXI, SXR & XPP), with the strongest demand at CXI. This provides evidence that instrumentation to support biology research, and especially nanocrystallography, should be a high priority for LCLS-II.

Required instrument specifications

- Desirable photon energy ranges:
    - Hard x-ray up to 16 keV (covering selenium k-edge)
    - Soft x-ray up to 2.5 keV to cover sulfur k-edge

- Highest peak intensity to achieve the highest possible number of photons in the shortest possible time
- Low noise, high dynamic-range, large area detectors
- Tandem operation of end stations to utilize the transmitted beam

LCLS-I has no instruments operating in the 2-5 keV region. This energy gap is a limitation and should be closed. This energy range will make accessible crystal phasing at the sulfur edge which could prove very important for solving new structures. We also note that this photon energy range has been desired by current LCLS users doing biological imaging. The proposed NXD package in Section III outlines a hard x-ray instrument using photon energies above 6 keV. However, a relatively simple reconfiguration of the existing LCLS-I soft x-ray beamline (presented in the Appendix) will allow operation in the 2-5 keV range and fill the current LCLS-I energy gap.

Crystallography and single-particle experiments have always shared common infrastructure, with experiment specific modifications. This flexibility can be beneficial and should be maintained while developing more stable systems for the high-demand field of nanocrystallography.

2. The Photochemical Cycle of Life: Understanding and Controlling Processes at Reaction Centers

Nearly all sources of energy, from wind to fossil to solar photovoltaic, rely on the sun as the primary energy source. This photon energy is highly abundant but it takes a very sophisticated and engineered system to funnel it into useful forms of energy. Nature has developed both efficient and cheap (in terms of mass production) molecular machines that master the challenge of transforming light energy from the sun into chemical energy which is easily stored and transported. In order to funnel light energy into specific channels, molecules use the approach that the fastest channel will be the most efficient. Nature also manages to protect and repair important molecules such as the genetic code or photosystem II that are damaged by sunlight or light induced radicals.

A formidable challenge: conversion of sun energy to other forms of energy

Molecular valence electrons are the primary absorbers of sunlight. These particles provide the binding forces between the nuclei and thus stabilize the molecule in a particular nuclear geometry. In the ground state, all forces among nuclei and electrons are balanced. If a photon is absorbed, the electrons reorganize, and the equilibrium is disturbed. What follows is a highly intertwined motion of nuclei and electrons. In order to perform a certain function, the motion of the molecule has to be directed into a particular channel. For example, a bond may need to be altered, like in the retinal isomerization as illustrated in Figure II-8.

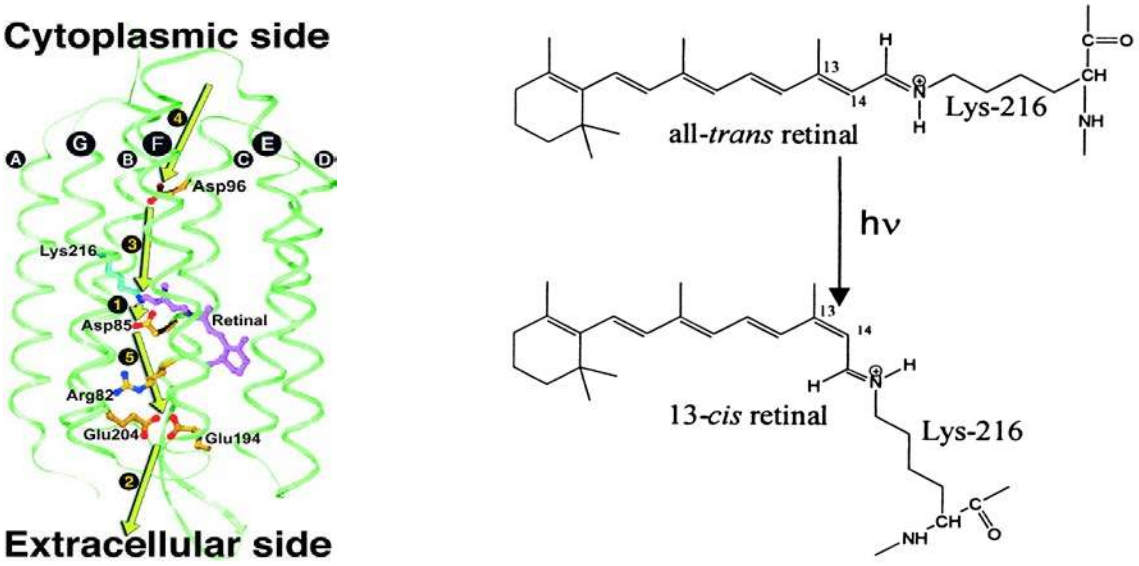

Figure II-8: (A) Bacteriorhodopsin structure and (B) light driven photoisomerization. Adapted from Neutze et al*., Biochim. Biophys. Acta: Biomembranes* **1565**, 144 (2002).

The light is not selective in the way a molecule changes its shape. This means the molecule needs to be constructed such that light excitation drives it into the particular desirable channel – or alternatively away from destructive channels. In this context, the function of a lot of molecules is a question of competing time constants. If a destructive mechanism occurs over a certain time scale, the molecule can function by simply speeding up the constructive channels. Since all nuclear dynamics after photoexcitation happen on a femto- to picosecond time scale, a molecular arms race in the ultrafast domain tries to funnel as much photon energy into usable forms of energy in the shortest time possible.

Our understanding of the molecular mechanisms in place is only beginning. Approximations that dominated molecular science for decades appear not to hold when it comes to efficient molecular machines for light conversion. One such example is the Born-Oppenheimer approximation, stating that nuclei and electrons inside the molecule can be treated separately because the light and fast molecular electrons adapt instantaneously to any nuclear geometry. As first proposed by Teller in the 1930's, this approximation breaks down at certain molecular geometries and it leads to an ultrafast transformation of electronic energy. In simulations, we have learned over the last two decades that this non-Born-Oppenheimer dynamics plays a big role in photochemistry and we will need sophisticated experiments with ultrafast x-ray pulses to shed new light on nature's molecular machines to learn about their dynamics. Such phenomena are also important for chemistry that requires multi-electron reactions, such as water splitting. Another frontier area is the influence of the environment on molecular photoreactions. Prominent examples here are the retinals, which perform specific functions highly dependent on the protein cage in which they are situated.

Three examples below make the case for new experiments with hard and soft x-rays from LCLS-II.

Bioengineering and chemical conversions with a twist

Biological systems have harnessed photo-induced charge transfer in photosynthesis and photo-induced isomerization in bacteriorhodopsin to fuel life. Such systems provide clear demonstrations of effective light-to-fuel conversions. By understanding, mimicking, and manipulating these ultrafast processes we have the opportunity to identify both molecular and supramolecular design rules for constructing artificial light conversion materials and devices.

Photo-isomerization reactions highlight the critical role of the supramolecular chemical environment on the rate and yield of a selected photoproduct. Ultrafast photo-isomerization of chromophores takes place in different locations within the molecule depending on whether the solvent is a protein (e.g., bacteriorhodopsin) or a liquid.

While we understand many of the details of *what* happens during ultrafast photo-isomerization in nature, we do not yet understand *why* it happens. A robust understanding of the interplay between reaction environment and photochemical outcome has wide ranging implications for directing light-driven chemical conversions, designing molecular sensors of local physical properties for biological imaging, and building photoactive molecular devices. Previous studies on reaction environments have generally emphasized either the solvent viscosity dependence of photo-isomerization dynamics, or the role of excited state charge transfer. Progressing beyond our current understanding requires a description of the *dual* importance of viscoelastic and electrostatic effects, a goal that will be enhanced by dynamical studies that more directly and comprehensively assess the photo-isomerization dynamics. While biochemical synthesis and ultrafast optical measurements have a demonstrated ability to influence and observe the outcome of photon driven chemistry, they have failed to identify the underlying physical and chemical properties of the reaction environment that dictate these outcomes.

Time resolving the structure of both the isomerizing chromophore and the protein environment about the chromophore during the ultrafast photo-isomerization will have a transformative effect on our ability to understand and potentially direct chemical conversions, but current technology has proven incapable of performing such measurements. A dedicated serial protein nanocrystallography end station with ultrafast optical laser capability would make such experiments possible. Coupling ultrafast protein nanocrystallography with site directed mutagenesis provides the ideal means of controlling and characterizing photo-isomerization dynamics in photoactive proteins. Site directed mutagenesis has been used to influence the photochemistry of bacteriorhodopsin (see Figure II-8) and control chemical reactivity. By coupling the known outcomes with time-resolved protein nanocrystallography, we have the opportunity to measure the time evolution of both the chromophore and the protein nuclear structure with atomistic detail. As highlighted in Section II.B.1, the hard x-rays at LCLS-II combine the high intensity and short pulse length needed to carry out these studies. These measurements will provide sufficient detail to constrain and benchmark quantum chemical dynamics simulations. By combining advanced biochemical synthesis, state of the art theory, and the unique capabilities of femtosecond resolution protein nanocrystallography, we will be able to identify design rules for supramolecular chemistry and potentially transform our ability to transform light to chemical fuel.

Replacing the leaf with inorganic artificial photosynthesis

Photo-Catalysts for Water Oxidation/Splitting and H^+ or CO_2 Reduction.

The rising demand for energy, the diminishing supply of economically feasible oil and natural gas reserves, and the environmental damage caused by the use of these fuels, have highlighted the need for alternative energy sources. Although many alternatives have been proposed, solar

energy is by far the most abundant and inherently clean energy source (Eisenberg and Gray, *Inorg. Chem.* **47**, 1697 (2008); Lewis and Nocera, *Proc. Natl. Acad. Sci. USA* **103**, 15729 (2006). Apart from direct electricity production there is also a strong demand for storable and transportable fuels that can be produced by H^+ or CO_2 reduction. Among the several possible electron sources, water emerges as an ideal substrate because of its ubiquity and energy storage potential. The potential of water as a source of energy is illustrated by this example: a third of the water in an Olympic-size swimming pool split every second would provide the power presently consumed by the earth's population (~ 13 TW). However, effective methods for water splitting have proven elusive, in part due to difficulties in managing the overall four-electron, four-proton redox chemistry. In nature, the water oxidation reaction is accomplished effectively by the oxygen-evolving complex (OEC) in Photosystem II, a multi-subunit membrane protein of green plants, algae, and some cyanobacteria, in which sunlight is used to oxidize water, generating most of the oxygen in the atmosphere (see also Figure II-6 and related section):

$$2H_2O \text{ ------> } O_2 + 4e^- + 4H^+ \qquad (1)$$

$$4e^- + 4H^+ \text{ ------> } 2H_2$$

Both hydrogen reduction and water oxidation reactions are performed in clean and efficient ways by natural enzymes: Hydrogenases and Photosystem II, respectively. Although these enzymes have inspired chemists to synthetically reproduce these reactions, there is still a lack of understanding on how to make artificial systems work. For example, the long-known water splitting reaction over platinum is still not fully understood, despite being widely used for fuel cells or electrolyzer applications. The production of dihydrogen using Pt is also too expensive to be viable on a large scale. Similarly, most water splitting catalysts described so far use rare and expensive metals such as platinum, ruthenium or iridium. The last decade has seen a lot of efforts being focused on the replacement of these expensive materials by non-noble, cheap transition metal catalysts such as manganese, iron, cobalt or nickel. However, few systems have proven to be successful so far as photocatalysts, one of the reasons being our lack of understanding of the mechanism by which two protons form an H-H bond or two water molecules form an O-O bond. A fundamental understanding of the electronic structure and therefore the reactivity of transition states of the photocatalysts is thus critical.

The artificial photosynthetic system needs to perform the same function as that of the plants, but with a robustness and efficiency that is greater than the best-known biological photosynthetic systems. In artificial photosynthesis, either a single material, or two absorbers (see Figure II-9) arranged in a tandem cell format connected electrically in series and current-matched spectrally must at minimum provide the thermodynamically required voltage of 1.23 V to split water, and must provide comparable voltages to reduce CO_2 to methanol or to

methane. In practice, some overpotential will always be present, with a minimal value likely involving operation at a total required voltage of 1.4-1.5 V. Some of the scientific challenges involve the development of earth Earth-abundant, robust materials needed to capture and convert sunlight, as well as the discovery and development of catalysts that drive the conversion of the absorbed solar energy into chemical fuels through key chemical fuel-forming transformations such as production of H_2 and reduced hydrocarbons from CO_2, water, and sunlight. Another essential component is the linking of the catalyst with the photoabsorber to allow efficient transfer of charges across the interface without any significant losses or chemical corrosion processes (see below).

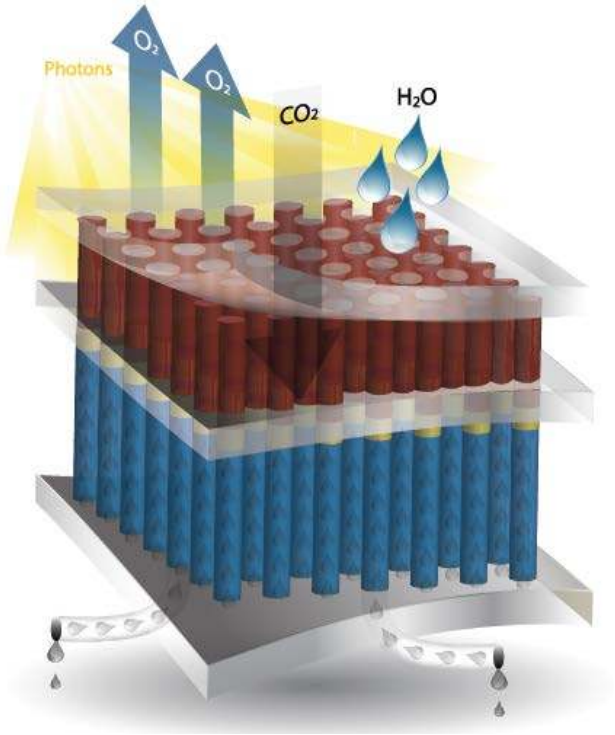

Figure II-9: Schematic of an artificial photosynthesis system with photoabsorbers at both the anode and cathode sides separated by a proton conductive membrane. The photoabsorber is coated with hetereogeneous catalysts providing low overpotentials for the oxidation and reduction of H^+ or CO_2. (JCAP brochure see http://solarfuelshub.org/about-jcap.)

Photo-absorption and Charge Separation. The ability of inorganic complexes to catalyze a wide array of chemical reactions and strongly absorb visible radiation makes them targets for the development of artificial photosynthetic catalysts. Research in artificial photosynthesis uses natural photosynthesis as a template for designing materials and devices to efficiently and cost-effectively convert photons into fuel. Following light absorption, the fast and efficient splitting of light-driven electronic excited states into charge separated electrons and holes represents

the first step in natural photosynthesis. The effective design of an artificial photosynthetic reaction center must incorporate ultrafast charge separation and minimize the perturbation to the nuclear structure induced by the light driven electronic excited state in order to inhibit undesirable photochemical and photophysical relaxation channels. Consequently, the ability to understand and eventually design molecular systems for solar applications requires a detailed understanding of electronic excited state chemical dynamics and the molecular properties that govern them.

Scientists have designed and synthesized a wide variety of inorganic complexes able to generate charge-separated excited states, but ultrafast relaxation of the charge-separated state greatly inhibits performance in many of these systems because a photocatalyst must reside in the excited state to drive a chemical conversion. Controlling the excited state dynamics of inorganic artificial photosynthetic systems, such as the carotene-porphyrin-fullerene triad shown in Figure II-10, first requires the characterization of the time-dependent charge distribution of the electron and hole and how this charge distribution influences the rate of electron excited state relaxation. Soft x-ray spectroscopy, including x-ray absorption, fluorescence and inelastic x-ray scattering, provide a unique set of tools for tracking time-dependent changes in charge distribution of atomic specificity and Ångström resolution.

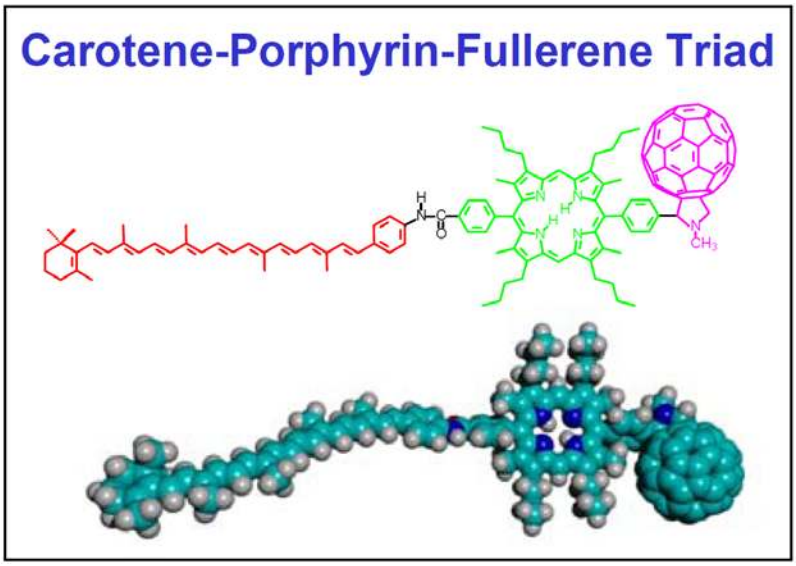

Figure II-10: Artificial photosynthetic triad, where the porphyrin (green) absorbs the light, the carotene (red) functions as the hole acceptor, and the fullerene (pink) acts as the electron acceptor. Ultrafast charge separation leads to efficient conversion of photon energy to chemical potential. Ultrafast x-ray methods provide the ability to map the time-dependent charge density in this triad with atomic spatial and temporal resolution. (DOE report on Basic Research Needs in Solar Energy Conversion).

Understanding, and eventually controlling, molecular conversion of light to electricity and fuel in inorganic chemistry requires understanding the non-adiabatic dynamics of electronic excited states, which in turn requires understanding the coupled motion of electrons and nuclei. This proves more challenging in inorganic chemistry than in organic chemistry because of the myriad energetically accessible electronic spin states and stronger spin-orbit coupling in these systems. Characterizing the excited state dynamics of inorganic artificial photosynthetic systems, requires determining the transition metal spin multiplicity with ultrafast time resolution. The critical role electronic spin plays in the properties of inorganic complexes limits the usefulness of optical spectroscopy for studying excited state relaxation dynamics on the ultrafast time scale where excited state quenching often occurs.

X-ray fluorescence with ultrafast time resolution can characterize the electronic relaxation and spin dynamics of these artificial light harvesting molecules. Simultaneous measurement of x-ray fluorescence and x-ray scattering presents an excellent opportunity to independently characterize the nuclear and electron spin dynamics that influence excited state relaxation in inorganic artificial photosynthetic systems. Self-seeded operations will also enable the simultaneous measurement of resonant inelastic and anomalous elastic x-ray scattering, a tour de force currently unachievable at LCLS. We also have the ability to measure time-dependent changes in the charge distribution with x-ray scattering and soft x-ray spectroscopy. This allows us to investigate the charge separation dynamics with atomic resolution and specificity.

Understanding nature's photoprotection mechanisms

Deoxyribonucleic acid (DNA) is the carrier of our genetic information encoded in alternating base pairs, or nucleobases. Light-induced damage to the base pair sequence can eventually lead to cell mutations resulting in cell death or cancer. The DNA in our skin is continually exposed to light, and the ultraviolet spectral region contains sufficient photon energy to damage DNA by either breaking the DNA double strand or by fragmenting the nucleobases. The nucleobases, like many other heteroaromatic molecules, absorb in the near ultraviolet (UV) region transmitted by the atmosphere. The DNA is therefore exposed to constant photochemical stress by excitation of higher lying electronic states. To avoid photochemical decomposition, the nucleobases have ultrafast pathways for funneling the population from the excited electronic state down into the ground state via non-adiabatic dynamics. Just as for the inorganic complexes involved in artificial photosynthesis, it is important to be able to understand non-adiabatic coupling in nucleobases, although in this case it serves as a photoprotection mechanism rather than a light harvesting mechanism.

Our current understanding of the photoprotection mechanisms in nucleobases is based on extensive theoretical studies paired with ultrafast absorption and valence shell ion/photoelectron spectroscopy. The UV absorption process in all bases involves rapid

dynamics, in which the molecule undergoes a multistep decay process on the timescale of a few hundred femtoseconds to picoseconds. An example of this mechanism for the nucleobase thymine is shown in Figure II-11. The interpretation of the transient states is complicated, and the relaxation from the excited state to the ground state may only be possible with a violation of the Born-Oppenheimer approximation. For pyrimidine nucleobases, the relaxation process is currently a matter of debate. Although all experiments agree regarding time constants (two time constants of about 100 fs and a few ps are measured), simulations even for the isolated molecules have resulted in contradictory interpretations.

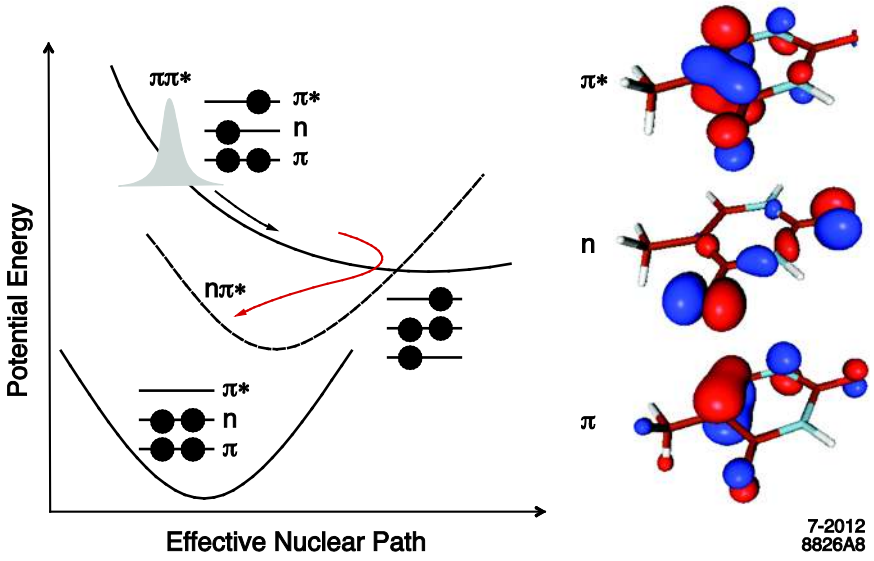

Figure II-11: Suggested photoprotection mechanism of the nucleobase thymine, molecular potential energy surfaces with orbital populations are on the right hand side, the orbital geometries are plotted on the left side. The ultraviolet light promotes an electron from the doubly filled pi orbital into the initially unoccupied π^* state. In this so called $\pi\pi^*$ state, the molecule is highly reactive with its environment. To counteract photoinduced reactions, the electronic energy is funneled into a lower lying $n\pi^*$ state via non-adiabatic dynamics, as given by the red arrow.

LCLS-II provides an opportunity to use ultrafast soft x-ray pulses to learn about nature's photoprotection mechanisms. Extremely short pulses, down to a single femtosecond in duration, provide a precision tool for probing non-BOA dynamics, complementing existing ultrafast spectroscopy methods. This will allow us to follow the electronic change as the nuclei move. In addition, at this timescale a new window opens: we will have the opportunity to follow pure electronic dynamics with motion periods on the order of attoseconds to a few femtoseconds.

Soft x-ray self-seeding at LCLS-II will result in high intensity, monochromatic pulses or two color pulses with a well-determined and stable spectrum from shot to shot. This capability opens the window to stimulated emission and Raman transitions to probe, and possibly also excite, the molecular valence electrons with picometer spatial fidelity.

Experimental work on isolated nucleobases will give us valuable data to evaluate the different theoretical approaches, and possibly tell us how in early bionic ages different nucleobases were selected under strong ultraviolet stress. After these challenges have been mastered, experiments on nucleobases inside DNA or RNA strands could provide insight into the real photoprotection of DNA inside living organisms.

Unique capabilities of LCLS-II

Our goal bound to the scientific examples outlined above is a detailed understanding of photoreactions on the level of individual atoms and electrons inside molecules and the molecular environment. The excitation mimics sunlight and is thus bound to ultrafast lasers in the visible, infrared and ultraviolet spectral range. The probing of the flow of energy after photoexcitation requires accurate space and time information on electronic and nuclear degrees of freedom.

LCLS-II capabilities include essential parameters for science on molecular light conversion. The advantages of LCLS-II parameters in the hard x-ray range are outlined in the scientific case for nanocrystallography. Hard x-rays will play a big role in understanding the influence of the molecular environment on light-driven processes. In addition to the serial nanocrystallography experiments, simultaneous x-ray spectroscopy and diffraction can be employed to study both the atomic and electronic structure changes on time scales ranging from femtoseconds to microseconds. In this 'probe-before-destroy' approach the study of electronic structure changes can be further extended to multiple metal sites by using dispersive x-ray emission spectrometers that cover several energy regions.

Soft x-rays are critical for applications such as artificial photosynthesis and understanding photoprotection. They are a precision tool for probing electronic valence dynamics on a picometer spatial scale, since they act on electrons in tightly bound core states. The core states also have extremely different binding energies, depending on the particular element and its position inside a molecule. This in turn makes soft x-rays an element- and site-selective tool to probe electronic structures of molecules.

The existence of highly monochromatic soft x-ray pulses, made possible by self-seeding at LCLS-II, allows us to tune to particular absorption edges of different elements inside the molecule and identify the change induced by light at many positions in the molecule. Pulse lengths down

to a femtosecond make it possible to explore interactions between electrons and nuclei and observe photoprotection as it happens.

With the advances in self seeding and intensity, we will be able to stimulate the emission of molecules in the soft x-ray spectral range, where fluorescence efficiency is low. This technology will therefore enable emission spectroscopy of gas phase molecules as well as advance knowledge about systems that are already used in spontaneous emission experiments.

It is possible to use two x-ray pulses at different energies to excite valence electrons in synthetic systems, similar to the effect of sunlight in nature. With the capability at LCLS-II for high intensity pairs of soft x-ray pulses with precisely tuned wavelengths, theoretical schemes can become experimental reality.

Required instrument specifications

- Optical laser parameters:
  - Wavelength range from visible to ultraviolet for molecular excitation
  - Pulse energies on the order of 100 μJ
  - Pulse duration on the order of a few femtoseconds for extremely fast systems or tens of femtoseconds for slower dynamics
  - Synchronization on the order of the laser pulse duration
  - Availability of lasers for both soft and hard x-ray instruments

- Hard x-ray parameters:
  - Photon energies extending from 5 keV (for x-ray spectroscopy) up to 18 keV (for x-ray scattering)
  - Pulse energies up to a few mJ per pulse
  - Self-seeded hard x-ray lasing for resonant inelastic scattering measurements and anomalous x-ray scattering
  - Pulse duration from a few femtoseconds to tens of femtoseconds
  - Spectral width from 0.25 eV for RIXS measurements to the full SASE bandwidth for protein crystallography
  - Time synchronization comparable to or better than the pulse duration
  - Focal diameters of a few hundred microns to a few microns, with an emphasis on beam diameters from 10 to 100 microns.

- Soft x-ray parameters:
  - Photon energies from 250 to 1800 eV for broad access of different absorption edges

- Pulse energies up to one mJ
- Pulse duration on the order of few femtoseconds to tens of femtoseconds
- Spectral width of the pulses on the order of 200 meV for absorption spectroscopy
- Seeded operation for small bandwidth operation with monochromator if necessary
- Two color seeded operation for stimulated emission probing creation of electronic wavepackets, jitter on single femtoseconds order, intensities up to 10^{17}-10^{18} W/cm^2
- Focal size on the order of 10 μm and larger

➢ Soft x-ray end station parameters:
- Gas phase sample environment equipped with: differentially pumped gas jet, effusive source, ultrahigh vacuum conditions, ion/electron velocity map imaging spectrometer, high efficiency electron spectrometer, angle resolved electron spectrometer, gas cell with fluorescence and absorption spectrometer
- Liquid phase sample environment equipped with: vacuum compatible liquid jet, transmission x-ray absorption spectrometer, x-ray fluorescence spectrometer
- Scattering detector and larger area photon detectors for gas and liquid experiments as well as optics and diagnostics for VIS/UV laser and x-rays

➢ Hard x-ray end station parameters:
- Liquid phase sample environment equipped with: liquid jet, liquid cell, transmission absorption spectrometer, x-ray fluorescence spectrometer
- Detectors: large area x-ray scattering detector and larger area photon detectors for gas and liquid experiments
- Optics and diagnostics for VIS/UV laser and x-rays

3. Information Technology: Approaching the Size and Speed Limits Set by the Laws of Physics

Our society is based on immediate access to information. We accept information storage and processing as a given and often forget the huge industry and complex science and technology behind providing these services. Moore's Law predicting an exponential increase in data storage density and processing speed requires that bits of magnetic hard drives and power-efficient transistors in our mobile phones and computers approach dimensions of only tens of nanometers. In order to continue along the path of Moore's Law and achieve needed gains in density and speed of data storage and processing, it is necessary to overcome fundamental scientific and technological limits. As present day information densities on hard disk drives are already heading towards the Tbit/in^2 threshold we need to find out if we can store and process *Tbit densities at THz speeds*.

The interactions between atoms, electrons and spins are at the heart of the rich variety of optical, magnetic and transport properties that emerge at nanometer length scales of the order of the mean free path and on the femtosecond timescales needed for electrons to traverse these distances. These are the dimensions of magnetic bits and electronic transistors in tomorrow's generations of information storage devices. Therefore, the search for advanced materials and novel concepts of ultrafast control of electrons and spins on nanoscale dimensions has become a topic of vital importance.

This research addresses several of the DOE Grand Scientific Challenges (*Condensed-Matter and Materials Physics*, Washington, D.C: The National Academies Press, 2010). We want to understand and control the properties of matter that emerge from complex correlations of the atomic or electronic constituents. A “first principles” approach to understanding fundamental properties of materials is conceptually, but deceptively, simple: one needs to solve a single Schrödinger equation to understand and predict the quantum behavior of electrons and ions in solids. Yet while the solutions of the Schrödinger equation, if found exactly, provide exquisite detail on the behavior of individual particles in a system, in many ways the diverse and mysterious phases of matter that emerge in complex materials are fairly ignorant of the fine details describing the behavior of individual ions and electrons. The phenomenon of “emergence” of novel and sometimes exotic phases of complex quantum matter underlies many advanced technology relevant materials. These include high temperature superconductivity, colossal magnetoresistance, multi-ferroics, and other unconventional behavior in transition metal and heavy fermion compounds, for example, that derive from the collective effects of strongly intertwined spin, charge, orbital, and lattice degrees of freedom.

Another important challenge is how to characterize and control matter in states very far from

equilibrium. The evolution of driven systems involves a broad class of phenomena that crosses many scientific disciplines, as the world around us is far from being in static equilibrium. Although non-equilibrium behavior is at the heart of exploring the speed limits of information technology, the fundamental understanding of non-equilibrium behavior in materials science is in its infancy. In equilibrium, the powerful formalism of statistical mechanics serves as a foundation to describe many of the macroscopic phenomena in materials as an aggregate behavior of more than 10^{23} interacting particles. We can use statistical mechanics when a system is thermally and mechanically in balance with its surroundings. However, this covers only a very small subset of the phenomena observed around us. Out of equilibrium we have no such theory to serve as a baseline, and therefore even our vocabulary to describe phenomena is desperately lacking. Often we resort to using equilibrium language by referring to "heating of electrons" or "changing free energy" when driving a system with fields, yet the concepts of temperature or free energy have no direct fundamental meaning in non-equilibrium.

In the following we present several examples of research where the capabilities of LCLS-II will be instrumental in advancing scientific knowledge that can lead to breakthroughs in information technology and related fields. We need to understand how materials properties emerge from correlations of the constituents (atoms, electrons and spins) and learn how to control these properties far from equilibrium. This concept extends beyond advances in magnetic data storage. It will play a crucial role in taking advantage of quantum materials properties, such as metal-to-insulator transitions and even superconductivity, to enhance future devices. Transient states displaying materials properties not found in thermal equilibrium may be used for novel forms of quantum computing performed during the lifetime of such states.

The unique capabilities of a fully instrumented LCLS-II will not only provide more photons than the present LCLS, but LCLS-II will more importantly enable a new quality of XFEL radiation – nearly transform limited, polarized pulses with the option of multiple pulses separated in energy and time. Such pulses, enabled by self-seeding, together with a large photon degeneracy parameter, i.e. the number of identical, simultaneously present photons in the sample, will ultimately enable the development of new research tools, such as the use of non-linear x-ray techniques for probing materials properties. The key to the use of non-linear x-ray phenomena in solids is not peak power but the utilization of a large degeneracy parameter (below ~ 10^8) at moderate peak power to avoid sample damage. In such experiments one keeps the majority of atoms in their ground state and avoids population inversion, as done in stimulated Raman scattering. This can be expected to profoundly alter the way we perform XFEL experiments decades from now. The use of seeded electron beams at LCLS-II will also allow unprecedented control of x-ray energy, intensity, and pulse length, enabling the destruction-free imaging of functional materials on the few-nm length scale. The combination

of two or more pulses that have variable delay and color will extend the non-linear tools readily available at optical wavelengths into the x-ray region with atomic and chemical specificity and the ability to measure energy-wavevector dispersions. Full polarization control will allow us to follow the evolution of emerging charge, spin and orbital order. Finally, the seeded beam of LCLS-II will provide a sufficient number of photons per bandwidth for probing inelastic charge, spin and orbital excitations in complex materials. This will enable us for the first time to determine the glue between electrons and spins in emerging transient phases far from equilibrium.

Understanding and controlling properties of magnetic materials

Most information available worldwide is stored magnetically, either readily accessible on modern hard disk drives or archived on magnetic tapes. This fuels the fifty billion dollar per year magnetic storage industry. The low price of hard disk drives implies that this will not significantly change in the future, despite strong efforts in developing solid-state memory applications. The next generation of hard disk drives will require novel magnetic materials. In order to advance knowledge of these materials, we need to understand and be able to manipulate interactions at the atomic level.

In magnetic materials the dominant interaction is magnetic exchange, which establishes long-range ferromagnetic or antiferromagnetic order. On a much lower energy scale, spin-orbit coupling determines the orientation of spins, which need to be oriented perpendicular to the surface of the magnetic disk in order to increase bit density. Control of spin-orbit-induced magnetic anisotropy energies in the meV range represents a significant theoretical and experimental challenge and calls for the design on the atomic level spin engineered materials, such as FePt alloys that possess alternating single atomic layers of Fe and Pt atoms.

Unfortunately, the large magnetic anisotropy induced by mesoscale grains prevents such materials from being magnetically switched by the magnetic fields available in miniaturized write heads. The future of magnetic hard disc drives is therefore believed to be in weakening magnetic anisotropy by heating the bit to close to the magnetic ordering temperature with miniaturized solid state lasers integrated into the write heads. Heating the material 'softens' the magnetic bits before the magnetic field of the read/write head switches the magnetization. A forefront question is whether this technology may be extended by eliminating lithographically produced field-producing coils in magnetic write heads altogether and simply switch the bits by use of optical laser pulses. To make such all-optical magnetic switching a reality we need to better understand the effect of optical pulses on the magnetization on the required nanometer length and sub-picosecond time scale. Only then can we develop suitable nano-engineered materials. The emergence and ultimate control of magnetic order following optical pulses requires the use of x-ray techniques that are capable of probing the system's intrinsic length

and time scales. LCLS-II is poised to enable research that could make all-optical switching a reality.

Controlling complex materials far from equilibrium

Of course, devices have to operate extremely fast. Current CPUs employ GHz frequencies and modern fiber-optic communication operates at even higher frequencies. If magnetic bits are switched quickly or transistors operate at very high frequencies, the materials processes are controlled by driving the system far away from equilibrium. Ultimately, the device performance is limited by the motions of electrons and spins that happen on the femtosecond time scale. It is clear that characterizing and controlling materials far away from equilibrium requires observing electron, spin and lattice dynamics on nanometer length scales. This challenge can only be overcome using XFEL radiation. Current experiments at LCLS-I lead the way. However, only the seeded beam available at LCLS-II will provide controlled intensity, pulse length and stability to allow damage-free access to the space-time dimensions needed to understand the flow of energy and angular momentum in information processing and storage. This can be expected to result in novel opportunities for basic research that in the spirit of the giant magneto-resistance discovery (Nobel Prize 2007) are likely to impact information technology.

Understanding energy flow on the nanoscale may allow us to create new technologies with decreased energy consumption. Developing spin based information technology applications requires us to understand the flow of angular momentum between various reservoirs such as spins, electrons (in form of orbital angular momentum) and the lattice. Figure II-12 illustrates our current understanding of non-equilibrium processes following ultrafast laser excitation of ferromagnetic metals. The simplest view is that of quasi-equilibrium steps involving thermalization of electronic, spin and phonon reservoirs at different times. This flow of energy between various degrees of freedom of the solid-state system is accompanied by angular momentum exchange governed by the magnetic interactions. The strongest is the magnetic exchange interaction. Its strength of typically up to ~1eV translates into relaxation times below ~10fs. The surprising outcome of recent experiments using femtosecond soft x-ray pulses is a very different magnetization dynamics of magnetic sub-systems (Ni and Fe in Figure II-12). These processes are currently discussed in terms of angular momentum transfer via spin currents. The non-locality of magnetization dynamics induced by such nanoscale spin transport requires corroboration using coherent imaging techniques at LCLS-II.

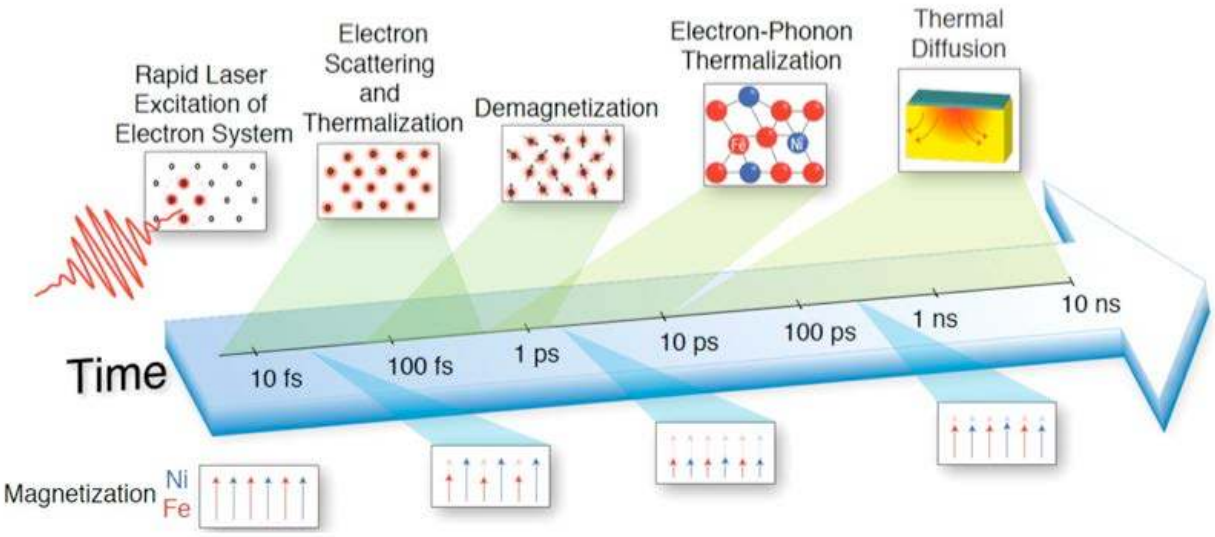

Figure II-12: Illustration of the laser-heating induced flow of energy from electrons to spins and ultimately to the lattice. This is accompanied by angular momentum exchange between different magnetic sub-systems. (from S. Mathias et al., *PNAS* **1094792** (2012))

All-optical switching

In contrast to the incoherent electron and spin dynamics discussed above, there are growing indications that spin excitations can be triggered coherently, allowing an even faster transfer of information. The writing of magnetic bits has successfully been demonstrated using circularly polarized optical laser pulses and is even patented, emphasizing its potential importance for the next generation of data storage devices (C.D. Stanciu, et al., *Phys. Rev. Lett*. **99**, 047601 (2007)). For this to become reality, all-optical switching has to be demonstrated at sub-100nm length scales and on materials where the written magnetic patterns remain stable. This requires investigating new materials that combine the magnetic hardness required for high-density recording with optical switchability.

One possible avenue toward all-optical switching is using the topological protection of certain magnetic structures (J. Wu, et al., *Nature Physics* **7**, 303 (2011)). Topological constraints eliminate certain scattering mechanisms, effectively making the generated structures more stable. One of the simplest magnetic topologies is that of a vortex, as shown in Figure II-13.

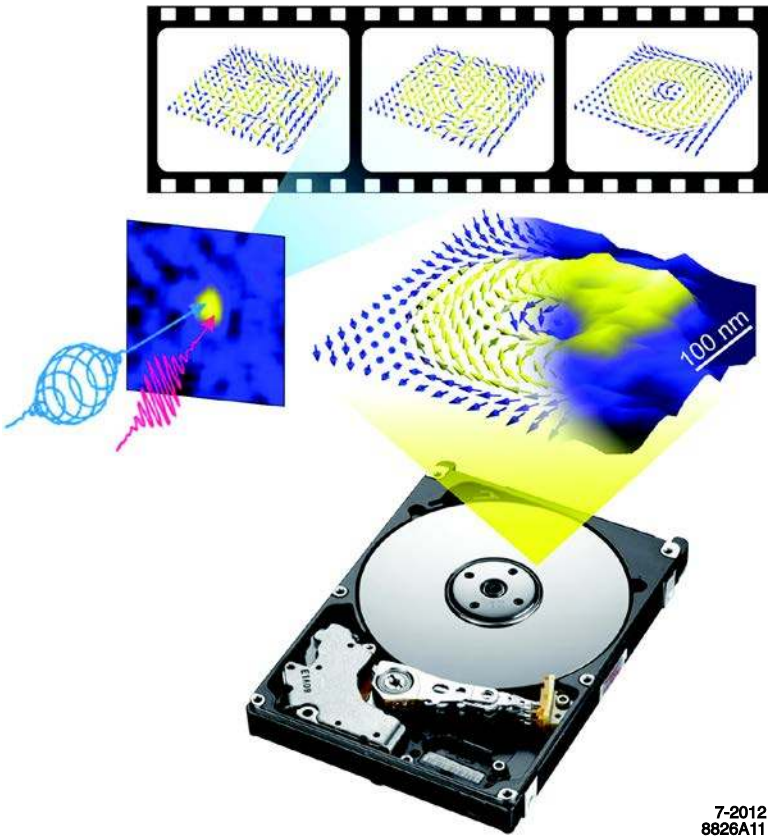

Figure II-13: Illustration how topological magnetic structures may represent magnetic bits on future hard disk drives (figure courtesy T. Rasing, University Nijmegen).

The generation of such magnetic structures is currently uncharted territory. It requires stroboscopic x-ray characterization combining peak brilliance, polarization control, nanometer spatial and femtosecond temporal resolution that will only be available at LCLS-II. The seeded stable, short, intense and fully coherent x-ray pulses from LCLS-II will provide a unique opportunity for imaging nanometer scale objects undergoing ultrafast, often non-repetitive, dynamical processes. Multiple images can be combined to produce a "molecular movie" to address how complex structures evolve from simpler materials. LCLS-I has pioneered the use of single shot x-ray imaging and established damage thresholds for electronic, magnetic and structural sample degradation (T. Wang, et al. *Phys Rev. Lett.* **108**, 267403 (2012)). The intensity stability of seeded beams at LCLS-II will be vital to reach the ultimate few-nm spatial resolution and still remain consistently below those damage thresholds.

Quantum materials: the semiconductor technology of the future?

One of the central issues in modern condensed matter physics research is understanding the novel quantum states emergent in complex materials in which spin, charge, lattice and orbital degrees of freedom are strongly intertwined. The coupled degrees of freedom can partition a material into electronically distinct domains that experience temporal and spatial fluctuations

over many time and length scales. These fluctuations reflect the competition between different symmetry-broken ground states in emergent matter, such as charge and spin stripes in transition metal oxides, electronic spatial inhomogeneity and superconductivity in high T_c cuprates, and ferroelectricity and magnetism in multi-ferroic compounds. The dynamics of spin, charge, lattice and orbital degrees of freedom are inherently complex, particular near phase transitions where symmetry-breaking occurs.

It is clear that in order to describe non-equilibrium behavior and the path towards emergence in complex materials, a more precise and correct vocabulary is needed. Several central questions need to be addressed:

- Can we disentangle intertwined degrees of freedom in the time domain to help us understand emergent phenomenon?
- Can we find new pathways to manipulate, induce and control the properties of emergent novel quantum states in photo-induced non-equilibrium states?
- What is the new paradigm for describing non-equilibrium spectroscopy?
- How do we measure low energy collective excitations that bear the hallmark of novel states and lead us into deeper understanding of emergence?

First steps have been taken to answer these questions at LCLS-I (W. S. Lee, et al., *Nature Commun*. **3**, 838 (2012)). For example, time-resolved elastic resonant soft x-ray scattering has enabled novel insight into the quasi-static evolution of charge, spin and orbital order. LCLS-II will enable the development of new experimental capabilities such as time-resolved *inelastic* resonant x-ray scattering to probe the nature of low-energy charge, spin and orbital excitations in emergent phases. These capabilities will bring to the scientific community entirely new approaches for understanding complexity in broad classes of energy-relevant materials.

Utilizing the spectacular electronic and magnetic properties of quantum materials in technological applications is expected to open up possibilities for new classes of ultrafast electronic devices. The potential impact on society is difficult to predict, but it may be as significant as the development of the transistor, which lead to the semiconductor resolution 50 years ago. In the following we mention two promising applications.

The first example is depicted in Figure II-14, illustrating the hypothetical response of atomically engineered hybrid structures of multiferroic and ferromagnetic layers to a pulsed electric field. The ferromagnetic layer switches magnetization direction when the electric polarization of the multiferroic layer is changed by applying an electric field. This provides a novel way of switching magnetic bits without the need for dissipating electric currents.

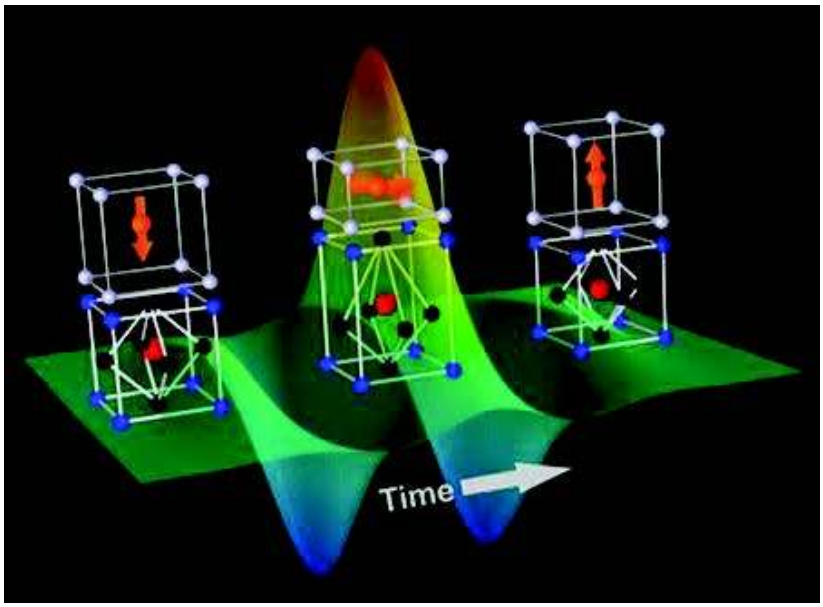

Figure II-14: Schematic of the influence of electric field induced polarization switching in a multiferroic bottom layer on the magnetic state of the top layer. Intense electric field pulses mimic for sub-ps durations the fields typically applied in devices during switching. (figure courtesy A. Lindenberg)

First experiments performed recently at LCLS-I show great promise in detecting coupled charge, spin and lattice motion in bulk multiferroics in the time domain (S. Johnson, ETH Zurich, private communication, 2012). It is more important to probe the interface properties of these heterostructures, where the intense and stable seeded beams at LCLS-II provide an advantage. Such studies will utilize the whole suite of facilities at LCLS-II ranging from hard x-rays probing atomic motion to soft x-rays with variable polarization to disentangle charge, spin and orbital contributions to the switching process.

The second application explores advances in low power electronics made possible by the response of quantum materials to external electro-magnetic stimuli (see Z. Yang, et al., *Annu. Rev*. *Mater. Res.* **41**, 337 (2011)). Figure II-15 illustrates how combining nanotechnology with quantum materials displaying metal-insulator transitions in applied electric fields can form a novel type of field effect transistor without dissipative leakage currents.

Single cycle THz pulses with frequency well below the lowest phonon frequencies can selectively trigger an electronic response in the time domain (M. Liu, et al., *Nature* **487**, 345 (2012)). LCLS-II will enable us to follow the temporal changes in the electronic gap with inelastic resonant x-ray scattering. This will not only establish speed limits for devices but also serve to disentangle the microscopic processes.

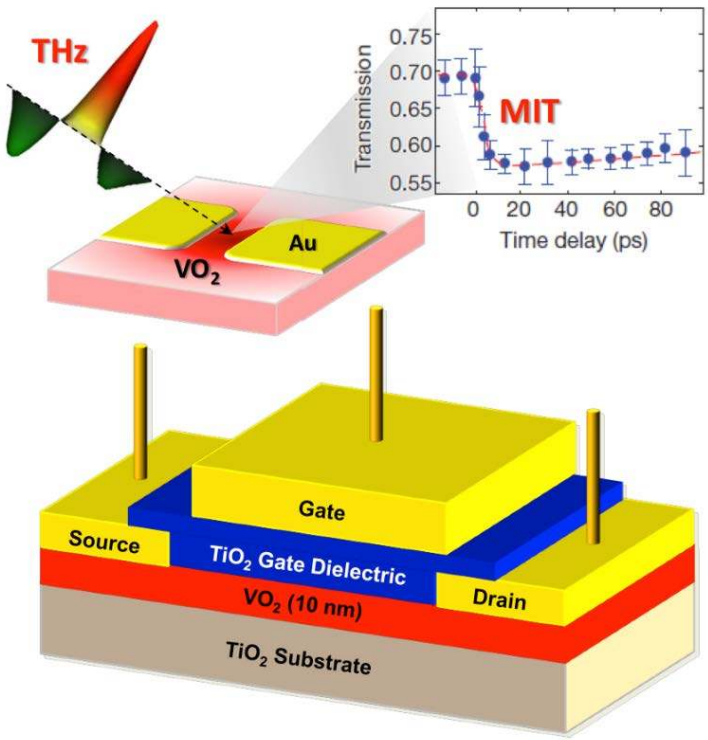

Figure II-15: Vision of a future field effect transistor where leakage currents are avoided by a correlated electron insulator that becomes metallic in an applied electric field. Liu et al. reported the first indication that the bandgap of VO_2 films is affected by ~1 MV/cm THz pulses (Liu et al. *Nature* **487**, 345 (2012)).

LCLS-II will enable the science described above by providing access to the inelastic x-ray spectrum of low-energy (meV to eV) excitations in solids. Understanding the low-energy excitation spectrum of systems is of fundamental importance because the ground state of a system is determined by the minimum energy associated with all low lying states, which determines the function of a system. Conventional resonant inelastic x-ray scattering (RIXS) has been impeded by the small x-ray scattering cross section, which in the soft x-ray region is about a factor of 10^3-10^4 smaller than the x-ray absorption cross section. Stimulated processes involve the cooperative act of photons on a timescale shorter than the Auger decay time (a few fs). Therefore, stimulated RIXS suppresses or eliminates the non-radiative Auger decay in favor of radiative decay and increases the scattered signal by orders of magnitude.

LCLS-II will enable stimulated RIXS in an optimized two beam geometry, as illustrated in Figure II-16. As mentioned earlier, stimulated RIXS or stimulated x-ray resonant Raman scattering does not require that the pump pulse creates a population inversion in the sample so that both pulses will typically have fluences that are well below the sample damage threshold.

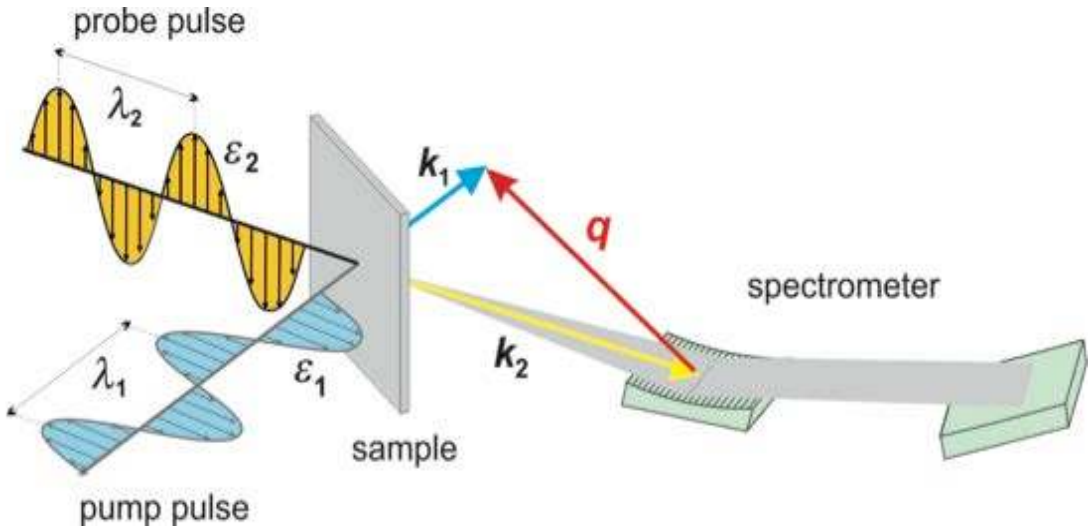

Figure II-16: Illustration of two beam stimulated x-ray Raman scattering. The pump pulse excites the sample while the probe pulse stimulates core hole decays. This requires that sufficient photons of the two beams are in the sample simultaneously, i.e. within the Auger decay time of the core hole (of order of 1-2 fs). This is only possible with x-ray lasers.

Stimulated RIXS will enhance the small radiative signal which would follow the pump pulse excitation by manipulating the intermediate state by means of suitable "stimulating photons" delivered by the probe pulse. Such photons need to have the right energy and polarization to assist spontaneous scattering events by driving a radiative transition from the intermediate core hole state to the final state before the non-radiative Auger decay sets in. The stimulated or cloned photons will emerge from the sample in the direction of the photons that induce the stimulated decay. This is achieved by beam splitting and delay, such that one beam with wavelength λ_1 and wavevector $\boldsymbol{k}_1$ excites while a second beam with wavelength λ_2 and wavevector $\boldsymbol{k}_2$ stimulates (see Figure II-16). This two beam geometry leads to dramatic (of order 10^6) increases in the momentum-dependent signal, combining the gain through suppression of the Auger decay with the gain in solid angle achieved by directing all stimulated photons into the detector. It can be shown by comparison of the absorption and scattering cross sections that *resonant* soft x-ray Raman scattering has the same stimulated cross section as *non-resonant* optical Raman scattering.

LCLS-II will complement these studies of electronic and spin excitations described above with access to lattice dynamics in the hard x-ray range. The possibility of taking quasi-static snapshots of lattice rearrangements during electronically-driven phase transitions has been described in Figures II-13 and II-14. Hard x-ray self- seeding at LCLS-II will dramatically enhance the sensitivity to even minute lattice changes. This will enable diffuse x-ray scattering studies of

transiently excited phonon modes throughout the Brillouin zone. Figure II-17 demonstrates how the excitation of coherent phonon oscillations enables extraction of phonon energies and thus a complete characterization. The combined LCLS II soft and hard x-ray capabilities offer the intriguing aspect of exploring all relevant aspects of electron, spin and lattice coupling directly in the time domain, especially for strongly out-of-equilibrium states that are thought to promote novel information technology applications.

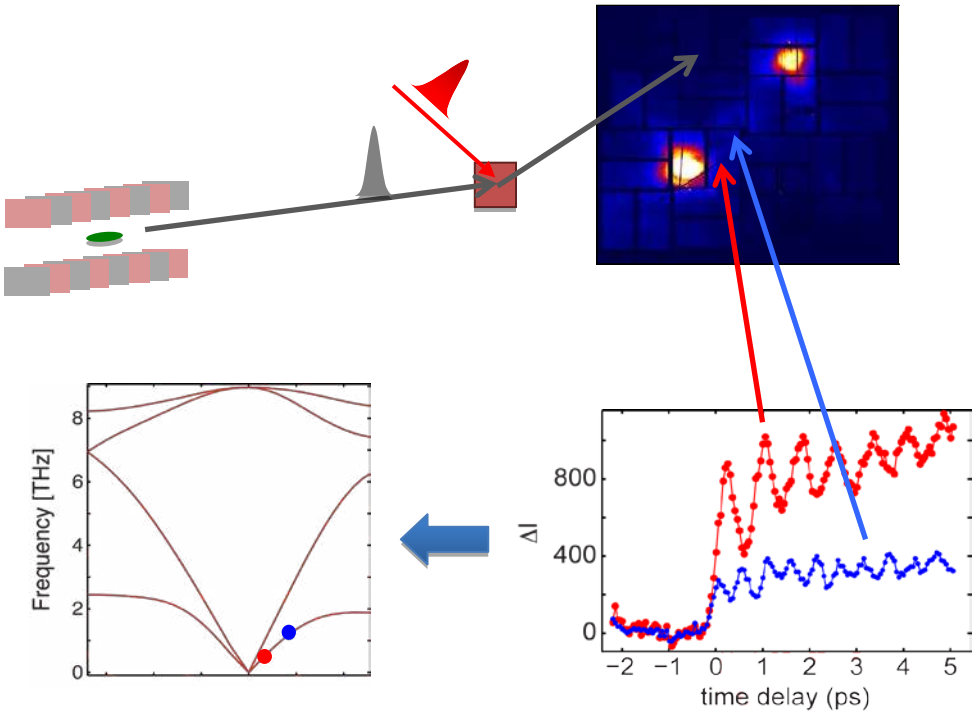

Figure II-17: Lattice distortions due to phonon modes contribute to the diffuse x-ray scattering yield between lattice Bragg peaks. LCLS allows probing of the phonon energies via coherent oscillations of the diffuse scattering intensity in optical pump – x-ray probe experiments as recently observed by M. Trigo et al. (unpublished).

Towards x-ray visualization of information transfer in molecular electronics

Since the smallest dimension of devices is the molecular length scale, the field of molecular electronics, focused on electrical transport through single molecules, may play an important role in the future of information processing. The exciton, an electron-hole pair that can move through solids as a unit, can act as a powerful quantum particle for transporting energy and information. Integrating molecules into devices requires a microscopic understanding of the injection of spin-polarized charge carriers, their excitonic motion within the molecule, and charge separation and transfer to other molecules.

The critical attributes of excitons have been exploited in a wide array of applications beyond information technology, including quantum computing, opto-electronics, and photovoltaics. In solar energy conversion, excitonic motion and ultimately charge separation into electrons and holes on different molecules has to occur rapidly to avoid recombination that would otherwise diminish device performance. Just imagine the new level of insight we could obtain if we were able to microscopically visualize in real time the complex charge motion within a molecule following the initial excitation step. This is one of the grand challenges limiting the efficiency of organic photovoltaic devices and their ability to provide low-cost energy.

By generating multi-exciton states in quantum confined systems where the size and shape and of the material can be controlled, we will be able to both control and observe the electronic evolution. These molecular building blocks can also be assembled and patterned into arrays to determine the mechanisms for quantum information transport and decoherence. The frequency and phase of the excitons report on the energy and information content of the system, making multi-dimensional correlation spectroscopy an optimal monitor of the time evolution of multi-exciton systems.

These processes can ideally be probed using seeded LCLS-II x-ray pulses. Such research will open up the field of non-linear x-ray spectroscopy. A two-color experiment, as shown schematically in Figure II-18, could probe intra-site electronic correlations, i.e. transport, in the time domain, similarly to present-day all-optical four wave mixing experiments with table-top femtosecond lasers.

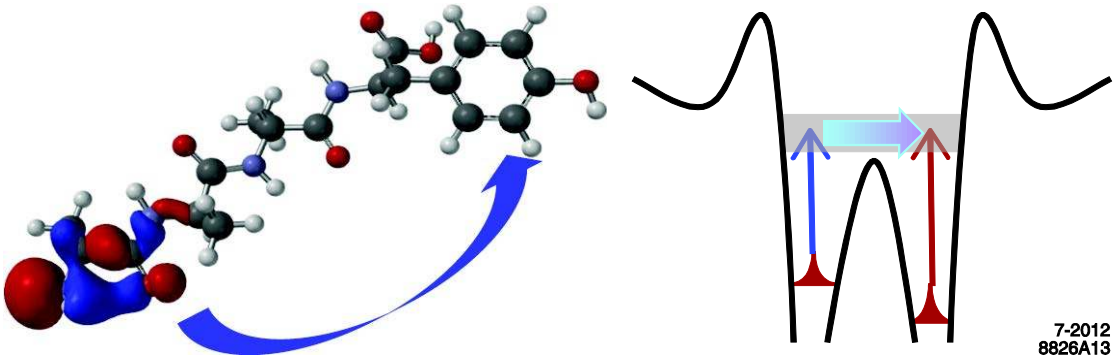

Figure II-18: X-ray spectroscopy of charge transport in molecules (left panel) can be expected to revolutionize molecular electronics. Multi-dimensional optical spectroscopy has been developed as a unique tool to probe the responsible electronic interactions. LCLS-II will enable transfer of these non-linear optical techniques into the x-ray regime (right panel). LCLS-I has already resulted in several demonstrations of non-linear x-ray science investigating atoms and molecules. The seeded nature of LCLS-II beams will enable element and orbital specific probes of ultrafast charge dynamics on ultra short length scales transforming the way we perform spectroscopy on a wide variety of materials.

Coherent imaging requirements

LCLS-II will be in a unique position to probe the femtosecond motion of electrons and spins at nanometer lengths via resonant coherent imaging. Since it is important to provide sufficient intensity for imaging while avoiding damage to the sample, the conditions for the onset of damage serve as a guide to the ultimately achievable resolution at LCLS-II. Full x-ray polarization control with circular polarization may enable ultrafast movies of electrons in functional materials. The following features are required for coherent imaging experiments.

- X-ray energy up to 1.8 keV tuned to absorption edges of magnetic elements
- Self-seeded beams for energy and intensity stability
- Narrow bandwidth (5000 resolving power) for coherent diffraction imaging mainly using soft x-rays
- Full polarization control for soft x-rays
- Timing to VIS-UV laser pulses on the order of 10s of fs, done either by active locking or by single shot timing tool
- Imaging detectors covering large solid angles to reach <10nm spatial resolution

Requirements for spectroscopic studies of emerging order

The wide range of available x-ray energies at LCLS-II offers unique opportunities for studying and controlling emergent charge, spin and orbital order. Hard x-rays typically probe atomic rearrangements, while soft x-rays allow access to transition metal L-edges where polarization control can separate electronic and spin degrees of freedom. A key feature is the synchronization to a THz source that allows peak electric fields of the order of 0.1GV/m. Such fields are typical for modern devices such as field effect transistors where voltages ~1V are applied across device dimensions of ~10nm. LCLS-II will complement elastic x-ray scattering following the evolution of excited states in real time with inelastic scattering that will simultaneously probe the relevant electronic, spin and lattice interactions as the states evolve. The pulsed nature of LCLS-II will enable pairing hard x-ray inelastic scattering probes of excited states with novel sample environments, providing extreme conditions such as high pressure or high pulsed magnetic fields. These studies require the following instrumentation.

- Narrow bandwidth (5000 resolution) for elastic and inelastic resonant soft x-ray diffraction and off-resonant elastic and inelastic hard x-ray scattering
- Full polarization control for soft x-rays
- Synchronized THz source
- Resonant elastic and inelastic soft x-ray scattering end stations

Also, as discussed in Appendix B, such studies would benefit from a hard x-ray inelastic scattering spectrometer for extreme sample environments.

Novel spectroscopy and scattering

Compared to other existing and future XFELs, LCLS-II has the unique advantage of significantly higher x-ray peak power. LCLS-II will be able to generate high enough peak power to drive stimulated processes, with pulse lengths approaching core-hole lifetimes. This would allow scientists to more readily develop and implement novel stimulated inelastic x-ray scattering techniques that could significantly enhance the potential of conventional, spontaneous inelastic scattering. In analogy to optical lasers, the development of such techniques can be done in the time domain with transient grating spectroscopy or the frequency domain using inelastic scattering with two x-ray colors or polarizations. This requires the development of a stimulated scattering 'toolbox' consisting of x-ray pulse splitters, polarizers and optics similar to what is now routinely available in the optical spectral region. In addition, two-color seeding schemes with a time delay between the pulses need to be developed in both hard and soft x-ray regions.

III. Proposed LCLS-II Instrumentation

A. Overview of LCLS-II Instrumentation

By providing two new XFEL beams, LCLS-II will triple the total amount of user beam time at the LCLS. The LCLS-II project itself will include one x-ray instrument, termed the "High Intensity Instrument" (HII), in the soft x-ray photon energy range. This instrument which is here renamed to SX-Ultra (see Figure III-2 below) will provide a focused non-monochromatic beam for high field atomic physics and imaging experiments. Additional x-ray instruments are needed to productively take advantage of the added beam time capacity. In the LCLS-II experimental hall there is space for up to six instruments.

History

In December 2011, a working group was formed to develop concepts for LCLS-II x-ray instruments. The group included LCLS instrument scientists, the leads of the LCLS laser, detector and engineering groups as well as scientists from the SLAC Photon Science Directorate. The group considered what has been successful at LCLS and what has not. Layouts were developed for different scenarios with between four and six instruments. The optimal number of instruments per undulator source was considered, taking into account LCLS beam time scheduling, the ability to rapidly switching x-ray beams between stations, simultaneous x-ray operation of several stations, and space in the existing near and far experimental halls and the new LCLS-II hall. These factors suggest that it is desirable to have three user stations per undulator. In the fully built out LCLS 2025 facility, three hard x-ray undulators will serve a total of nine hard x-ray stations, and one soft x-ray undulator will serve three soft x-ray stations. Our LCLS-II instrumentation scope presented below is consistent with this vision.

On March 19-22, 2012, we held the LCLS-II New Instruments Workshops at SLAC. An international group of 154 people attended. The workshop charge asked to:

> Define LCLS science opportunities created by the enhanced capabilities and capacity of LCLS-II with focus on: 1. biological sciences, 2. materials science, 3. chemical sciences, and 4. atomic, molecular and optical physics. In each of the four identified science areas establish a priority list of desired user experiments including the ability of placing samples in the beam, preparing the desired state of the sample (e.g. by optical, THz methods), synchronizing the transient states with the x-ray pulses and the required detectors for the x-ray and particle signals from the sample. Identify important x-ray beam parameters to address the envisioned science opportunities, such as photons per pulse, pulse length, 120-Hz-based pulse trains, band width and spectral purity,

polarization, special requirements in transverse (diffraction limited) and longitudinal (transform limited) coherence.

After the workshops we received nineteen 2-page contributions on specific scientific topics and their instrumentation requirements. A report summarizing results of the workshops (http://slac.stanford.edu/pubs/slacreports/reports19/slac-r-993.pdf) served as input for the present white paper.

Figure III-1: Attendees at the LCLS-II New Instruments Workshops

The LCLS-II instrumentation scope and priorities presented below are based on experience with LCLS user operations, feedback from users and discussions held at the workshops. The recent rounds of LCLS proposals, with all but the MEC station ready for user operation, requested time predominantly on the hard x-ray coherent x-ray imaging (CXI) and x-ray pump probe (XPP) and on the soft x-ray AMO and SXR instruments. The LCLS facility plan envisions decommissioning the AMO and SXR instruments and creating a new soft x-ray suite of three instruments in the LCLS-II experimental hall. This strategy is consistent with the above-mentioned plan of three stations per undulator source and the LCLS' emphasis on hard x-rays above 2.5 keV.

Before describing the required facilities, it is useful to define some key terms. The term "beamline" describes an optical transport and manipulation system that delivers x-rays to an "end station" which may be exchangeable. An end station consists of equipment to introduce and manipulate samples, and all necessary detectors and spectrometers to examine particles and x-rays emitted from the sample, and may also incorporate special optics for additional manipulation, such as refocusing of the incident beam. We shall use the term "instrument" to mean a complete user-ready facility that includes a beamline with all required optics and a completely integrated end station.

Proposed instruments

Figure III-2 gives the overall schematic and engineering layouts of the proposed LCLS-II experimental hall and indicates the location of three soft and three hard x-ray stations.

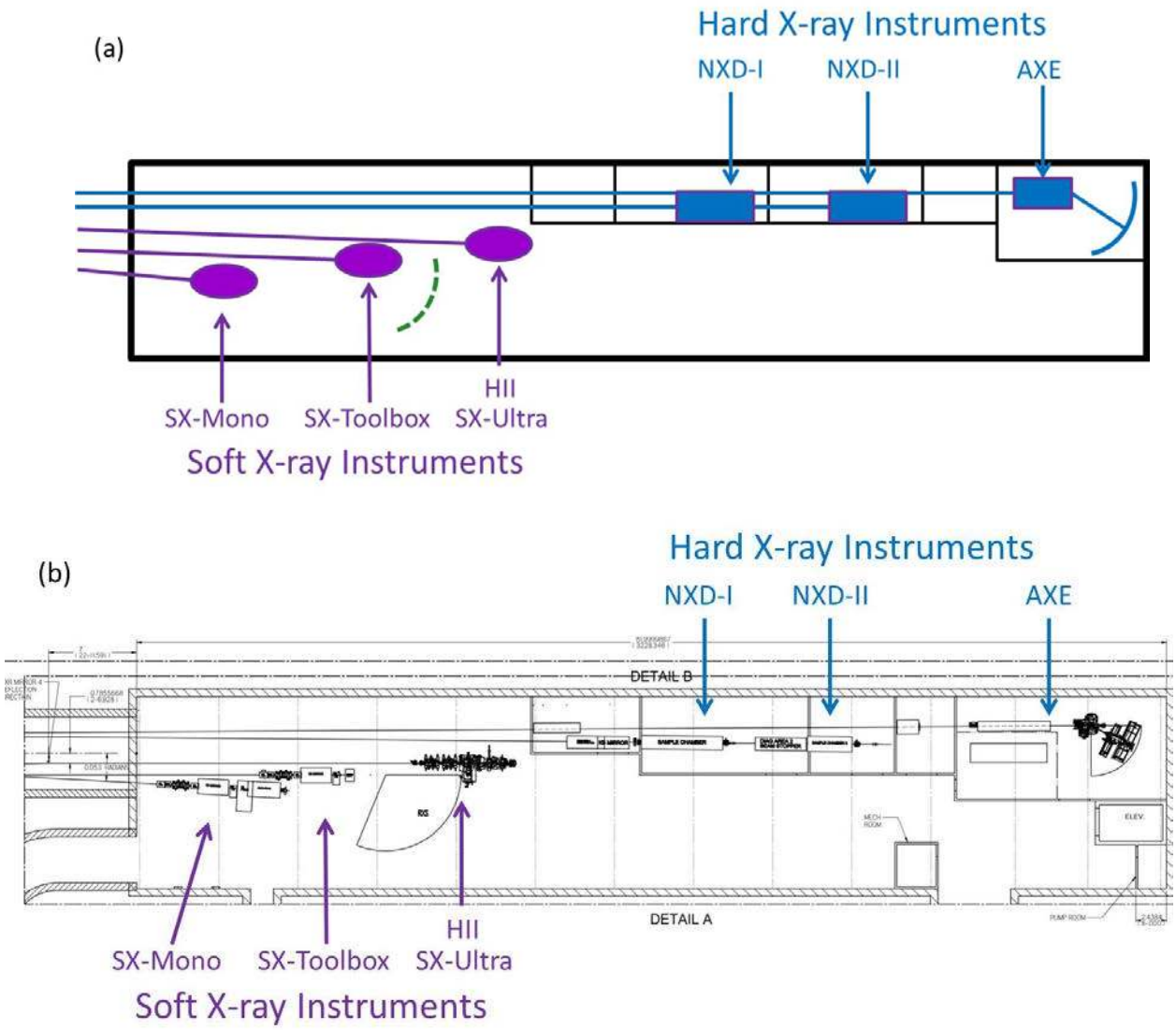

Figure III-2: (a) Schematic and (b) engineering layouts of the x-ray instruments in the LCLS-II Experimental Hall.

The soft x-ray instruments are located at the front end of the hall because of the larger divergence of the soft x-ray compared with hard x-ray radiation. From our experience with soft x-ray operation at LCLS, hutch walls are not required for radiation shielding. The soft x-ray package, serving atomic, molecular and materials science, consists of three instruments: HII, SX-Mono and SX-Toolbox. The HII instrument is part of the LCLS-II scope; however, a new end station incorporating tight focusing optics is included here (SX-Ultra). The SX-Mono instrument,

which will replace the present SXR instrument, contains a grating monochromator and a resonant scattering end station for material science. The SX-Toolbox instrument uses the same monochromator as SX-Mono but has two separate exit slits that form part of an x-ray optical toolbox as illustrated by Figure III-9. A multi-spectroscopy end station for chemical reactivity will be attached to SX-Toolbox. We envision a high resolution resonant inelastic scattering (RIXS) end station as indicated by the green dashed line in Figure III-2 and discussed in Appendix A. The high resolution RIXS end station is not included in the LCLSI-II instrument scope. The soft x-ray instrument suite is designed to accommodate scientific needs in chemistry and materials science, discussed in Sections II.B.2 and II.B.3.

The hard x-ray instruments are located at the far end of the LCLS-II hall. They need to be enclosed within radiation shielding hutches as indicated in Figure III-2. The highest priority instrument overall is for Nanocrystal X-ray Diffraction (NXD) and consists of two experimental stations as described in Section III.B. The front station, NXD-I, is dedicated to accurate structure determinations and the back station, NXD-II, to screening for well diffracting crystals. The NXD Instrument is ideal for protein nanocrystallography, supporting the science case described in Section II.B.1.

The hard x-ray package, described in Section III.D, comprises the Ångstrom X-ray Experiments (AXE) Instrument and serves a variety of hard x-ray spectroscopy and elastic scattering experiments in materials sciences and chemistry. It combines the capabilities of the present X-ray Pump Probe (XPP) and X-ray Correlation Spectroscopy (XCS) instruments. It is envisioned that the present XCS instrument will be converted in the future to hard x-ray inelastic x-ray scattering (IXS) as discussed in Appendix B. The AXE Instrument will tackle science topics such as molecular light conversion, discussed in Section II.B.2, and understanding materials of technological importance, Section II.B.3.

Hard x-ray self-seeding

The LCLS-II scope includes two SASE undulator sources: HXR for hard x-rays and SXR for soft x-rays. The instrumentation packages presented here propose to enhance these undulators for self-seeding, adding monochromators and electron chicanes as well as additional undulator modules for sufficient amplification of the seeded x-ray pulse. While filling the 286-meter long undulator hall with modules would provide full saturation, for this proposal we have chosen a cost-effective undulator configuration which produces one-half the maximum x-ray pulse energy at 2000 eV for soft x-rays and 18 keV for hard x-rays.

The LCLS-II SASE XFEL produces x-ray radiation that is transversely but not longitudinally coherent. The XFEL spectrum and its temporal pulse shape are spiky in their structure since the XFEL relies on shot noise for SASE startup. However, each spike is fully coherent. In contrast,

self-seeding, in principle, creates a single coherent spike of enhanced intensity. It is accomplished by use of two undulators and an x-ray monochromator located between them as shown in Figure III-3. The first undulator operates in the exponential gain regime of a SASE FEL. After the exit of the first undulator, the electron beam is guided through a dispersive bypass (a four-dipole chicane) that smears out the microbunching induced in the first undulator. The SASE output enters the monochromator, which selects a narrow band of radiation as the seed. At the entrance of the second undulator the monochromatic x-ray seed is combined with the electron beam and is amplified to saturation.

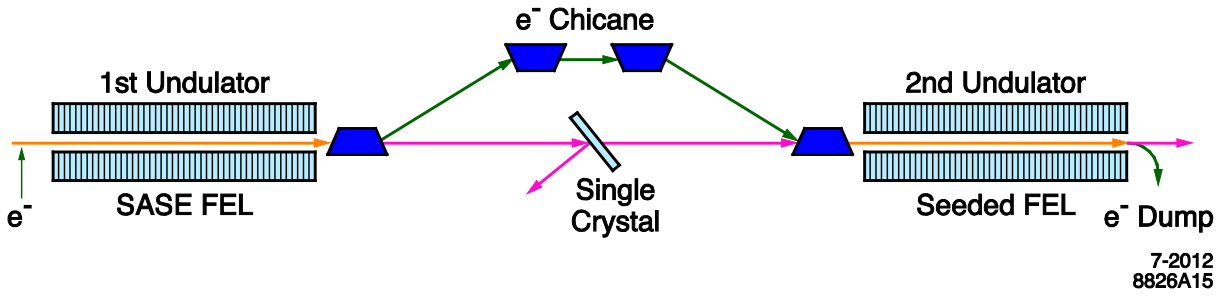

Figure III-3: Schematic of the LCLS(-II) hard x-ray self-seeding FEL, which consists of two undulator systems separated by photon monochromator and electron by-pass chicane.

The hard x-ray self-seeding scheme, illustrated in Figure III-3, delivers a self-seeded FEL beam at the Ångstrom wavelength scale with a factor of about 40 bandwidth reduction, as demonstrated by the experimental data shown in Figure III-4.

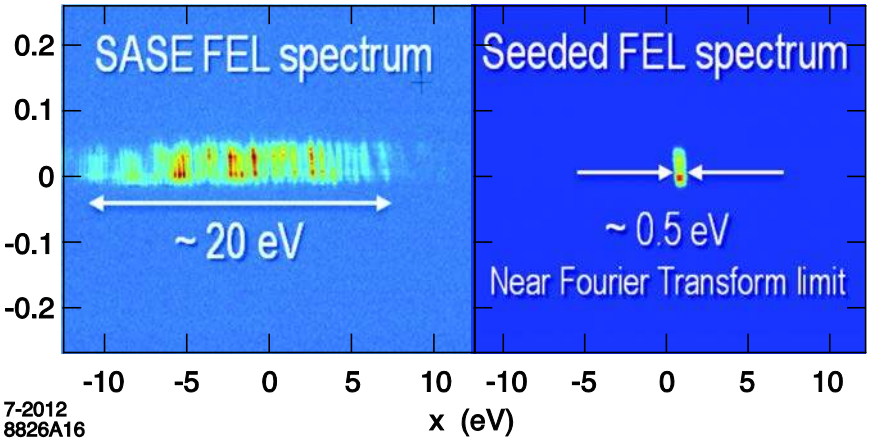

Figure III-4: SASE and Seeded spectra recorded on single shots at the LCLS. The left panel is SASE with 150 pC, 3kA peak current, un-seeded. The FWHM bandwidth of the SASE spectrum is 20 eV (0.2% at 8.3 keV photon energy). The right panel is the seeded beam with the same electron beam parameters. The FWHM bandwidth of the seeded beam is 0.5 eV (5×10^{-5}).

General instrumentation/infrastructure requirements

The LCLS-II x-ray transport optics and diagnostics provide one soft x-ray path and a minimal hard x-ray configuration for commissioning the HXR undulator. The instrumentation packages add soft x-ray offset mirrors for two additional x-ray beam paths and a complete set of hard x-ray optics and diagnostics. The goal of the optics and diagnostics is to fully characterize the x-ray pulses, giving information on the intensity, spectrum, focusing and timing to the experiments on a pulse-by-pulse basis.

Roughly 65% of LCLS-I experiments to date have required an optical laser system to either pump or probe the sample being investigated. Proposed instrument packages include four ultrafast Ti: laser systems for the NXD, AXE, and HII instruments and the SX beamlines. Experience at LCLS-I suggests that each instrument should have its individual laser system located in one of two rooms, increasing reliability and allowing users to easily set up before their scheduled beam time. We will develop a suite of new x-ray detectors through a mixed approach of in-house work at SLAC and outside collaborations. These detectors will have many more pixels than the current detectors at LCLS and have a higher dynamic range in order to enable, for example, structure determination on large molecular complexes at the highest possible resolution.

Prioritized LCLS-II instrumentation packages:

Based on the needs of the scientific community, we have prioritized the instrument packages as listed below. The following sections describe detailed requirements for each instrument.

1. Nanocrystal X-ray Diffraction
2. Soft X-ray
3. Hard X-ray

B. Nanocrystal X-Ray Diffraction Package

Primary scientific opportunity addressed:

- The Biological Cycle of Life: Understanding the Structure and Function of Macromolecular Assemblies

1. Introduction

The use of micron- and sub-micron-sized crystals of protein for structure determination has been an early success for LCLS-I and is expected to continue as a high-demand research area in the coming years, in direct analogy to the evolution of macromolecular crystallography at third-generation x-ray user facilities. The package of instrumentation required to deliver a fully optimized Nanocrystal X-ray Diffraction (NXD) instrument is described in this subsection. This system will provide a purpose-built small-crystal facility at LCLS-II to the general user community. The benefits of a dedicated facility include the opportunity to provide a stable foundation of LCLS-proven components and provide a workhorse for protein structure determination. This instrument complements the CXI instrument at LCLS-I by providing a high-throughput backdrop against which high-risk, extraordinary-outcome research can be performed at the more flexible CXI instrument, which will continue to provide tighter focusing necessary for the work towards single molecule imaging using hard x-rays.

In order to fully utilize the potential of LCLS-II for protein nanocrystallography, the x-ray instrumentation alone is not sufficient. The fully implemented system also requires additional undulator modules beyond the LCLS-II baseline to provide SASE saturation at higher photon energies (up to 16 keV) for molecular systems requiring higher resolution and a larger energy-bandwidth by operating in the "over-saturation" regime of the XFEL. Front-end optics and diagnostics, as well as x-ray beam transport to the instrument, are also included in this package. The optical front-end must be compatible with x-rays up to 16 keV to allow the exploitation of the selenium k-edge, with some margin, for Multi-wavelength Anomalous Dispersion (MAD) phasing and to capture higher-resolution data sets arising from this higher photon energy. Below is a description of the all-encompassing package needed to deliver a fully-functional Nanocrystal X-ray Diffraction system.

2. Package Concept

Most small-crystal protein crystallography experiments at LCLS-I are currently performed using liquid-jet sample delivery systems that constantly replenish the sample at the interaction region. While we anticipate increasingly sample-efficient delivery technologies, we believe that these new technologies will share certain characteristics with the current liquid-jet method. In particular, the beam will continue to be minimally attenuated by the sample delivery system. This is highly desirable, as both the attenuation of the diffraction signal and the undesired scattering from the sample's protective environment, e.g., the buffer in which the sample is delivered in a liquid jet, are minimized.

The transmitted beam, after it passes through the hole in the middle of the 2D diffraction detector, will typically contain close to 10^{11} photons per pulse with a nearly unchanged brightness. We will provide this "spoiled" or "spent" beam to a second end station downstream of the main instrument, in a separate hutch. This concept is beneficial on two key levels. First, the "spent" beam is not simply lost in a beam dump, rather the scheme will provide a way to reuse this beam and increase the capacity of LCLS-II, providing tandem sequential operation of both end stations. Secondly, it has been observed that classical x-ray sources, such as storage rings, are not adequate tools to determine the quality of small crystals or even to predict their diffraction quality at LCLS. The second hutch of the NXD suite will provide access to crystal screening non-invasively and make the use of the primary NXD hutch more efficient.

We call the primary hutch of the NXD suite "NXD-I." Here, the most challenging measurements requiring the highest power density, highest flux and tightest focusing will be performed. We envision that most pump-probe experiments requiring optical laser excitation will occur in the NXD-I and include that system in the NXD-I specification. The secondary instrument, "NXD-II," is located is a completely separate hutch to allow the configuration of and access to the current experiment on either end station with minimal effect on the other. A rendering of the proposed NXD suite is shown in Figure III-5 with, from left to right, front end components, an optics hutch, the NXD-I hutch and the separate NXD-II hutch.

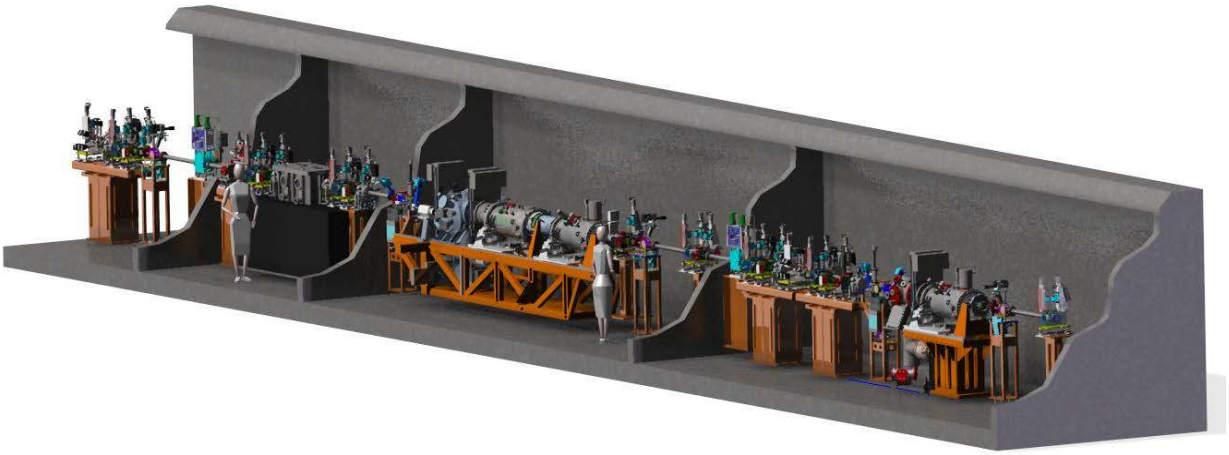

Figure III-5: Rendering of the proposed Nanocrystal X-Ray Diffraction (NXD) suite at LCLS-II showing—from left to right—LCLS-II common optics; an optics hutch containing KB focusing mirrors; the main experimental hutch (NXD-I) with sample environment, detectors and diagnostics; and finally the last hutch that utilizes the refocused beam (NXD-II).

3. Specifications

The highest expected demand for the NXD-I instrument is for the study of small macromolecular crystals in the few-micron to sub-micron range where diffraction will be used to obtain a structure at the highest resolution possible. Therefore, the need for hard x-rays is clear. The higher energy limit available at the NXD instruments must at least reach the selenium K edge to allow MAD phasing, as is typically done at crystallography beamlines at storage ring sources. The energy range must exceed the selenium edge by a margin of at least 2 keV for proper MAD phasing and therefore a cutoff energy of 16 keV is desired, which has the benefit of allowing higher resolution measurements.

The 16 keV cutoff defines a maximum mirror angle—which, in conjunction with the maximum reasonable mirror length afforded by current technology, limits the lowest usable photon energy to that at which the beam overfills the mirror apertures. We expect 6 keV to be the lowest useable energy, although lower energies will still be transmitted with less efficiency. Table III-1 lists the beam and instrument parameters for both NXD-I and NXD-II.

Table III-1: Specifications for nanocrystallography instruments

	NXD-I	NXD-II
Photon energy range	6 - 16 keV	6 - 16 keV
Bandwidth	As wide as possible for SASE Well-defined and controlled with seeding	As wide as possible for SASE Well-defined and controlled with seeding
Optics	Bendable KB mirrors	Be lenses
Spot size	0.5 – 3 μm	1 – 10 μm
Monochromator	No	No
Sample environment	Flexible environmental chamber	Flexible environmental chamber
Detector needs	4000x4000 pixels 100 μm pixel size 10,000 dynamic range	4000x4000 pixels 100 μm pixel size 10,000 dynamic range
Laser pulse duration	50 – 300 ns	50 – 300 ns

4. Source Enhancements

Additional undulators for higher photon energies

In order to achieve the desired performance, which includes high pulse-intensity up to 16 keV and an energy bandwidth as wide as possible, we will install additional undulator modules beyond the LCLS-II baseline. A total of 6 additional modules will allow SASE saturation up to 16 keV and also allow operation in the over-saturation regime of the SASE process, which will lead to an increased energy bandwidth. This increased bandwidth may allow less partial Bragg integration with a single LCLS-II pulse, reduce the time needed for data collection, and—perhaps most importantly—minimize the sample consumed to collect a full data set.

Hard x-ray self-seeding and TW production

The NXD instrumentation package will include hard x-ray self-seeding (see Figure III-3) and additional undulator modules to bring the seeded XFEL to saturation. Although the saturation power for the seeded XFEL is expected to be about the same as the SASE power at 20-50 GW, the temporal uniformity of the seeded pulse allows for a more aggressive post-saturation undulator taper with the potential to generate up to 1 TW power. The path to TW pulses involves additional undulator modules at a later date.

5. Front End and Beam Transport Systems

As the first envisioned instrument on the hard x-ray line of LCLS-II, the NXD package must include a full front end system and beam transport from the undulator to the end station. In the long term, when other instruments are added to the LCLS-II hard x-ray line, the front end optics and diagnostics will become shared devices among all instruments. The proposed front

end and beam transport is envisioned from the start to include all devices needed to eventually accommodate the fully built-out LCLS-II and the necessary mirrors, and beam pipes to deliver the beam to another future hard x-ray station is included. The following devices are required for the front end and beam transport systems:

- Mirror distribution system
- Single shot spectrometer
- Beam imagers
- Intensity monitors
- Wave front monitor
- Pulse shutter
- Attenuator system
- Timing distribution system

6. NXD-I Instrument

Expected use and impact of the instrument

The NXD-I system, which also includes the optics hutch, is expected to be the main workhorse of the NXD suite. Challenging experiments on novel protein structures, as well as dynamic studies of molecular structure in systems such as photosystem II, will be performed in NXD-I. The smallest focus of the NXD system will be available with the full, undisturbed high intensity beam. Therefore, this is the hutch where most of the work with the smallest crystals will take place, allowing the determination of novel structures of molecules that resist the formation of large crystals. The NXD-I instrument will also allow the study of small crystals at room temperature, permitting the exploration of more native structures and multiple conformations, as is the case for some molecular systems. These measurements are not currently possible at a third-generation source where cryo-cooling of the crystals is required. The NXD-I instrument will also be the ideal location for dynamics studies of reactions using fast mixing techniques, again at room temperature.

The NXD-I instrument is designed to provide a flexible focus in the range of 0.5 to 3 μm, which will allow both sub-micron and few-micron crystals to be studied. Based on early experience at LCLS-I, this range seems to be ideal for fulfilling user demand. A larger beam size will be possible by placing the sample out of the x-ray focus if desired. The system allows sufficient flexibility in the position of the sample and detector to provide a very flexible beam size at the sample.

The NXD-I system is conceptually simple and builds upon demonstrated components already used at LCLS-I, but geared toward a more dedicated and robust crystallography system. The following key components are proposed.

Optics hutch

An optics hutch is proposed as a narrow and rarely accessed area, which should be fully-enclosed with good temperature control. This will allow Kirkpatrick-Baez (KB) mirrors and other devices to be located in a separate room and ensure their stable operation.

Kirkpatrick-Baez focusing optics

The primary focusing optics, which deliver the beam to the NXD-I station, will be a pair of bendable KB mirrors that will allow a minimum focus of 0.5-1 µm FWHM and a maximum focus of 3-5 µm FWHM when the mirror bending is changed to move the focal plane as far downstream as possible. The mirrors will be located close to the downstream wall of the optics hutch, with the sample chamber capable of being located close to the upstream wall of the main hutch, minimizing the focal length and therefore the focal spot for optimum signal from the smallest crystals. The bendable mirrors will provide flexibility in the focal spot size by varying the focal length. Long, state-of-the-art mirrors are required to reflect up to 16 keV.

Diagnostics and optics

Diagnostics will be placed upstream and downstream of the sample location, allowing them to be removed from the upstream side of the sample in cases where they are found to disturb the beam excessively. In this case, the downstream diagnostics would be used to look at the beam passing through the detector in the NXD-I hutch. Some simple optics are necessary to control the beam profile and intensity. The following set of diagnostics and optics is proposed for the NXD instruments:

- Beam imagers
- Intensity monitors
- Wave front monitor
- Slits
- Reference laser to allow offline alignment of the experiments

Sample environments

The sample chamber and detector chambers will be mounted on a long stand with rails, allowing the distance between the sample chamber and the KB mirrors to be varied to allow a largest spot of 3-5 µm. Allowing both the sample chamber and the detector chambers to slide downstream will provide a very flexible system, which will allow different focal sizes and different sample-to-detector distances to be used. The use of bendable KB mirrors, which are

expected to be available with suitable figure quality, allows the focal plane to be changed without changing the mirror angles and therefore allows a single beam axis, making a single, large fixed stand possible and simplifying the instrument's implementation. Although fixed targets may be needed both in air and in vacuum, the majority of the experiments are expected to be carried-out in low vacuum and often using liquid jets. Therefore, environmental chambers are preferred to high-vacuum chambers, allowing more flexibility in the sample environment. The chambers should be large enough to accommodate various sample configurations and extra diagnostics such as x-ray emission spectrometers. Other desirable features include easy integration of pump lasers, rapid venting and a cryogoniometer.

Detectors

While the CSPAD detector has proven itself to be adequate for the current crystallographic experiments using CXI at LCLS-I, improved nano-crystallography detectors are required in the future. First, low order Bragg spots arising from the interaction of the LCLS-II x-ray pulse and a micron-sized crystal will saturate the detector. This has deleterious effects upon structure determination by disallowing the absolute determination of structure factors. The new instrument will require a detector that provides a dynamic range exceeding 10^4. Since the scattering signal falls off quickly, a detector that simultaneously also provides single-photon discrimination is needed. A detector that uses self-selecting gains, similar to the KPix circuit chip designed at SLAC, to achieve these specifications is currently under design. Secondly, the lost area due to the CSPAD tiling should be reduced. Active-edge sensors, which were developed at Stanford, and through-silicon vias are being explored to improve the sensitive fill factor. Finally, a 4000 x 4000 pixel array is highly desired to increase the angular acceptance of the detection system, enabling structure determination at the highest possible resolution, even on large molecular complexes.

The primary detectors for NXD-I and NXD-II will need to meet the above requirements, but the secondary detector for low-angle measurements at NXD-I could be much smaller with 2-3 megapixels.

Spectroscopic measurements in combination with diffraction have proven to be valuable at LCLS-I to characterize the electronic state and therefore assess the damage threshold of metal compounds in macromolecules. A spectroscopy detector with high energy resolution is foreseen for such measurements at the NXD instruments. This detector is likely to be used with an energy dispersive device to obtain higher energy resolution using the small pixel size of the detector.

The detectors proposed for the NXD instruments are listed in Table III-2. The HXRD-10K detectors are those required for diffraction measurements. These provide the necessarily large

number of pixels needed for the study of large molecular complexes along with the necessary dynamic range.

Table III-2: Types of detectors needed for the NXD science with their specifications.

Detector	Pixel Size (μm)	Array Size (pixels)	Energy Resolution	Maximum Signal	Energy Range
HXRD-10k	100	16,000,000	1000 eV	80 MeV	4 – 25 keV
HXRD-10k	100	3,000,000	1000 eV	80 MeV	4 – 25 keV
HXRD-100	50	256,000	300 eV	800 keV	2 – 25 keV

Optical laser

A nanosecond optical laser system will be used at the NXD-I instrument with the aim of characterizing the excited state structure of photoactive macromolecules (see timescales in Figure II-6). This system will be a portable, turn-key unit that will couple into the sample chamber.

7. NXD-II Instrument

Expected use and impact of the instrument

The LCLS user community currently lacks a small-crystal screening facility. Such a facility would be of great benefit, particularly due to the observation that third-generation x-ray facilities cannot reliably predict the quality of diffraction patterns observed from a given sample at the LCLS. The proposed downstream end station of the NXD suite (the NXD-II instrument) would provide an ideal opportunity to establish a small-crystal screening facility. The proposed NXD-II system has nearly all of the functionality of the main NXD-I hutch, allowing the transparent switch-over of a sample from the screening facility to the primary crystallography facility in the NXD-I hutch. While we foresee a high user demand for the screening facility, the downstream instrument could also be used for other forward scattering experiments, so long as these do not require the very highest flux density possible at LCLS-II. The NXD-II instrument would, for example, be an ideal location for studying larger crystals, mounted on a support of some kind, at atmospheric pressure and room temperature. Such measurements would be ideal for the common cases of metalloproteins where resolution at a synchrotron is severely limited by radiation damage. The short pulses of LCLS-II could allow higher resolution structural determination on these larger crystals.

The NXD-II instrument will utilize the beam that is left over after passing through the sample in the NXD-I hutch and passing through the holes in the NXD-I detectors. This minimally disturbed beam will then be refocused to the proper plane into the NXD-II hutch where a fully functional nanocrystallography system, similar to that in NXD-I, with similar sample environments, detectors and diagnostics will be available. A great example of the usefulness of NXD-II is the case of dynamic studies where it would be very valuable to spend a few hours screening different sample preparation runs and selecting the best sample before moving over to the highly complex time-resolved measurements in the NXD-I hutch. This will greatly increase the efficiency of beam time use at LCLS-II.

Below is a description of the key components required for the NXD-II instrument.

Refocusing optics

The beam must be refocused before delivery to the NXD-II interaction region. For this purpose, we propose the use of refractive lenses because the lenses will not offset the optical axis of the beam. This has an added benefit of allowing the detector in the second hutch to be used to measure extremely-low-angle scattering from the sample in the first hutch, in cases where low-angle scattering measurements are required. This could very well turn out to be important for MAD phasing and for accurate quantitative structure factor determination, as the low order Bragg spots provide information about the shape transform, and therefore the size, of small

crystals. A current limitation of the CXI instrument is the maximum detector distance of 2.6 m. The proposed NXD suite would allow the furthest downstream detector to be positioned up to ~15 m away, facilitating the measurement of shape transforms from larger crystals.

The location of the refractive lenses for refocusing will depend on the location of the primary focus and therefore on the curvature of the primary KB mirrors that focus the beam for NXD-I. Short focal lengths imply a large beam divergence, which would require the lenses to be located further upstream for efficient refocusing. Therefore, two sets of lenses are proposed, one mounted to the first detector chamber behind the detector in NXD-I and the other at the upstream end of the NXD-II hutch.

Diagnostics and optics

NXD-II will be equipped with a full complement of beam diagnostics and optics to operate independently from NXD-I. Diagnostics should exist before and after the sample location, allowing them to be removed from the upstream side of the sample in cases where they are found to disturb the beam excessively. The following devices are required for the independent operation of the NXD-II hutch:

- Pulse Shutter
- Attenuators
- Slits
- Beam Imagers
- Intensity monitors
- Wave front monitor

Sample environments

The NXD-II sample environments will have the same capabilities for sample delivery as the NXD-I hutch to allow easy transfer of sample from one to the other. However, due to the reduced intensity and larger spot size at NXD-II, it is envisioned to be useful for other more specific, less challenging measurements. For example, it is expected that the NXD-II system will be used often for fixed samples rather than liquid jets. Therefore, multiple sample delivery systems will need to be supported, including the liquid jets, fixed target scanning systems and a cryostage. The NXD-II hutch could be used for measurements in air for crystal screening or for samples that diffract sufficiently strongly despite the air scattering.

Detectors

The same detector requirements as for NXD-I apply to NXD-II with the difference that no small-angle detector is planned for NXD-II since the measurements requiring such a detector would be done on NXD-I. A single 16 Megapixel detector as described for NXD-I is envisioned for NXD-II.

8. Role in LCLS Complex

The proposed layout with tandem operation of two instruments with the reuse of the beam will provide dedicated nanocrystallography capabilities that will greatly expand the capacity of the LCLS for crystallography. This new instrument will complement the existing CXI instrument by adding dedicated nanocrystal diffraction capacity, providing a stable, user-friendly instrument, and by enabling higher-photon-energy diffraction experiments. CXI will remain available for nanocrystallography work, especially those studies requiring the smallest LCLS x-ray spot size of 100 nm. A dedicated nanocrystallography setup at LCLS-II will provide a robust tool for structural studies while allowing more exploratory research using the existing CXI instrument to continue to push the limits towards single molecule imaging using hard x-rays.

C. Soft X-ray Package

Primary scientific opportunities addressed:

- The Photochemical Cycle of Life: Understanding and Controlling Processes at Reaction Centers
- Information Technology: Approaching the Size and Speed Limits Set by the Laws of Physics

1. Introduction

LCLS-II provides a foundation to discover mechanisms necessary to develop functional materials and control chemical processes. Soft x-rays access these mechanisms through an understanding of electronic structure and order with elemental and chemical specificity. The soft x-ray instrument suite upgrade to LCLS-II presented here delivers unique experimental access to femtosecond time-scales and nanometer length-scales. This is achieved by a new ability to deliver, control and detect precision x-ray pulses.

2. Package Concept

Attacking the scientific questions to understand the photochemical cycle of life (Section II.B.2) and advance information technology (Section II.B.3) requires a diverse set of instrumentation. Figure III-6 presents an overview of the key soft x-ray components that will provide performance enhancements over LCLS-I and thus enable new discovery at LCLS-II. Note that only the SX-Ultra branch line is funded within the LCLS-II baseline project.

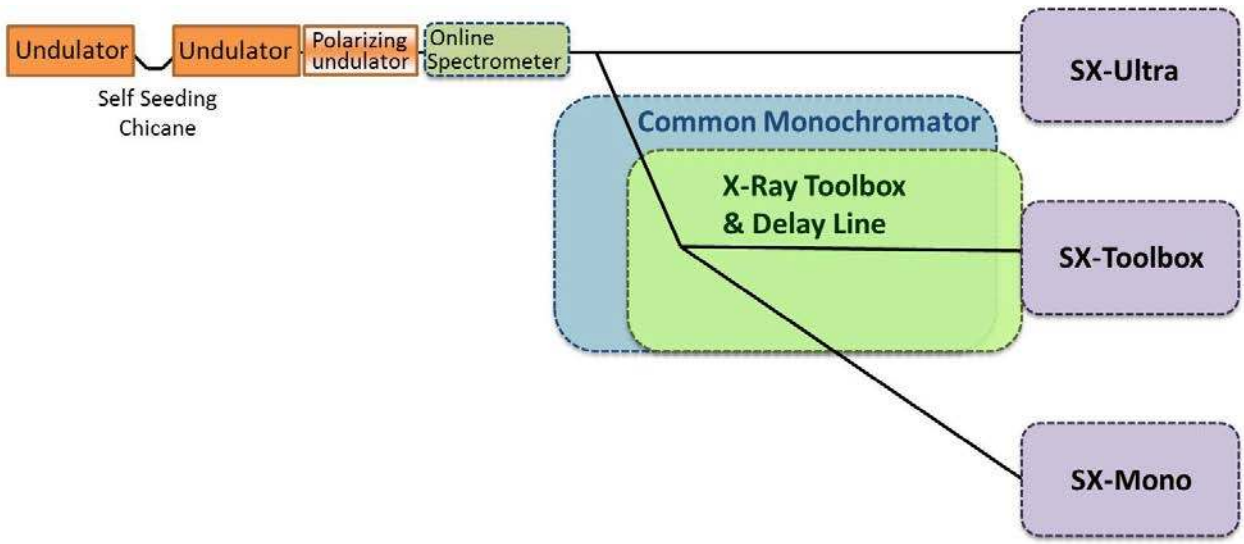

Figure III-6: Layout of the LCLS-II soft x-ray instrumentation.

3. Instrument Specifications

The soft x-ray suite, serving chemistry and atomic, molecular, and materials sciences, consists of three instruments: SX-Ultra, SX-Toolbox and SX-Mono. The SX-Toolbox is the most novel component of the soft x-ray instrument suite, as it combines ultra-short x-ray pulses with optical tools in an approach that will revolutionize nonlinear spectroscopy. The basic components of the SX-Ultra instrument are part of the LCLS-II scope. The SX-Toolbox and SX-Mono instruments share a grating monochromator, with the former being augmented by a diversified x-ray pulse manipulation tool kit. The SX-Toolbox beamline is complimented by an end station to study chemical reactivity while the SX-Mono beamline delivers beam to a resonant scattering station for materials studies. While these end stations are purpose-built, they are not fixed and can be installed on any beamline or exchanged with experiment-specific instrumentation. Space is reserved for expansion and we envision a high-resolution resonant inelastic scattering (RIXS) end station, described in Appendix A, to be installed on SX-Toolbox.

Table III-3: Specifications for soft x-ray instruments

Instrument	SX-Toolbox	SX-Mono	SX-Ultra
Photon energy range	250-1800 eV	250-1800 eV	250-2500 eV
Optics	Tool box + KB	Bendable KB	Ultrafocus KB
Spot size	1 mm to 5 µm	1 mm to 1 µm	100 nm
Monochromator	Yes	Yes	No
Resolving power	1,000 – 30,000	1,000 – 30,000	
Primary end station	Multi-spectroscopy	Resonant scattering	High-intensity imaging and spectroscopy
Main Detectors	X-ray grating spectrometer	Movable area detector	Photon and particle area detectors, particle spectrometers
Detector needs	1000x1000 pixels 10 µm pixel size 120 Hz	1000x1000 pixels 10 µm pixel size 120 Hz	1000x1000 pixels 100 µm pixel size <1 ns time resolution
Optical Laser	Yes	Yes	Yes

4. Source Enhancements

Understanding the origins of magnetism or following chemistry in real-time begins with exquisite control over x-ray pulse properties such as polarization and bandwidth. Command of these parameters is common for conventional lasers, but unprecedented for a soft x-ray FEL. Enhancements to the soft x-ray source include:

- Self-seeding**:** narrow bandwidth, wavelength stability and higher brightness
- Polarization control**:** tunable linear and circular polarization
- Two color pulses: simultaneous delivery of independent wavelength pulses
- Delayed pulses: independent delay of two pulses up to 1 ps

Soft x-ray self-seeding

By delivering more x-rays in each pulse at the energy and within the bandwidth prescribed by the experiment, seeding will open a new class of resonant scattering and imaging experiments. Even if peak brilliance is not required, experimental efficiency will improve by a factor of fifty, such that most experiments previously taking an entire five-shift run to complete will gather as much data in one hour. To realize this improvement, self-seeding will stabilize the photon energy to 0.005% and narrow the bandwidth to 0.01% for every pulse.

Following the success of hard x-ray self-seeding, a compact soft x-ray self-seeding system shown in Figure III-7 is being designed and will be tested at LCLS-I in late 2013. LCLS-II should include a similar soft x-ray self-seeding system that covers the photon energy range from 250 to 1800 eV with a resolving power of the order of 10,000.

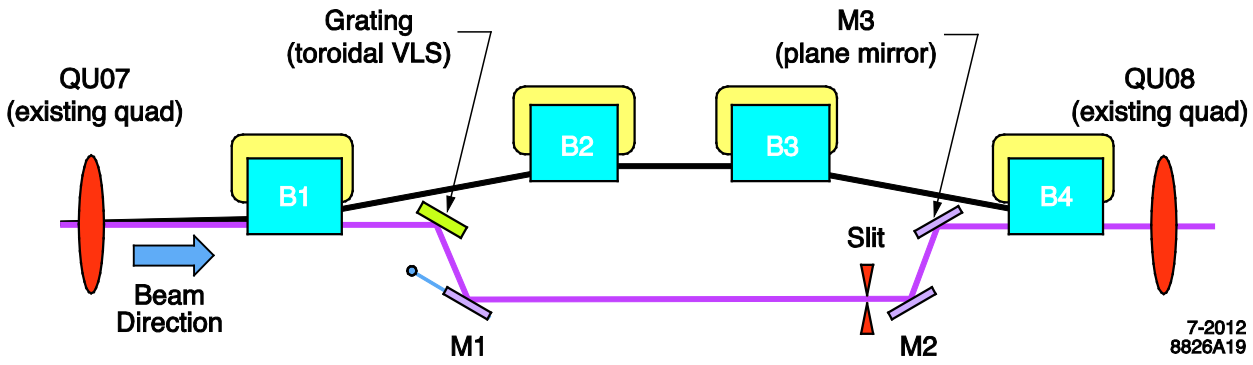

Figure III-7: Schematic of the soft x-ray self-seeding section. The x-ray delay is tunable up to 1 ps, and a compact chicane can be used to delay the electron bunch to match the x-ray delay. This chicane also enables two color and delayed pulse operation. The grating and slit form a monochromator to define the energy of the seed photons.

Polarization control

Examining emergent properties in ferromagnetic and quantum materials, which arise from electron spin correlation, requires polarization control. Circularly polarized soft x-rays have the powerful ability to couple to electron spin with element specificity. However, the LCLS-II variable-gap planar undulator is only designed to generate intense high brightness, linearly polarized x-ray pulses. While the planar undulator design is well understood and expected to be tunable within tight FEL tolerances, it lacks polarization control, required for separation of charge/spin response.

Efforts at LCLS-I have created circular polarization with dichroic magnetic multilayer filters. These have demonstrated the ability to capture femtosecond images of magnetic materials, but the filter only transmits 1% of the incident flux, which limits sensitivity and resolution. We need a different approach in order to improve transmission rates.

At hard x-ray energies polarization control can be accomplished by quarter-wave-plate diamond optics, but in the soft x-ray region the dual requirement of variable polarization and photon energy tuning is best accomplished by the undulator source itself. The LCLS-II design reserves space for adding polarization control with APPLE or DELTA type undulator modules after the last planar undulator. These undulator modules will work as afterburners, producing right or left circular or elliptical polarized radiation from the micro bunched electron beam leaving the planar LCLS-II undulators. The linearly polarized radiation produced by the planar undulator during the microbunching process will be a small background component, keeping the total degree of circular polarization slightly below 100%. As an example, with 16 m of polarizing undulator modules, polarization degrees above 90% are expected at milli-Joule pulse energy levels for the 250 to 1500 eV photon energy range. Increasing the number of the polarizing undulator modules will further enhance both the intensity and the degree of the polarized radiation.

Two color pulses

With two variable gap undulator modules it is possible to generate two-color x-ray pulses. When a Gaussian electron bunch enters the first undulator module, the middle of the bunch reaches saturation faster and thus produces significantly more photons than the head and tail of the bunch. The second undulator module is tuned to a different gap (and hence a different photon energy) and because the center of the bunch is ‘spent’ it will not strongly emit x-rays. However, the head and tail of the bunch are still ‘fresh’ and can generate SASE x-rays up to saturation. This technique can create two color pulses with energies that differ by as much as the full tuning range for a given electron energy in SASE mode or as little as the SASE bandwidth in seeded mode.

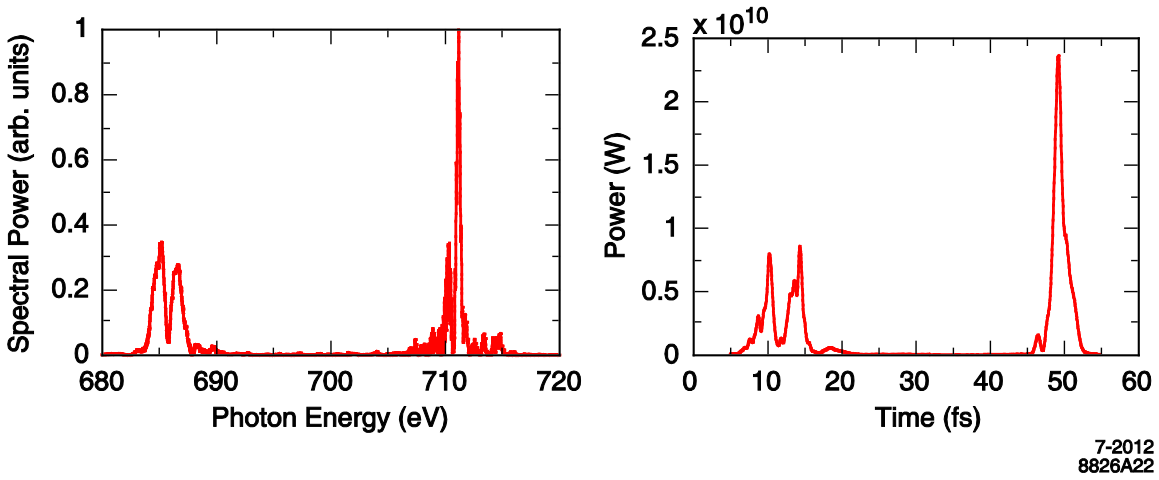

Figure III-8: Two-color soft x-ray pulses near 700 eV with pulse separation of ~40 fs set by the self-seeding chicane.

Delayed pulses

Capturing the ultra-fast dynamics of electronic processes requires two pulses separated in both photon energy and time. The self-seeding chicane can produce two-color pulses with a delay from 1 fs (jitter limited) to the maximum of 1ps afforded by the chicane. Figure III-8 shows simulated two-color pulses near 700 eV using the existing hard x-ray self-seeding chicane at LCLS-I with a 40 fs delay between the two pulses. Because the pulses originate from independent sources they are not mutually coherent. A split and delay line, like the one described in Section III.C.6, is needed to generate coherent, delayed pulses.

5. Front End and Beam Transport Systems

Enhanced x-ray pulse characterization and control are essential for examining complex chemical systems. It is important to characterize incoming photons upstream of the individual beamlines in order to normalize the signal and make necessary adjustments for each experiment. The baseline LCLS-II design includes a pulse fluence detector and attenuator, which is not sufficient for the complex experiments envisioned. The following enhancements will provide detection sensitivities that rival the state of the art at synchrotron sources:

- Single shot spectrometer to measure energy resolution in real time
- Beam imagers to measure beam size and profile
- Wave front monitor to optimize the beam optics, especially for imaging
- Pulse shutter to select individual pulses
- Timing distribution system to lock the x-ray pulse to the optical laser pulse

6. SX-Toolbox and SX-Mono Instruments

Expected use and impact of the instruments

The x-ray optical toolbox**,** with a highly configurable set of x-ray gratings, mirrors and slits, is the cornerstone of the SX-Toolbox instrument. Advanced spectroscopy methods will require independent temporal and spatial control of x-ray pulses in a way that is only available at optical wavelengths, in addition to the spectral control the monochromator delivers. The toolbox takes advantage of the monochromator and focusing mirror, augmented by additional mirrors and slits, that enable diverse experimental setups. This creates a soft x-ray beamline with the flexibility in configuration usually associated with optical laser components. The resonant spectroscopy end station attached to this beamline exploits these pulses to better understand chemical reactivity. This combination of beamline and end station provides the perfect development platform for advances in nonlinear spectroscopies that will become standard techniques at soft x-ray FELs.

The SX-Mono branch is ideal for investigating the evolution of electron correlation in nanoscale and mesoscale structures in condensed matter systems. Pump-probe methods with multiple beams and wavelengths can excite, control and interrogate electronic structure. The resonant diffraction end station attached to this beamline allows users to investigate long range electronic order.

Monochromator

The SX-Toolbox and SX-Mono instruments share a common monochromator, which provides a beam with tightly controlled photon energy. The flexible monochromator is capable of working in several modes of operation as shown in Fig. III-9 (a) and (b). A collimating mirror (CM) tangentially collimates the beam coming from the source. The combination of a grating and plane mirror (PM) select the photon energy without disturbing the beam collimation. A focusing mirror (FM) re-focuses the beam onto the exit slit.

The monochromator can be operated in multiple modes: high resolution, high flux (medium resolution) or higher order suppression. To optimize flux over the entire 250-1800 eV range we propose using three interchangeable gratings of 300, 600 and 1200 lines/mm groove density. For example, with a 1200 lines/mm grating, the achievable resolution is 30,000 for energies up to 1.4keV and almost 25,000 at 1.8 keV. The monochromator elements CM and the grating are used in conjunction with additional optics to define the SX-Mono exit beam, as shown in Figure III-9 (b).

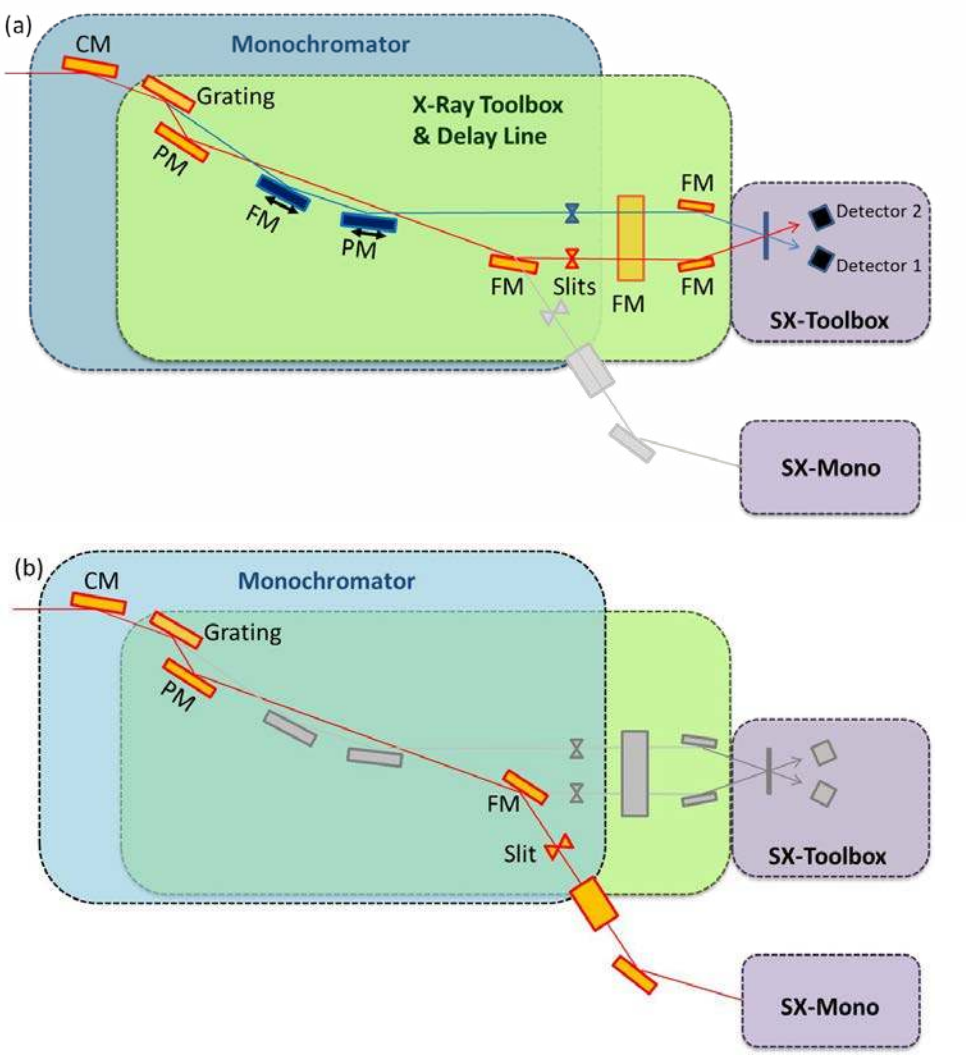

Figure III-9: Schematic of the monochromator serving both the SX-Toolbox beamline as shown in (a), and for the SX-Mono beamline shown in (b). The SX-Toolbox beamline is capable of generating delayed pulses and features modular x-ray optical components. At the end station of the SX-Toolbox beamline, split pulses can be combined with control over angle, position, arrival time and photon energy.

Pulse delay

The SX-Toolbox beamline consists of two exit beams, shown as red and blue in Figure III-9 (a), that serve as input for the x-ray tool box. The red beam path is simply deflected by the focusing mirror onto one exit slit. The blue beam path constitutes that of the non-dispersed zeroth order beam and utilizes two additional mirrors. The zeroth order beam (blue) exits parallel to the monochromatic beam (red), and has a variable time delay accomplished by moving the two delay mirrors as indicated.

As mentioned under "Delayed pulses" in Section III.B.4, the chicane can generate two independent pulses. Thus, by combining the two-pulse input to the monochromator with the split and delay capability of the SX-Toolbox it is possible to produce two pairs of coherent, delayed pulses.

X-ray optics toolbox

The monochromator design in Figure III-9 (a) constitutes the first element of our envisioned x-ray optics toolbox that delivers two x-ray pulses of different photon energies, angles and at variable delay times to the sample as shown. The two offset exit beams from the monochromator/beam splitter in Figure III-9 (a) are combined at the sample under different angles by a set of insertable mirrors. The different beam directions facilitate experiments such as stimulated Raman scattering.

Diagnostics and optics

Both the SX-Toolbox and SX-Mono instruments require the following set of simple optics and diagnostics is to characterize the XFEL beam, align optics and pre-align experiments:

- Beam imagers
- Absolute Intensity monitor
- Wave front monitor
- Slits
- Reference Laser to allow offline alignment of the experiments

Kirkpatrick-Baez focusing optics

The SX-Mono beamline includes a Kirkpatrick-Baez (KB) mirror system that is not complicated by the multiple beam configurations in SX-Toolbox. The shorter working distance improves focusing capability to 1 µm.

Chemical reactivity and spectroscopy end station

This end station, connected to SX-Toolbox, is specifically designed to take full advantage of the precisely conditioned pulses delivered by the x-ray toolbox to follow chemical bond formation of reactions on native time scales and characterize intermediate states. Chemical reactivity will be studied with x-ray emission spectroscopy using two dedicated sample environment systems: a UHV system for surface science and catalysis and a high pump-speed vacuum system for gas phase and liquid jet sample environments.

X-ray emission spectra will be measured with two dedicated varied line spacing plane grating spectrometers attached to the sample environment chamber. The spectrometers can be independently tuned to optimize operation over a larger energy range, but can also be tuned to

the same energy to double the signal. A full frame rate (120 Hz) soft x-ray sensitive area detector will be collaboratively developed for use on these spectrometers. The specifications for the spectroscopy detector are given in Table III-4. Given the challenges associated with reaching these specifications, multiple approaches are being pursued to design this detector in parallel with the similar detector for the resonant diffractive imaging end station.

Table III-4: Soft x-ray spectroscopy detector specifications.

Detector	Pixel Size (μm)	Array Size (pixels)	Energy Resolution	Maximum Signal	Energy Range
Soft x-ray spectroscopy area detector	10	1,000,000	60 eV	100 keV	250-1,800 eV
Soft x-ray scattering area detector	< 10	1,000,000	60 eV	10 keV	250-1,800 eV

Resonant diffractive imaging end station

The materials science community will use this end station to understand charge, spin and electron correlation in emergent materials. The increased spectral brightness afforded by the seeded beam will enable characterization of excitations on the scale of tens of meV. Moreover, nanoscale islands of electronic order can be imaged with coherent scattering.

The sample environment can be cooled to 10 Kelvin on a six-axis manipulator. The diffracted signal will be detected on a 120 Hz area detector sensitive to soft x-rays. In vacuum, motion of the detector will provide access to sufficient momentum transfer to investigate nanometer-scale order in correlated materials. The specifications for the scattering detector are given in Table III-4. The small (sub 10 micrometer) pixel size will allow the detector to resolve coherent scattering speckles. Image reconstruction will provide insight into the interplay between mesoscale order and electron and spin correlation.

Optical laser and timing system

A commercially available ultrashort pulse laser system will generate up to 20 mJ per pulse for pump-probe experiments using the SX-Toolbox. These pulses can then be converted to the excitation wavelength prescribed by experiments ranging from single THz oscillations to sub 100nm ultraviolet radiation.

Like the SX-Toolbox instrument, the SX-Mono will have femtosecond optical excitation capabilities. Moreover, the generation of peak THz fields on the order of 0.1GV/m will be important on the SX-Mono instrument to mimic electric fields present in devices.

The arrival time jitter of the x-ray pulse must be measured and corrected to achieve pulse width limited temporal resolution. This applies to both instruments. An arrival time monitor exploiting the ability of the x-ray pulse to alter the optical properties of a thin, x-ray transmissive, film allows for an arrival time measurement.

7. SX-Ultra Instrument

Expected use and impact of the instrument

The ultra-high intensity end station will serve the needs of experiments for which the highest possible photon density is required and for which the spectral contrast from the seeded source is sufficient or a large bandwidth is advantageous. Biological imaging experiments (Section II.B.1) should be performed at the longest possible wavelength supporting the required resolution, since the scattering cross section decreases with increasing photon energies. The SX-Ultra end station will be optimized for delivering the maximum amount of photons from the sulfur and phosphorous K-edges to the water window.

For the AMO community the SX-ultra branch line will be a quantum leap towards non-linear x-ray physics. Laser based research at the intensity frontier has led to many unexpected discoveries. Prominent examples in the optical regime range from high-harmonic generation and attosecond pulse creation to fusion in laser-driven cluster nanoplasmas. In the extreme non-linear regime electrons are driven non-perturbatively by the electric field of the laser pulse. Since the intensity required to access non-perturbative ionization scales inversely with the wavelength of the light, current x-ray free-electron lasers miss the non-perturbative regime by roughly two orders of magnitude in power density. LCLS-II, with its high peak output from the seeded soft x-ray undulator in combination with the SX-ultra high-transmission 100 nm focus beamline, offers the potential to break into the non-linear x-ray physics regime. Compared to the current state-of-the-art high intensity soft x-ray beamline at LCLS a factor of one thousand increase in power density appears possible. The higher source power, combined with an improved design of focusing optics incorporated into the experimental station, can deliver power densities exceeding 10^{21} W/cm^2 on target. The main challenge will be the control of the slope errors of the focusing mirrors and the mitigation of beam damage.

Beam transport and focusing optics

The beam transport from the source to the end station will be provided within the LCLS-II baseline. We need to enhance the basic beamline with ultimate focus optics to deliver a 100

nm x-ray spot and a harmonic rejection system. Prefigured fixed focal length mirrors will be used to achieve the 100 nm focal spot. As the focal length will be short, the optics must be incorporated into the experimental end station.

End station

The end station will be designed as modular system. Focusing optics and the interaction chamber form the core of the system, with multi-stage differential pumping sections between the two in order to protect the optics from the target samples. The interaction chamber will include various sample delivery options, as well as electron and ion spectrometers perpendicular to the beam. Pixelated charged particle detectors will allow momentum-resolved multi-coincident electron and ion imaging experiments. Development of an integrated circuit chip with sub-nanosecond time resolution is underway. When mated with a custom sensor and other system components, the performance goals listed in Table III-5 should be met.

Downstream of the interaction region will be a port for large-area photon detectors for imaging experiments. At present there are a couple of detectors that come close to meeting these requirements. Collaborations with these existing detector groups as well as new technologies are being pursued. This modular multi-purpose system will allow for imaging and spectroscopy of dilute gas-phase targets.

Table III-5: SX-Ultra detector specifications.

Detector	Pixel Size (μm)	Array Size (pixels)	Energy Resolution	Maximum Signal	Energy Range
Soft x-ray area detector	25	1,000,000	60 eV	150 keV	250-2,500 eV
Charged particle spectrometer	100	500,000	10 meV	100 eV	0.1 – 100 eV

Optical laser and timing system

The SX-Ultra design will incorporate an optical pump laser system. This system will be a shared with the other soft x-ray instruments described above. A timing jitter diagnostic will deliver the relative arrival time of the optical and x-ray laser with femtosecond precision.

Diagnostics and optics

A suite of diagnostics will be implemented to optimize the focal point and to measure the x-ray pulse properties on a shot-by-shot basis. The diagnostics suite will be located after the

interaction region so that the properties of the beam on target can be accurately measured. The suite will include the following:

- Beam imagers
- Absolute Intensity monitor
- Wave front monitor
- Reference Laser to allow offline alignment of the experiments

8. Role in LCLS Complex

The instrumentation presented in the soft x-ray package captures all of the capabilities of the LCLS complex at photon energies below 2500 eV. Although the current LCLS-I undulator source is able to produce photons with energies below 2000 eV, the LCLS-II soft x-ray source will have significantly more capabilities and far superior performance in comparison. As such, the LCLS-I soft x-ray instrumentation will be decommissioned and LCLS-II will take over as the state-of-the-art for soft x-ray experiments.

D. Hard X-ray Package

Primary scientific opportunities addressed:

- The Photochemical Cycle of Life: Understanding and Controlling Processes at Reaction Centers
- Information Technology: Approaching the Size and Speed Limits Set by the Laws of Physics

1. Introduction

The LCLS-II hard x-ray undulator will be a world leading source with the enhancements specified in the nanocrystal x-ray package (Section III.B.4). The scientific topics addressed by the hard x-ray package are nearly identical to those addressed by the soft x-ray package: characterizing the behavior of photoexcited molecules and materials of technological importance. However, hard x-ray probing techniques yield complimentary information to soft x-ray techniques. While the soft x-ray tools will be used to primarily characterize the electronic structure of a system, hard x-rays excel at directly measuring the atomic arrangements. As such, in many cases both probing techniques are needed to fully elucidate the fundamental mechanisms involved at the earliest stages of ultrafast processes due to the various couplings of electronic and atomic structure. In addition, hard x-rays have the ability to penetrate deeply into materials and probe bulk effects. This attribute is also an advantage for sophisticated sample environments with entrance and exit windows.

2. Package Concept

The hard x-ray package places a general purpose hard x-ray instrument, the Ångstrom X-ray Experiments instrument (AXE) at LCLS-II, illustrated in Figure III-10, to take full advantage of the world leading properties of the LCLS-II hard x-ray source. In addition to this instrument, the package builds upon the source enhancements presented in the nanocrystal x-ray diffraction package (Section III.B.4) by extending the seeded photon energy range to 18 keV by adding undulator modules. No additional enhancements are needed to the hard x-ray front end system since it will be fully built out in the NXD package.

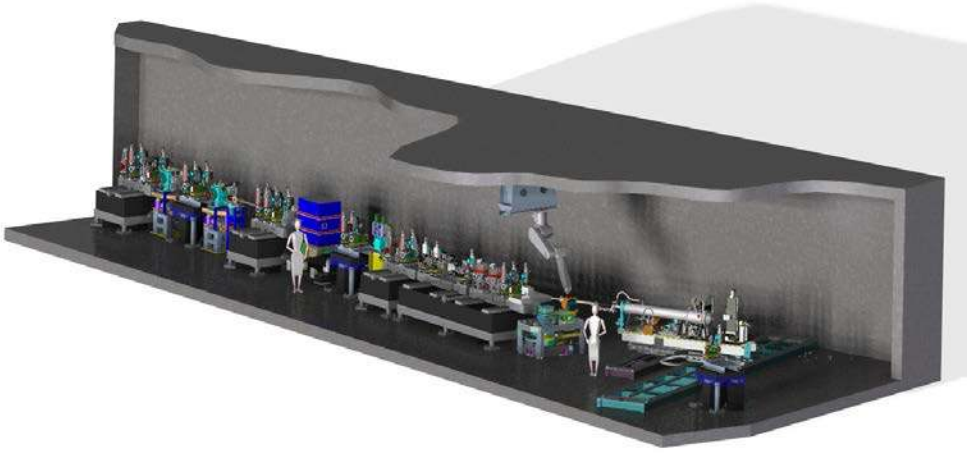

Figure III-10: Rendering of the proposed general purpose AXE hard x-ray instrument at LCLS-II.

3. Instrument Specification

The AXE instrument will operate in the 5 to 18 keV photon energy range, with the majority of use expected in the higher end of the range. The lower energy cutoff is set by the expected operational limit of the monochromator system. The upper limit is defined by the mirror distribution system energy cutoff. An inline focusing system, based upon refractive lenses, will be used to create a varying x-ray spot size on the sample. The system will be capable of generating spot sizes from the unfocused beam size down to 2 microns. The AXE monochromator is an inline system that can be retracted. As such, the x-ray bandwidth can be tuned from the natural SASE bandwidth of 10^{-3} to either 10^{-4} or 10^{-5} via Si (111) or Si (333) operation of the AXE monochromator. Table III-6 shows the specifications the AXE instrument.

Table III-6: Specifications for AXE instrument.

	AXE
Photon energy range	5 - 18 keV
Bandwidth	10^{-3} to 10^{-5}
Optics	Refractive lenses
Spot size	2 – 300 µm
Monochromator	Yes
Sample environment	Diffractometer system
Intense scattering Detector needs	3000x3000 pixels 100 µm pixel size 10,000 dynamic range
Weak scattering Detector needs	3000x3000 pixels 50 µm pixel size Low noise
Optical Laser	Yes

4. Source Enhancements

Six additional undulator modules are needed to extend the seeded LCLS-II photon energy to 18 keV. This extension is required to effectively probe conformational changes in disordered systems (molecules in liquid or gas phase, proteins in liquid, amorphous systems) via scattering techniques. In addition, the extension to harder x-rays has many advantages in terms of probing bulk materials, mitigating x-ray induced sample damage and coupling the x-ray beam into and out of complex sample environments while covering a wide range of reciprocal space.

5. Ångstrom X-ray Experiments (AXE) Instrument

Expected use and impact of the instrument

The AXE instrument will fully exploit all x-ray beam properties of the LCLS-II hard x-ray undulator: high brilliance on the first harmonic up to photon energies of 18 keV, short pulse duration, narrow self-seeding bandwidth and full transverse coherence. The AXE instrument design will emphasize flexibility, ease-of-use and rapid reconfiguration capability. This instrument will accommodate a wide variety of sample environments (in-air, vacuum, cryogenic temperatures, high pressure, etc.) and will execute a wide variety of x-ray probing techniques (WAXS, SAXS, XAS, XES, XPCS, CXDI). In many instances, AXE will be capable of performing simultaneous combinations of the aforementioned x-ray probing techniques.

The majority of AXE experiments will involve creating and probing non-equilibrium states of molecular and condensed matter systems. These states typically will be generated with an optical laser. A complete ultrafast optical laser system is therefore included in the design of the AXE instrument. This system contains wavelength conversion capabilities to populate specific degrees of freedom within a sample, a timing system capable of achieving a ~ 10 fs resolution and amplification stages to reach the desired level of excitation densities. AXE will also have the capability of performing x-ray pump/x-ray probe experiments via a split-and-delay system.

Diffractometer system

A diffractometer system will be incorporated into the AXE instrument to position samples and their environments into the XFEL beam with high precision. The diffractometer system will be re-configurable, allowing per-experiment optimization. AXE will have three detector arms to perform the intended x-ray probing techniques: a robotic positioner, a horizontal two-theta arm and a large horizontal detector arm. The robotic positioner can operate in both spherical and Cartesian coordinates because it offers the flexibility of placing a detector on an upper hemisphere with a radius up to 1 m. The horizontal two-theta arm is intended for studies

requiring high-resolution energy analysis of scattered or emitted photons, and for high-resolution diffraction studies. The large horizontal detector arm will be capable of positioning a detector up to 4 meters from the sample at a scattering angle up to 90°. This arm is intended for small angle x-ray scattering,, x-ray photon correlation spectroscopy, x-ray emission spectroscopy and coherent x-ray diffraction and imaging studies.

Monochromator

The in-line, silicon based monochromator system will be able to precisely and repeatably scan the incident photon energy, which is helpful for experiments that exploit resonance effects. The system can select from two silicon reflections, (111) and (333), to optimize the energy bandwidth for each experiment. This allows us to control the Q-resolution, the longitudinal coherence, and also to clean up the self-seeding spectrum from its SASE background.

Diagnostics and optics

The following set of simple optics and diagnostics is proposed for the AXE instrument to characterize the FEL beam, align optics and pre-align experiments:

- Beam imagers
- Intensity monitors
- Slits
- Reference laser to allow offline alignment of the experiments

Split and delay system

A split and delay unit allows users to control the lag time between two successive pulses, with a time delay ranging from the pulse duration to 1 ns. Such an approach not only offers the possibility of generating double-pulse exposures as required for ultrafast-XPCS, but also provides x-ray pump/x-ray probe capabilities. In combination with an optical laser pulse, it will broaden the possibility of investigating stimulated dynamics. The split and delay system will rely on silicon Bragg optics, including thin Bragg crystals as splitters and mixers. The device throughput will be maximized by using (111) and (220) reflections.

Detectors

Two detector systems will be incorporated into the AXE instrument to accommodate the wide variety of experiments and techniques that will be performed: a multi-megapixel, large dynamic range detector (HXRD-10k) and a low noise, high-energy resolution, small pixel area detector (HXRD-100). The detailed AXE detector specifications are displayed in Table III-7.

The HXRD-10k system, also used on the NXD instruments, is best for experiments that generate intense scattering patterns (e.g. protein crystallography and solution phase scattering). This

system will have single photon sensitivity (8 keV), moderate pixel size (~100x100 um^2), large well depth (10,000 photons/pixel) and 9 megapixels.

The HXRD-100 system will be used for experiments that generate weak scattering patterns (e.g. x-ray photon correlation, emission and inelastic spectroscopy studies). This system will have a very low noise (fraction of a 8 keV photon), small pixel size (~50x50 um^2), limited well depth (100 photons/pixel) and 9 megapixels.

Table III-7: AXE detector specifications.

Detector	Pixel Size (μm)	Array Size (pixels)	Energy Resolution	Maximum Signal	Energy Range
HXRD-10k	100	9,000,000	1000 eV	80 MeV	4 – 25 keV
HXRD-100	50	9,000,000	300 eV	800 keV	2 – 25 keV

Optical laser and timing system

Many experiments on AXE will be of the pump-probe variety. As such, a state of the art optical laser system will be incorporated into the instrument. The laser system will be similar to the systems currently installed on many of the operating LCLS instruments (up to 20 mJ pulse energy, 120 Hz, a complete spectrum of wavelengths) but will have a shorter pulse duration (30 fs). The temporal resolution, via an x-ray/optical timing diagnostic, is expected to reach a ~10 fs resolution. In addition, the system will have wavelength conversion options to tune the photon energy to a particular sample resonance, which is important for most molecular and biological systems.

6. Role in LCLS Complex

Third generation synchrotron user facilities, such as the Advanced Photon Source at Argonne National Laboratory, typically have more than 30 beamlines, with each beamline containing multiple experimental stations. These facilities have the luxury of constructing very specific, purpose-built instruments due to the large quantity of instrument locations available. LCLS, on the other hand, has a very limited number of experimental stations for a given undulator source. This limitation, in combination with our observation of a rapid evolution of scientific scope being addressed by LCLS-I, makes it important to construct at least one flexible, general purpose instrument for each unique undulator source at the LCLS complex. AXE fulfills this role at the LCLS-II hard x-ray undulator source and will be capable of performing experiments that are not feasible on the purpose-built NXD-I and NXD-II instruments.

AXE is analogous to the general-purpose LCLS-I XPP instrument, one of the most in-demand instruments at LCLS to date. Although there is some overlap between these instruments, there are many noteworthy differences:

- AXE will typically run at higher photon energies since the LCLS-II hard x-ray source will be capable of self-seeding at photon energies up to 18 keV. The LCLS-I source is currently limited to 10 keV and does not have the undulator length required to saturate the self-seeded beam at high photon energies.
- AXE will be equipped with an integrated two-theta arm on the diffactometer system, which will be ideal for studies requiring crystal energy analyzers.
- AXE will utilize a 4 meter horizontal detector arm that is capable of reaching a 90 degree scattering angle
- AXE will contain a x-ray split and delay system

The long detector arm and small pixel, low-noise detector system will permit x-ray photon correlation spectroscopy studies. This capability will permit the repurposing of the LCLS-I X-ray Correlation Spectroscopy (XCS) instrument into an inelastic spectroscopy station (see Appendix B).

Appendix: Other Instrumentation needs toward LCLS 2025

E. RIXS End station: Resonant Inelastic Soft X-ray Scattering

High-resolution soft x-ray RIXS has emerged as a powerful spectroscopy technique for the study of atom-specific energy, momentum, and polarization dependent elementary excitations in various samples. It can be used to probe low-energy charge, spin, orbital, and lattice excitations in correlated materials or to reveal element specific excited states in molecular systems, for example, the states involved in electronic energy flow between different functional groups in a molecule.

Because of the large resonant x-ray cross section, RIXS is compatible with small-volume samples in contrast to inelastic neutron scattering. It also allows the separation of charge and spin excitations by polarization dependent studies. State-of-the-art soft x-ray RIXS studies are presently performed at the Swiss Light Source and the ESRF and they utilize the high *average* brightness of these sources. At LCLS, time resolved RIXS studies of excited electronic states become possible. Such studies can be carried out in a pump-probe mode where the sample is "prepared" by an optical or THz pump pulse and the x-ray probe pulses reveal the evolution of low lying excited states that contain the relevant information on the excitation and equilibration processes. Such studies have not yet been carried out at LCLS but are planned in the near future. LCLS offers another potentially revolutionary advantage. In contrast to synchrotron radiation sources where within a femtosecond time interval no more than a single photon is typically present in the sample, the LCLS pulses contain up to 10^9 equivalent photons within a femtosecond SASE spike. This opens the door for stimulated resonant Raman scattering as discussed in conjunction with Figure II-16. In anticipation of time dependent and stimulated RIXS studies we have developed a concept for a soft x-ray RIXS endstation that is briefly sketched below. We anticipate rapid developments in this area and upcoming LCLS-II instrumentation workshops may well lead us to include such an end station as part of the soft x-ray suite.

The RIXS instrument (see Table A-1) will be equipped with a spectrometer that can resolve fine energy features at moderate time resolution. It will also allow time-resolved RIXS by pump-probe techniques. The goal for this station is to be able to perform at a resolving power near 30,000 and cover a range of 400 to 1700 eV photon energy. This would give 30 meV energy resolution, which would be state of the art. Pulse broadening limits the possible time resolution to between 70 and 300 fs, depending on the photon energy.

Table A-1: Parameters for RIXS instrument

Photon energy range	400-1700 eV
Bandwidth	0.003 %
Laser pulse duration	< 300 fs
Spot size	2 μm to 2 mm
Monochromator	Yes
Resolving power	30,000
Sample environment	Ultrahigh vacuum
Detector needs	Spectrometer, fast CCD

One important point to consider for spectroscopy development is the damage threshold of materials for the type of fluences available at LCLS-II. At LCLS-I, solid samples can handle a typical spot size of about 300 μm^2 with minimal attenuation for 3 mJ and 1 eV bandwidth pulses, which places constraints on the energy resolution. This damage concern is reduced somewhat by the lower transmission of the high resolution monochromator in the SX-Toolbox beamline. We also note that stimulated RIXS reduces Auger decay and may well help in circumventing electronic damage.

One method to improve energy resolution would be to use a line focus, such that the overall fluence is preserved. For instance, considering a spot size with dimensions of 3 μm in the dispersive direction by 300 μm in the orthogonal direction, and a 7m spectrometer (a length compatible with the layouts of the LCLS-II experimental hall), preliminary calculations give a resolution near the 30 meV goal. Further optical design work will optimize the monochromator and spectrometer performance. The size of the spectrometer necessitates a permanent installation at LCLS-II.

F. IXS Instrument: Inelastic Hard X-Ray Scattering

The implementation of the AXE instrument in the LCLS-II experimental hall not only increases the capacity and capabilities of the existing XPP instrument but it also supports the user program of the XCS instrument located in the far hall of LCLS-I. The long scattering arm of the XCS instrument provides the opportunity to reconfigure this instrument for high resolution inelastic scattering (IXS). It is envisioned that this type of spectroscopy, which depends on average brightness, has high potential when combined with the hard x-rays of LCLS. LCLS-II offers the opportunity for time-resolved studies while exceeding the average brightness of existing synchrotron radiation sources.

IXS at LCLS-II may revolutionize the field of hard x-ray inelastic experiments because of the unique properties of the LCLS-II hard x-ray undulator: high peak power, moderate repetition rate, small isotropic divergence and beam size, energy tunability of the first harmonic up to 25

keV and, most importantly, fully saturated seeded pulses. A comprehensive review of the currently available IXS capabilities at 3rd generation storage rings shows that operating IXS instruments can provide on average about 5 x 10^9 ph/s/meV incident within the 5 to 25keV energy range. LCLS-II is expected to deliver fully saturated seeded pulses with an average of at least 1 x 10^{12} ph/s/meV over the same energy range. LCLS-II would therefore provide meV bandwidth pulses with a factor of 200 more intensity than is presently available. It would dramatically change the performance and scientific output of these photon-hungry experiments, due to the time-average brightness of LCLS-II. In addition, it would most importantly offer the unique opportunity to perform single-shot experiments in transient states, which is currently unavailable at any other facility.

Instrumentation for medium energy resolution (typically 0.1eV) IXS is fundamentally different from that needed for high energy resolution (typically 1meV) IXS. Therefore, two dedicated experimental setups are envisioned, with required parameters as listed in Table A-2.

Table A-2: Parameters for IXS instruments

	Medium resolution	**High resolution**
Photon energy range	5 - 15 keV	12 – 25 keV
Bandwidth	0.5 eV	0.5 eV to < 1 meV
Spot size	50-100 µm	50-100 µm
Monochromator	Yes	Yes
ΔE/E	10^{-4}	10^{-6}
Sample environment	Not critical	High P, high magnetic field
Detector needs	50-100 µm pixel size	50-100 µm pixel size

Medium energy resolution setup

A conventional medium resolution setup would be required in order to fully explore the dynamics of the transition metals by means of resonant or non-resonant inelastic x-ray scattering techniques.

This setup does not require a high resolution monochromator, but would use the fully saturated seeded hard x-ray beam. However, a standard diamond(111) or eventually Si(333) double crystal monochromator, as required to clean the seeded beam from its SASE pedestal, is needed. It will provide a energy bandwidth of around 0.5eV, as determined by the x-ray line width, and should cover an energy range from 5 to 15 keV. The lower limit is defined by the optics damage threshold.

A 6-circle diffractometer with a 2θ-arm reaching scattering angles up to 170 degrees is required to reach the scattering wave vectors of interest. The detector arm will have the capability to

house multiple medium resolution crystal analyzers organized in Rowland geometry with a radius of 1-2 meters. Several wave vectors should be measured simultaneously. Multiple sets of crystal analyzers are required to perform efficient Resonant IXS over the entire energy range.

Such an instrument does not require any extreme focusing capabilities, as typical beam sizes are in the 25 to 100 μm range.

High energy resolution setup

A state of the art high resolution setup would be required in order to access very small energy transfers (i.e. down to the sub-meV range) up to the large wave vector range of interest. This is in particular of fundamental interest when probing dynamics in amorphous systems, where the concept of Brillouin zone is absent. High energy resolution setups usually require elaborate x-ray optical schemes based on high order reflections from perfect silicon crystals.

This setup would therefore also require a standard C*(111) or eventually Si(333) double crystal monochromator to be used as a pre-monochromator. The energy resolution of the monochromator in backscattering mode dictates the photon energy range specified in Table A-2. A [Si(nnn), n=5,7,8,9,11,13] backscattering monochromator can provide an incident x-ray beam with a bandwidth ranging from 7 down to <1 meV, in order to achieve meV to sub-meV resolution. The existence of the monochromator reduces the bandwidth compared to that of the medium resolution instrument. More complex in-line monochromators, such as the combination of a Channel Cut [CC] (220) with a backscattering CC (15 11 3) and terminated by a additional CC (220), provide a 1.25meV bandwidth at 21.657 keV. The system will require a 4 circle diffractometer to orient crystalline samples.

The system will most importantly require meV resolution [Si(nnn), n=5,7,8,9,11,13] diced crystal analyzers with a bending radius of about 7 meters. This will also require a detector arm operating in the horizontal scattering geometry with a sample to crystal analyzer distance of 7 meters. As many as ten to fifteen crystal analyzers would be used simultaneously, thus offering the possibility of measuring many scattering wave vectors on a single shot basis.

G. TXI Instrument: Tender X-ray Imaging

The proposed NXD instrumentation package not only will provide a stable hard x-ray protein crystallography system but will also have the added benefit of freeing up beamtime on the existing CXI instrument of LCLS-I for more challenging experiments using hard x-rays. However, neither the existing LCLS-I instruments nor proposed LCLS-II instruments will be capable of efficiently utilizing photons in the range of energies between 2.5 and 5 keV. This energy range is

often requested by existing LCLS-I users, especially for biological imaging and single molecule imaging experiments. It provides a good compromise between achievable resolution and scattering cross-section, and calculations indicate it can be a very valuable tool for imaging. Also, the energy range of 2 to 5 keV (tender x-ray range), slightly below and above the sulfur K-edge, could provide a very important tool for phasing protein crystal diffraction patterns for de novo structural determination. This energy gap at the LCLS complex should be closed and the TXI instrument proposes to accomplish that.

Since the proposed soft x-ray package (Section III.C) moves all soft x-ray capabilities to the new LCLS-II source, the current hutches 1 and 2 of LCLS-I will become vacant and are ideal locations for a beamline that uses photon energies of 5 keV and below.

Package Concept

The tender x-ray range can be achievable with simple modifications of the LCLS-I soft x-ray optical branch. The intention is to reuse the existing optical system, with mirrors at the same locations, using the same incidence angle, and deliver the beam on the same axis at the experimental hutch. This will require minimal intervention and modification of the existing devices. The higher photon energy range will be achieved by replacing the existing mirrors with either optics coated with heavier material or multilayer optics.

Specifications

The proposed TXI beamline will require high reflectivity optics up to as close to 5 keV as possible. The low photon energy cutoff will be determined by the radiation damage threshold of the coating material chosen but is desired to be 2 keV or lower. The beamline will also require focusing to a few microns in order to provide high power density at the sample to allow crystallography studies of small crystals as well as single molecule imaging applications.

Table A-3. Parameters for the tender x-ray Beamline

Photon energy range	**2 - 5 keV**
Spot size	1-3 µm
Monochromator	No
Sample environment	Vacuum
Detector needs	100 µm pixel size, high dynamic range

Needed instrumentation and enhancements

Several systems will need to be reconfigured to meet the needs of the TXI instrument:

- New LCLS-I Front End Optics: replace 4 mirrors with either optics with heavy coatings or multilayers to reflect photon energies up to 5 keV
- New KB Mirror System: replace the existing KB mirror system at the AMO instrument with a mirror system with a coating or multilayer that will be reflective up to 5 keV
- Slits: required to efficiently block the beam at the higher energy range
- Diagnostics: beam viewers and intensity monitors will be added inside hutch 1 of LCLS-I

End stations

Large area detectors are expected to be important for imaging and crystallography applications, but no end station will be specifically developed for this beamline. The TXI will instead rely on movable end stations from LCLS-I, as well as those planned for the LCLS-II soft x-ray instruments. User-supplied end stations could also be considered for use at the TXI beamline when suitable.